Instructions to the Practical M48: Analysis of Z^0 decays

Physikalisches Institut
der Friedrich-Alexander-Universität Erlangen-Nürnberg

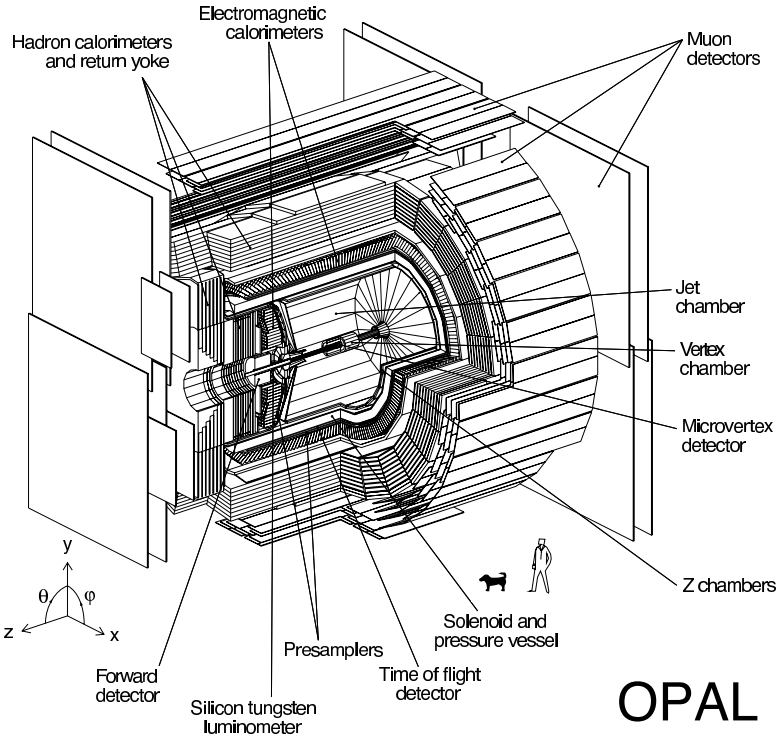

Last modification: March 2024
(Revision 2.0)
*r*odrigo.lang@fau.de

Contents

Materials (additional document)

List of Figures

List of Tables

1. Introduction

Overview and goal of the practical

This practical is to give you a first impression on the experiments and methods of analysis of modern particle physics. As an example for that kind of experiment the OPAL-Detector is used – one of four big detector systems, that have been used to investigate the physics of electron-positron collisions at the LEP-accelerator/CERN by international collabrations between 1989 and 2000.

The name *Omni-Purpose Apparatus at LEP* expresses the fact, that OPAL is a „general purpose particle detector“, a type of detector system that has been used – and is used right now at the LHC (Large Hadron Collider) – for many years in high energy physics.

The data collected by LEP-detectors over the years can be evaluated with regard to different questions. To illustrate the methods of detection and analysis, the identification of fundamental properties of elementary particle physics based on measurements of the shape of the Z^0-resonance is to be reproduced.

Contents of the practical, methods and previous knowledge

The goal of this practical is to introduce you to the following aspects of physics:

- Elementary particles and their interactions,
- interactions of particles and radiation with matter,
- modern particle detector systems and particle identification,
- physics with e^+e^--storage rings at high energy.

For that purpose, the following methods and utilities will be used:

- Classification of individual events on the basis of measured data of different subdetectors of the OPAL-detector, put into graphs with the OPAL-event-display Grope,
- computerised statistic evaluation of big datasets (working with histograms and selective cuts),
- model fitting to measured data to determine the model parameters; verification of the qualitiy of the fit with statistic methods (e.g. χ^2-check)
- other means like the programming languages Python and C++ for the execution of the evaluation.

The practical will be executed at a personal computer with the operating system Linux in **r**oom TL 209 over the course of **t**wo days. Preselected and preprocessed datasets as well as basic programs for their analysis are available. These programs are to be used and partialy expanded in the practical. For the most part, the evaluation is done with the program package Root, which has been developed at CERN. Previous knowledge of C++ and Linux as well as the use of programs for symbolic computation like Matlab, Maple or Mathematica are advantageous but will not be expected. Basic knowlege of particle physics are required.

During the course of this practical you will determine important parameters of elementary particle physics, for example the mass and lifetime, or the decay width repectively, of the Z^0-boson (see adjacent figure), the weak mixing angle ($\sin^2\theta_W$), the color rotation (Farbfaktor) of the strong force and the number of neutrino generations, based on data of a big experiment.

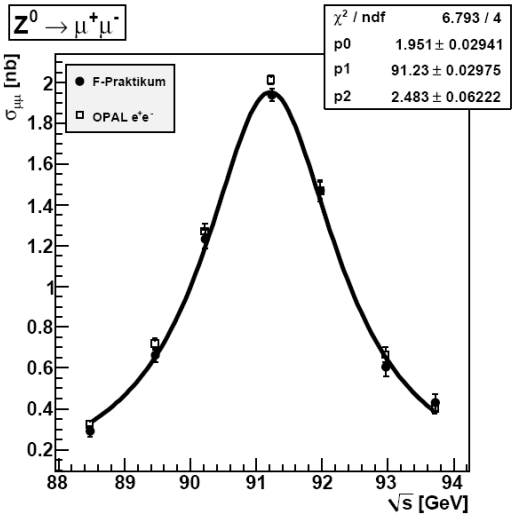

Figure 1.1.: Z^0-resonance curve as outcome of the practical

Notes to preparation and literature

This practical is rather conceptional because you don not have access to the experimental setup and will not do any „measurements“ on your own, but instead only evaluate already existing data (this is a typical situation when working in certain areas of physics, especially in high energy physics and astrophysics!). Because of that, it is especially important to be well prepared before beginning the practical. The instructions and material are intentionally extensive and should be understood as an offer of information, that you can work with selectively based on your previous knowledge.

What follows is a (wide) selection of additional literature (partly in German), that could be useful to extend upon the instructions and the attached materials depending on your previous knowledge and interests.

- particle physics in general:
  1. Chr. Berger: *Elementarteilchenphysik*, Springer, 2006
  2. D. Griffiths: *Introduction to Elementary Particles*, John Wiley & Sons, 1987
  3. F. Halzen, A. D. Martin: *Quarks and Leptons*, John Wiley & Sons, 1984
  4. D. H. Perkins: *Introduction to High Energy Physics*, Addison-Wesley, 2000
- particle detection:
  1. C. Grupen: *T*eilchendetektoren, Spektrum Akademischer Verlag, 1998
  2. K. Kleinknecht: *Detektoren für Teilchenstrahlung*, Vieweg+Teubner, 2005
  3. W. R. Leo: *Techniques for Nuclear and Particle Physics Experiments*, Springer-Verlag, 1994
- statistics and data processing:
  1. R. J. Barlow: *Statistics*, Wiley, 1989
  2. G. Cowan: *Statistical Data Analysis*, Oxford University Press, 1997

Note: This practical is offered in similar form at many other universities as well. The basics (especially the preprocessed datasets) have been adopted from the University of Bonn; we'd like to thank our associate there for their support.

2. Basics of particle physics

After a short introduction to the measurands and utilities in section 2.1, the sections 2.2 and 2.3 will explain the Z^0-boson and its properties in context with the *s*tandard model of elementary particle physics. Section 2.4 will concentrate on the analyses, that can be done regarding the parameters of the Z^0-boson during this practical. Lastly, section 2.5 contains a compilation of the most important formulas and relations.

2.1. Cross section and decay width

To specify event rates and the probability of a reaction, the so called *c*ross section is used. It is possible to assign a (cross-sectional) area to every particle. Figuratively speaking, a reaction takes place, when the interaction partner of a particle hits this area. The cross section (σ) is measured in barn: $1\,\mathrm{b} = 10^{-24}\,\mathrm{cm}^2$. The name refers to the fact that this is still as huge as a barn door compared to the scale of particle physics (engl.: *b*arn = Scheune). The cross sections $\sigma(\mathrm{e}^+\mathrm{e}^- \to \mathrm{f}\bar{\mathrm{f}})$ of the electron-positron-annihilation in different pairs of fermions and antifermions at energies close to the Z^0-mass are at the scale of some nb. The cross section of a specific sub-process, for example $\mathrm{e}^+\mathrm{e}^- \to \mathrm{q}\,\bar{\mathrm{q}}$, is referred to as partial cross section (labelled σ_f below).

In experiments, the cross section is not measured directly, but instead the number N of events that occured during a specific time frame. To calculate the cross section σ, one needs a factor that contains information about the accelerator (collimation of the beam, rotational speed, etc.): the luminosity $\mathscr{L}$. This leads to

$$\sigma = \frac{N}{\int \mathscr{L}\,\mathrm{d}t},$$

whereat $\int \mathscr{L}\,\mathrm{d}t$ is called the integrated luminosity.

Another important quantity is the decay width Γ, that allows statements about the average lifetime τ of a resonance state. For many particles, this lifetime is too short to determine it by meassuring flight distances. Due to the Heisenberg uncertainty principle, it is, however, possible to estimate τ based on the energy uncertainty that is given by the (total) width Γ. Given the resonance curve follows a Breit-Wigner distribution (compare section D in the supplementary material), Γ corresponds to the full width at half maximum (*F*WHM, ger: Halbwertsbreite), and the lifetime can be determined with

$$\tau = \frac{\hbar}{\Gamma}.$$

Looking at a specific decay channel $\mathrm{f}\bar{\mathrm{f}}$ on its own, its fraction of the decay width is called partial width Γ_f ($=\Gamma\times$ branching ratio). The sum of all partial widths has to be the total decay width.

2.2. Elementary particles and their interactions

An important goal of particle physics has always been the search for a unified concept that explains the variety of natural phenomena. It became apparent that all physical processes can be reduced to a small number of components and forces. According to the current understanding, the basic elements are elementary particles without structure. They are devided into two groups depending on their spin (fermions with half-integral and bosons with integral spin, as seen in table 2.1). The fermions, further devided into three so called generations of quarks and leptons, are the fundamental components of matter, whereat the bosons convey the fundamental forces as so called vector bosons (spin = 1) : electromagnetic, weak and strong force.

Table 2.1.: Particles of the Standard Model of elementary particle physics. (a) Fermions are differentiated in left handedIsospin-doublet and right handedIsospin-singlet[1]. (b) The four fundamental forces (gravity is listed here for the sake of completeness, but is not covered by the Standard Model) are conveyed by exchanging specific Bosons.

(a) Fermions

	Fermionmultipletts			I	I_3	Q_f	color
Leptons	$\begin{pmatrix}\nu_e\\ e\end{pmatrix}_L$	$\begin{pmatrix}\nu_\mu\\ \mu\end{pmatrix}_L$	$\begin{pmatrix}\nu_\tau\\ \tau\end{pmatrix}_L$	$1/2$	$+1/2$ $-1/2$	0 -1	—
	e_R	μ_R	τ_R	0	0	-1	—
Quarks	$\begin{pmatrix}u\\ d'\end{pmatrix}_L$	$\begin{pmatrix}c\\ s'\end{pmatrix}_L$	$\begin{pmatrix}t\\ b'\end{pmatrix}_L$	$1/2$	$+1/2$ $-1/2$	$+2/3$ $-1/3$	r, g, b
	u_R	c_R	t_R	0	0	$+2/3$	
	d_R	s_R	b_R	0	0	$-1/3$	

(b) Bosons as transmitters of interaction

Interacton	Charge	Mediator	Mass [GeV/c^2]
strong	color charge	Gluon	0
electromagnetic	electr. charge	Photon γ	0
weak	weak charge	$W^\pm$, Z^0	80 and 91
gravity	mass	Graviton	0

These interactions are described as quantum field theories that are based on local gauge symmetry, in the so called Standard Model. The strength of the interaction is given by the respective coupling constant. The fourth fundamental force, gravitation, is very weak and can be neglected in particle physics.

The theory of the electroweak interaction (Glashow, Salam and Weinberg) was spectacularly confirmed by the discovery of the massive vector bosons $W^\pm$ and Z^0 (mediators of the weak interaction) in 1983 at CERN. To describe the strong interaction between quarks, a gauge theorie called

[1] I represents the weak isospin and I_3 its third component. The weak isospin is a quantum number that corresponds to a certain symmetry of fermions: it takes into account, that the particles in a isospin doublet behave like identical particles regarding the weak force. On top of that, it is possible to describe the transitions in these doublets, that are conveyed by the weak force, using this formalism.

quantum quantum chromodynamics (QCD), was developed. This theroy describes the strong force using the exchange of eight massless vector bosons, the gluons.

The annihilation of electrons and positrons is especially effective for testing the basic statements of the Standard Model. The biggest advantage of the e^+e^- storage rings, compared to hadron storage rings, are the well-defined initial state and final states. From there, it is basically possible to calculate the cross sections for the individual channel based on known theories.

According to the Standard Model, the annihilation of electrons and positrons mainly creates pairs of leptons and antileptons and pairs of quarks and antiquarks. Quarks and emitted gluons subsequently fragment into hadrons.

2.2.1. Electroweak interaction

Quantum electrodynamics (QED) is a gauge theory and describes the interaction of charged particles through the exchange of a photon. To explain the weak interaction, a similar gauge theory was sought. The theory first introduced, using W^+ and W^- bosons, could only describe the behaviour at low energies. In search for a working gauge theory, the $SU(2)$-symmetry was chosen. This led to the introduction of three gauge bosons, W^+, W^- and W^0, and with that to the important prediction of neutral current (through the exchange of a W^0). The coupling strength of this field is determined by the „weak charge“ g (corresponding to the charge e in the electrical field), with the following relation to the fermi contant G_F (derived of the μ-lifetime):

$$G_F = \frac{\sqrt{2} \cdot g^2}{8 M_{W^\pm}^2} = 1.16637 \cdot 10^{-5}\,\mathrm{GeV}^{-2} \tag{2.1}$$

with the mass $M_W^\pm$ of the charged W-bosons.

At high energies, the coupling strength of this field is very similar to that of the electromagnetic force. This encouraged the unification of both interactions. For this reason, another symmetry $U(1)$ with a field particle Y^0 was introduced for the electromagnetic interaction. The symmetry $SU(2) \times U(1)$ affects the left handed fermion pairs (compare table 2.1).

Only in case of the charged W bosons, the gauge particles of the theory are identical to the physical state. The fastest solution would be to identify Y^0 with the photon. This would, however, correspond to a coupling of Y^0 and neutrinos, which the photon does not have. Therefore, one should assume that the photon field is a quantum mechanical mixture of the W^0 and Y^0 fields:

$$|\gamma\rangle = \cos\theta_W\,|Y^0\rangle + \sin\theta_W\,|W^0\rangle.$$

In addition, there is a second electrically neutral field, the Z^0, which is also a mixture and is orthogonal to the photon field.

$$|Z^0\rangle = -\sin\theta_W\,|Y^0\rangle + \cos\theta_W\,|W^0\rangle.$$

The mixing angle is named Weinberg angle θ_W after one of the pioneers of the so called „electroweak theory“.

In the original formulation of this theory, all gauge bosons were massless. The problem was rewriting the theory to give three of the four particles mass without destroying the other properties of the original theory. This was done using the Higgs-Kibble mechanism (symmetry breaking), that leads to the prediction of another neutral, massive particle with spin = 0, the Higgs boson.

The three parameters of the electroweak theory were measured at low centre-of-mass energies first:

- $\alpha_{\mathrm{em}} = e^2/(4\pi\varepsilon_0\hbar c)$, the electroweak fine structure constant
- G_F, the Fermi constant (based on the μ lifetime)
- $\sin^2\theta_W = e^2/g^2$, (based on comparison of neutrino reactions with $W^{\pm}$- (charged current) and Z^0-exchange (neutral current)).

All other properties can be expressed using these parameters. For example the mass of the W boson is connected to the coupling constant and the Weinberg angle θ_W in the following way:

$$M_{W^{\pm}}^2 \cdot \sin^2\theta_W = \frac{\sqrt{2}\cdot g^2}{8G_F}\cdot\sin^2\theta_W = \frac{\pi\cdot\alpha}{\sqrt{2}G_F}. \tag{2.2}$$

The masses of the vector bosons $W^{\pm}$ and Z^0 fulfill this correlation:

$$\frac{M_{W^{\pm}}}{M_{Z^0}} = \cos\theta_W. \tag{2.3}$$

The masses of the fermions and the Higgs particle are not predicted by this theory.

2.2.2. Strong interaction

Quantum chromodynamics (QCD) is the theory of the strong interaction and like QED, it is a gauge theory. Instead of the electrical charge, there is the color charge (*c*olor: red, green, bue) of the quarks as source of the fields. Therefore, each quark has one internal degree of freedom N_c , that allows it to take three different states. Force only occurs between particles with color. The quanta of the fields are again massless particles with spin = 1, the gluons. The corresponding symmetry for the strong interaction is $SU(3)$, which means there are eight different gluons.

Compared to photons, which carry no electrical charge themselves, the gluons have a complicated color charge consisting of one color and one anticolor index. That means that gluons, in contrast to photons, can interact with each other via the stron force. As a result, the strong force is rather weak at short distances (asymptotic freedom), but becomes very strong at higher distances (> some 10^{-13} cm).

Instead of the electromagnetic coupling constant α, that characterises the strength of the force, there is the QCD coupling constant α_s. Like in QED, vacuumpolarisation leads to a running coupling constant $\alpha_s(q^2)$. In contrast to QED, $\alpha_s(q^2)$ declines with a rising q^2:

$$\alpha_s(q^2) = \frac{12\pi}{(33-2N_f)\cdot\log(q^2/\Lambda^2)}. \tag{2.4}$$

Λ is the scale parameter of QCD, that has to be determined in experiments; N_f is the number of quark types, also called flavour, that are relevant for the process ($N_f = 5$ at $E_{\mathrm{cm}} \approx M_Z$) and q^2 is the squared characteristic momentum transfer. For small values of q^2, which means large distances, α_s gets big enough so that the interaction can not be described in terms of perturbation theory. At this point, one has to use phenomenological models.

One important application of QCD is the description of the hadronic final states at the e^+e^-annihilation.

The so called „fragmentation“ (see figure 2.1) starts with a quark-antiquark pair that flies apart. Due to their movement, the force between the quarks gets very strong. In the QCD field between the quarks, additional quark antiquark pairs are formed out of the high field energies. These are instantly affected by the strong force. This pocess continues until q^2 is small enough. The quarks group together and form color neutral hadrons. The particles fly approximately in the same direction of the original quarks. This leads to the formation of two bundles of particles (*J*ets)

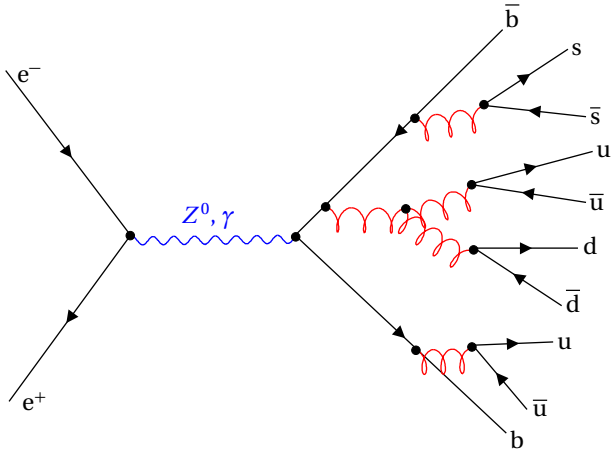

Figure 2.1.: Scematic depiction of fragmentation using the process $e^+e^- \to (Z^0, \gamma) \to b\bar{b} \to$ hadrons as example.

At hight centre of mass energies, there are increasing numbers of emissions of hard gluons, which means there are also events with more than two particle jets. This cascading transition form colored quarks into colorless (white) hadrons, also called fragmentation, can not be seen directly in experiments; only the stable particles of the final state can be measured.

2.3. Physics at energies close to the Z^0 resonance

The following processes can be seen when analysing e^+e^-interactions:

1. elastic e^+e^-scattering (Bhabha scattering).
2. annihilation of the e^+e^-pair in a virtual photon or Z^0, that subsequently turns into a fermion antifermion pair (not e^+e^-)
3. inelastic e^+e^-scattering, whereat two virtual photons (one per field of the incoming particles) can interact and produce hadrons. (This process is called „two-photon reaction (Zwei-Photon-Reaktion)“.)
4. annihilation of the e^+e^-pair in two or three real photons.

Each of these processes gets more complicated due to the fact that either the e^+, the e^- or both can emmit real photons.

The Standard Model describes the creation of fermion-antifermion pairs at e^+e^-interaction

$$e^+e^- \to (\gamma, Z^0) \to f\bar{f}$$

with the exchange of the neutral gauge bosons, the photon and the Z^0.

The electromagnetic interaction of charged fermions is induced by the electrical charge Q_f of the participating fermions. In case of the weak neutral current, each fermion has two couplings, the vector coupling g_V and the axial vector coupling g_A:

$$g_V^f = I_3^f - 2Q_f \sin^2\theta_W, \tag{2.5}$$

$$g_A^f = I_3^f. \tag{2.6}$$

(I_3^f is the third component of the weak isospin (weak charge).)

At interaction energies close to the Z^0 mass, the production of real Z^0 particle is possible and the cross section shows a resonance rise in a magnitude of $(M_Z/\Gamma_Z)^2 \approx 10^3$, as can be seen in figure 2.2, comparing a model prediction and measured data. This resonance allows for precise measurements of the properties of the Z^0 boson.

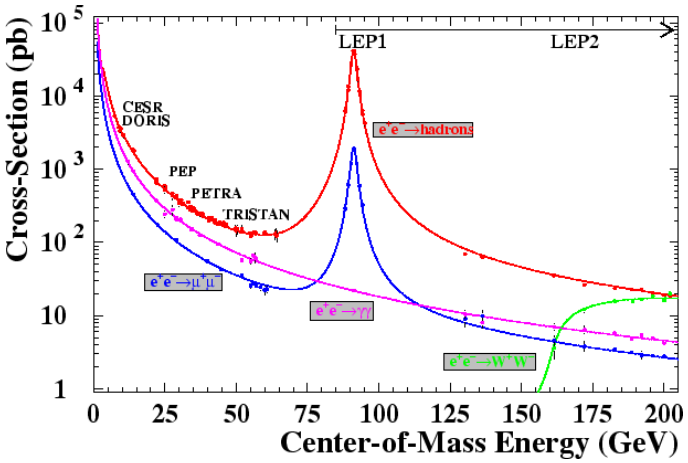

Figure 2.2.: Cross sections close to the Z^0 resonance.The continuous line represents the prediction of the Standard Model, the dots represent the data measured in different accelerator experiments.

In the end state $f\bar{f}$ the following fermion antifermion pairs show up:

Charged leptons:	e^+e^-, $\mu^+\mu^-$, $\tau^+\tau^-$,
Neutral leptons (Neutrinos):	$\nu_e\,\overline{\nu}_e$, $\nu_\mu\,\overline{\nu}_\mu$, $\nu_\tau\,\overline{\nu}_\tau$,
Quarks:	$u\bar{u}$, $d\bar{d}$, $s\bar{s}$, $c\bar{c}$, or $b\bar{b}$
	(not $t\bar{t}$, because of its high mass $M_t \approx 171.2\,\mathrm{GeV/c^2}$).

The most important parameters of the Z^0 boson are its mass and the partial decay widths of the different end states, that sum up to the total decay width of the Z^0 boson:

$$\Gamma_Z = \Gamma_e + \Gamma_\mu + \Gamma_\tau + \Gamma_{had} + N_\nu\Gamma_\nu + \Gamma_{unknown} \tag{2.7}$$

Here, Γ_ν is the decay width of the Z^0 boson in each of the N_ν different kinds of $\nu\bar{\nu}$ pairs. All occuring quark-antiquarc decay channels are merged to the hadronic decay width

$$\Gamma_{had} = \sum_{q\neq t}\Gamma_q$$

which is reasonable since the different quark channels can not be identified separately.

$\Gamma_{unknown}$ contains the decay processes that are not included in the Standard Model. So far, no such processes have been found, which means $\Gamma_{unbek.}$ is consistent with zero. Three kinds of neutrinos (ν_e, ν_μ, ν_τ) were known before the experiments at LEP were conducted. Therefore, one of the most important questions was: Are there additional generations of leptons with light neutrinos? (The answer given by the LEP experiments, which can also be retraced based on the measurements of the OPAL detector in the course of this practical, is shown in figure C.1 in the supplementary material!)

The Feynman diagrams for the process $e^+e^- \to f\bar{f}$ in the lowest order is shown in figure 2.3. The cross section, also called Born cross section in this order, consists of a pure Z^0 exchange term, a

pure γ exchange term and an interference term:

$$\sigma(e^+e^- \to f\bar{f}) = \sigma_Z + \sigma_\gamma + \sigma_{Z\gamma}. \tag{2.8}$$

Disregarding the fermions' masses one finds:

$$\begin{aligned} \sigma_Z &= \sigma_{QED} \cdot (v_e^2 + a_e^2) \cdot (v_f^2 + a_f^2) \cdot |\chi(s)|^2 \\ \sigma_\gamma &= \sigma_{QED} \cdot Q_f^2 \\ \sigma_{Z\gamma} &= \sigma_{QED} \cdot (-1) \cdot Q_f \cdot v_e \cdot v_f \cdot \mathrm{Re}(\chi(s)), \end{aligned} \tag{2.9}$$

with

$\chi(s)$	=	$\frac{s}{(s - M_{Z^0}^2) + i s \Gamma_Z / M_Z)}$	propagator,
σ_{QED}	=	$\frac{4\pi}{3} \cdot \frac{\alpha^2}{s} \cdot N_c^f$	QED cross section,
N_c^f	=	1 for leptons, 3 for quarks	color rotation,
Q_f			electrical charge in units of e,
v_f	=	$\frac{I_3^f - 2Q_f \sin^2\theta_W}{2 \sin\theta_W \cos\theta_W}$	
	=	$\frac{g_V^f}{2 \sin\theta_W \cos\theta_W}$	coupling constant (compare equation (2.5)),
a_f	=	$\frac{I_3^f}{2 \sin\theta_W \cos\theta_W}$	
	=	$\frac{g_A^f}{2 \sin\theta_W \cos\theta_W}$	coupling constant (compare equation (2.6)),
s	=	E_{cm}^2	squaredcentre of mass energy,
M_{Z^0}	=	$91.188\,\mathrm{GeV/c^2}$	mass of the Z^0 boson,
$\sin^2\theta_W$	=	0.2312	Weinberg angle.

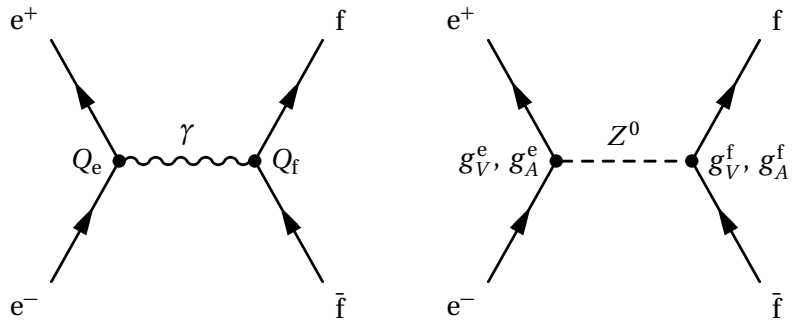

Figure 2.3.: Feynman diagrams for the process $e^+e^- \to f\bar{f}$ in the lowest order (s channel).

The cross section close to the Z^0 mass is dominated by the Z^0 exchange term, that follows the typical Breit-Wigner distribution for the exchange of spin = 1 particles (compare section D of the supplementary materials). Neglecting the other contributions, one finds, using the partial decay

width

$$\begin{aligned}\Gamma_f &= \frac{N_c^f\,\alpha(M_Z^2)}{3}\cdot M_{Z^0}\cdot\left(v_f^2+a_f^2\right)\\ &= \frac{N_c^f\cdot\sqrt{2}}{12\pi}\cdot G_F\cdot M_{Z^0}^3\cdot\left((g_V^f)^2+(g_A^f)^2\right),\end{aligned} \tag{2.10}$$

the following formula for the cross section:

$$\begin{aligned}\sigma_f &= \frac{12\pi\,\Gamma_e\,\Gamma_f}{s\,M_Z^2}\cdot|\,\chi(s)\,|^2\\ &= \frac{12\pi}{M_{Z^0}^2}\cdot\frac{s\,\Gamma_e\,\Gamma_f}{(s-M_{Z^0}^2)^2+(s^2\Gamma_Z^2/M_{Z^0}^2)}\end{aligned} \tag{2.11}$$

and for the cross section of a pair of fermions $f\bar{f}$ near the resonance peak ($s=M_{Z^0}^2$):

$$\sigma_f^{\text{peak}} = \frac{12\pi}{M_{Z^0}^2}\cdot\frac{\Gamma_e}{\Gamma_Z}\cdot\frac{\Gamma_f}{\Gamma_Z}, \tag{2.12}$$

which means that it only depends on the ratio between the partial and the total width. Γ_e represents the coupling of Z^0 and electron/positron in the initial state (following equation (2.10)), Γ_f is the coupling of Z^0 and the fermions in the final state.

Scanning the resonance curve, one finds – as indicated by the denominator of the fraction in equation (2.11) – the same width Γ_Z for each process. The maximum cross section σ_f^{peak} for the individual processes, however, is defined by the relative contribution of the decay channel (the partial decay width).

The decay width predicted by theory for the individual fermions are shown in table 2.2.

Table 2.2.: Partial decay widths for the different fermion pairs disregarding their masses.

Channel	Partial width
$\Gamma_e=\Gamma_\mu=\Gamma_\tau=\Gamma_\ell$	83.8 MeV
$\Gamma_{\nu_e}=\Gamma_{\nu_\mu}=\Gamma_{\nu_\tau}=\Gamma_\nu$	167.6 MeV
$\Gamma_u=\Gamma_c$	299 MeV
$\Gamma_d=\Gamma_s=\Gamma_b$	378 MeV

2.3.1. Bhabha scattering

The reaction $e^+e^- \to e^+e^-$, also called Bhabha scattering, has to be viewed seperately, because there are additional Feynman diagrams. Apart from the Feynman graphs of the common e^+e^-pair annihilation in fermion-antifermion pairs (s channel) shown in figure 2.3, there are pure scattering diagrams (t channel, compare figure 2.4). s and t represent the Mandelstam variables, that are explained in section A of the supplementary materials.

Only the s channel adds to the Z^0 width. The final states of s and t channel are identical, which means that one single event can not be allocated to one or the other decay channel. The statitical distribution of the scattering angle, however, is different and we will use it in this practical to determine the fraction of the s channel to suppress the background of t channel events. For this, we look at the differential cross section $\frac{d\sigma}{d\Omega}$, that does not depend on the angle ϕ (centered around the beam axis), but on the angle θ (between the incoming and outgoing electrons). The following applies:

$$\frac{d\sigma}{d\Omega} \propto \begin{cases} \left(1+\cos^2\theta\right) & s \text{ channel}, \\ (1-\cos\theta)^{-2} & t \text{ channel}. \end{cases} \tag{2.13}$$

At high scattering angles θ, the s channel is dominant, at small θ, however, the t channel.

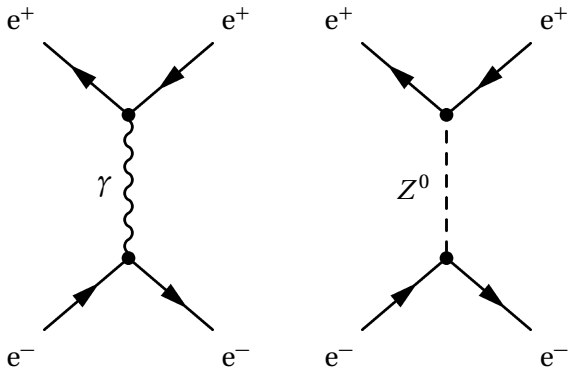

Figure 2.4.: t channel contribution to the reaction $e^+e^- \to e^+e^-$.

2.4. Overview: Extraction of the parameters of Z^0

In this section, we want to summarise, which properties of the Z^0 boson and its interactions we can extract from the measurements, and how to do that:

- Fitting a Breit-Wigner courve to the cross section σ_f as a function of the centre of mass energy E_{cm} close to the Z peak gives us
  - the mass M_{Z^0} of the Z^0 boson,
  - the total decay width Γ_Z, and
  - the peak cross section σ_f^{peak}.
- The fraction of the cross sections σ_f of different decay channels gives us
  - the partial decay widths Γ_ℓ and Γ_{had}, as well as
  - the relative strength of the coupling of Z^0 and the particular $f\bar{f}$ final states.

One defines the relations

$$R_{\mathrm{e}}^0 \equiv \frac{\Gamma_{\mathrm{had}}}{\Gamma_{\mathrm{e}}}, \quad R_{\mu}^0 \equiv \frac{\Gamma_{\mathrm{had}}}{\Gamma_{\mu}}, \quad R_{\tau}^0 \equiv \frac{\Gamma_{\mathrm{had}}}{\Gamma_{\tau}},$$

that merge, assuming *l*epton universality, to a single parameter[2]

$$R_{\ell}^0 \equiv \frac{\Gamma_{\mathrm{had}}}{\Gamma_{\ell}}. \tag{2.14}$$

- The relation between the partial width Γ_f and the Weinberg angle θ_W

$$\Gamma_f = N_c^f \frac{\sqrt{2}}{12\pi} G_F M_{Z^0}^3 \cdot \left[1 + \left(1 - 4|Q_f| \sin^2 \theta_W\right)\right] \tag{2.15}$$

as per equation (2.5), (2.6) and (2.10) (with $\left(I_3^f\right)^2 = \frac{1}{4}$) allows for the identification of the relation between the coupling strength of the weak and electromagnetic interactions ($\sin^2 \theta_W = e^2/g^2$).

- Comparing the measured invisible decay width Γ_{inv}, or rather the ratio R_{inv}^0 with the predictions of the Standard Model for this ratio

$$R_{\mathrm{inv}}^0 = N_{\nu} \left(\frac{\Gamma_{\nu}}{\Gamma_{\ell}}\right)_{\mathrm{SM}} \tag{2.16}$$

one can determine the number N_{ν} of light neutrino generations (assuming $N_{\nu}\Gamma_{\nu} = \Gamma_{\mathrm{inv}}$, which means no further contributions).

[2]Here, Γ_{ℓ} is the partial width of the decay of Z^0 in a *m*assless charged lepton. Since the mass of the τ lepton $M_{\tau} = 1777\,\mathrm{MeV/c^2}$ can not be neglected, one finds that, even when assuming similar coupling strength because of lepton universality, $\Gamma_{\tau}^{\mathrm{mess}}$ is reduced by approximately 0.23% compared to Γ_{ℓ}.

2.5. Units, formulas and relations

Often, in particle physics, a set of units is chosen where $c = 1$ and $\hbar = 1$. Correspondingly, masses and particle momentum are also expressed in units of energy (MeV, GeV,...).

For explicit calculations, however, the correct values of c and $\hbar$ have to be used to find the correct values of the desired variables!

What follows, is an overview of the physical dimensions of different parameters with and without $c = 1$ and $\hbar = 1$:

Parameter	**D**imension		**T**ranslation		
	$c = 1, \hbar = 1$	normaly			
Mass	GeV	$\mathrm{GeV/c^2}$	1 kg	=	$5.61 \times 10^{26}\,\mathrm{GeV}$
Length	GeV^{-1}	$(\hbar c)/\mathrm{GeV}$	1 m	=	$5.07 \times 10^{15}\,\mathrm{GeV}^{-1}$
Time	GeV^{-1}	$\hbar/\mathrm{GeV}$	1 s	=	$1.52 \times 10^{24}\,\mathrm{GeV}^{-1}$
Current	GeV	$\sqrt{c/\hbar}\cdot\mathrm{GeV}$	1A	=	$1.24 \times 10^{-6}\,\mathrm{GeV}$
Cross section	GeV^{-2}	$(\hbar c/\mathrm{GeV})^2$	1 b	=	$2.57 \times 10^{3}\,\mathrm{GeV}^{-2}$

Units			
1 fm	=	10^{-15} m	Unit of length („1 fermi“)
1 GeV	=	$1.602\,176\,487(40) \times 10^{-10}$ J	Unit of energy
1 b	=	$10^{-24}\,\mathrm{cm^2} = 10^{-28}\,\mathrm{m^2}$	Cross section „Barn“
1 nb	=	$10^{-9}\,\mathrm{b} = 10^{-33}\,\mathrm{cm^2}$	

Constants (according to [PDG08])			
c	=	299 792 458 m/s	Speed of light
e	=	$1.602\,176\,487(40) \times 10^{-19}$ C	Elementary electric charge
$\hbar$	=	$6.582\,118\,99(60) \times 10^{-22}\,\mathrm{MeV \cdot s}$	Planck constant/2π
$\hbar c$	=	$0.1973\,\mathrm{GeV \cdot fm} = 197.3\,\mathrm{eV \cdot nm}$	
M_{Z^0}	=	$91.1876(21)\,\mathrm{GeV/c^2}$	Z^0 mass
G_F	=	$1.166\,37(1) \times 10^{-5}\,\mathrm{GeV}^{-2}$	Fermi coupling constant
m_e	=	$0.510\,998\,910(13)\,\mathrm{MeV/c^2}$	Electron mass
m_p	=	$938.272\,031(23)\,\mathrm{MeV/c^2}$	Proton mass

Formulas and Parameters			
electromagnetic coupling constant at an energy of 91.2 GeV	$\alpha(M_{Z^0}^2)$	=	$\dfrac{1}{128.87}$
strong coupling constant at an energy of 91.2 GeV	$\alpha_s(M_{Z^0}^2)$	=	0.12
third component of the weak isospin	I_3^f	=	$\begin{cases} +1/2 & \text{for } f = \nu,\ \mathrm{u},\ \mathrm{c} \\ -1/2 & \text{for } f = \mathrm{e}^-,\ \mu^-,\ \tau^- \\ & \text{as well as for } \mathrm{d}', \mathrm{s}', \mathrm{b}' \end{cases}$
weak vector coupling constant	g_V^f	=	$I_3^f - 2Q_f \sin^2\theta_W$
weak axial vector couping constant	g_A^f	=	I_3^f
propagator of the Z^0 boson	$\chi(s)$	=	$\dfrac{s}{(s-M_{Z^0}^2)+is\dfrac{\Gamma_{Z^0}}{M_{Z^0}}}$
cross section for $\mathrm{e}^+\mathrm{e}^- \to \mathrm{f}\bar{\mathrm{f}}$	$\sigma_f(s)$	=	$\dfrac{12\pi}{M_{Z^0}^2}\dfrac{s\Gamma_\mathrm{e}\Gamma_f}{\left(s-M_{Z^0}^2\right)^2+\left(s\dfrac{\Gamma_{Z^0}}{M_{Z^0}}\right)^2}$
partial decay width for $\mathrm{e}^+\mathrm{e}^- \to \mathrm{f}\bar{\mathrm{f}}$	Γ_f	=	$\dfrac{N_c^f\sqrt{2}}{12\pi} G_F M_{Z^0}^3 \left((g_V^f)^2+(g_A^f)^2\right)$
color rotation of the fermion f	N_c^f	=	$\begin{cases} 1 & \text{for leptons} \\ 3 & \text{for quarks} \end{cases}$

3. Particle detection and classification with the OPAL detector

In this chapter, the individual components of the OPAL detector and their function are introduced shortly, and, building on this, the methods of particle identification in this experiment are explained.

3.1. The OPAL detector at the LEP accellerator

The LEP storage ring (*L*arge Electron Positron Collider) was operating between 1989 and 2000 at the european laboratory for core and particle physics CERN[1] (Genf). It generated a huge ammount of measured data, that allowed for especially precise studies of the physics of electron positron collisions at high energies. Most of you might know the 27 km long LEP tunnel, that, since the deconstruction of LEP, contains the *L*arge Hadron Collider (LHC) today, from the media (and probably also from the lectures on particle physics).

In the first operating stage (LEP-I, 1989 to 1995), the maximum centre of mass energy was $E_{\mathrm{cm}} = \sqrt{s} \approx 110\,\mathrm{GeV}$ – just enough to produce Z^0 bosons with a mass of $\approx 91\,\mathrm{GeV/c^2}$ with the reaction $\mathrm{e^+e^-} \rightarrow Z^0$. With this, Z^0 bosons could be generated with good statistics for the first time[2] and their properties could be measured with an accuracy not reached before (compare figure C.2). The data used for this practical are from this measurement phase.

For the second operating stage (LEP-II, 1996 to 2000), the accelerator was upgraded to a maximum centre of mass energy of $E_{\mathrm{cm}} = \sqrt{s} \approx 200\,\mathrm{GeV}$, which allowed for an increased production of $W^{\pm}$ pairs ($M_W \approx 80\,\mathrm{GeV/c^2}$) in the reaction $\mathrm{e^+e^-} \rightarrow W^+W^-$.[3]

Detector components

Like most experiments in high energy physics, the OPAL detector is built in onion-like layers of subdetectors, that are optimised to work together to reconstruct the interactions that occur in the centre at the collision point. The following main components make up the detector, starting in the middle (compare figure 3.1):

- The *c*entral tracker is there to measure the trajectory and momentum of charged particles in a magnetic field.
- The electromagnetic calorimeter (ECAL) measures the energy of electrons, positrons and photons.
- With the hadronic calorimeter (HCAL), the energy of hadrons is determined.

[1] `http://www.cern.ch`

[2] In total, approximately 18 million Z^0 events were measured during LEP-I. This gave the accelerator the nickname „Z^0 factory“.

[3] Approximately 80000 $W^{\pm}$ events were registered during LEP-II

- In the muon chambers, muons are identified and their momentum is measured.

A detailed description of the OPAL detector can be found in the supplementary material, section B.2.4.

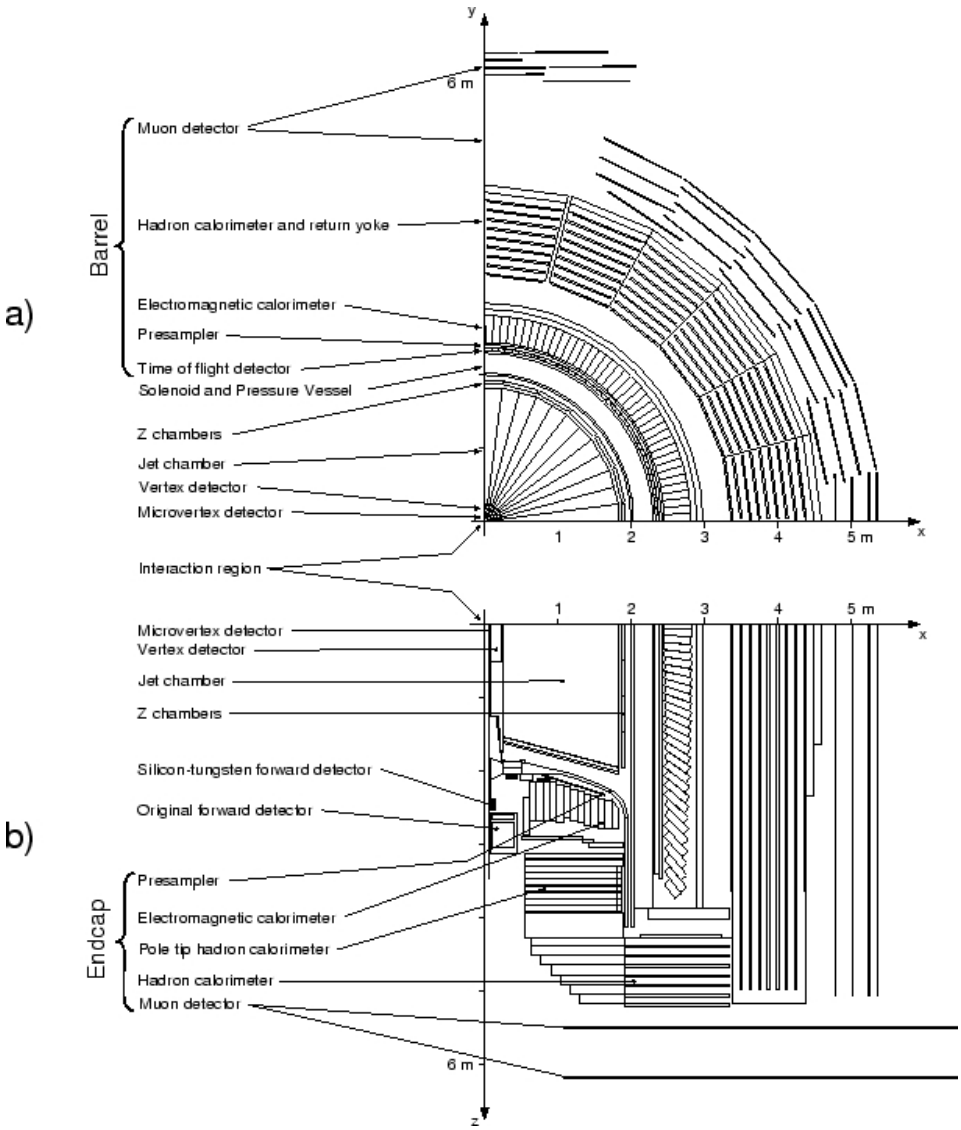

Figure 3.1.: Sectional view of the OPAL detector. (a) transverse section (x-y plane), (b) longitudinal section (x-z plane). The coordinate system has been defined as follows: the origin is at the nominal e^+e^-collision point, the x axis is horizontal and points to the centre of LEP, the y axis is vertical and the z axis points in the direction of the electron beam. The polar angle Θ is measured from the z axis and the azimuth angle φ from the x axis around the z axis to the y axis.

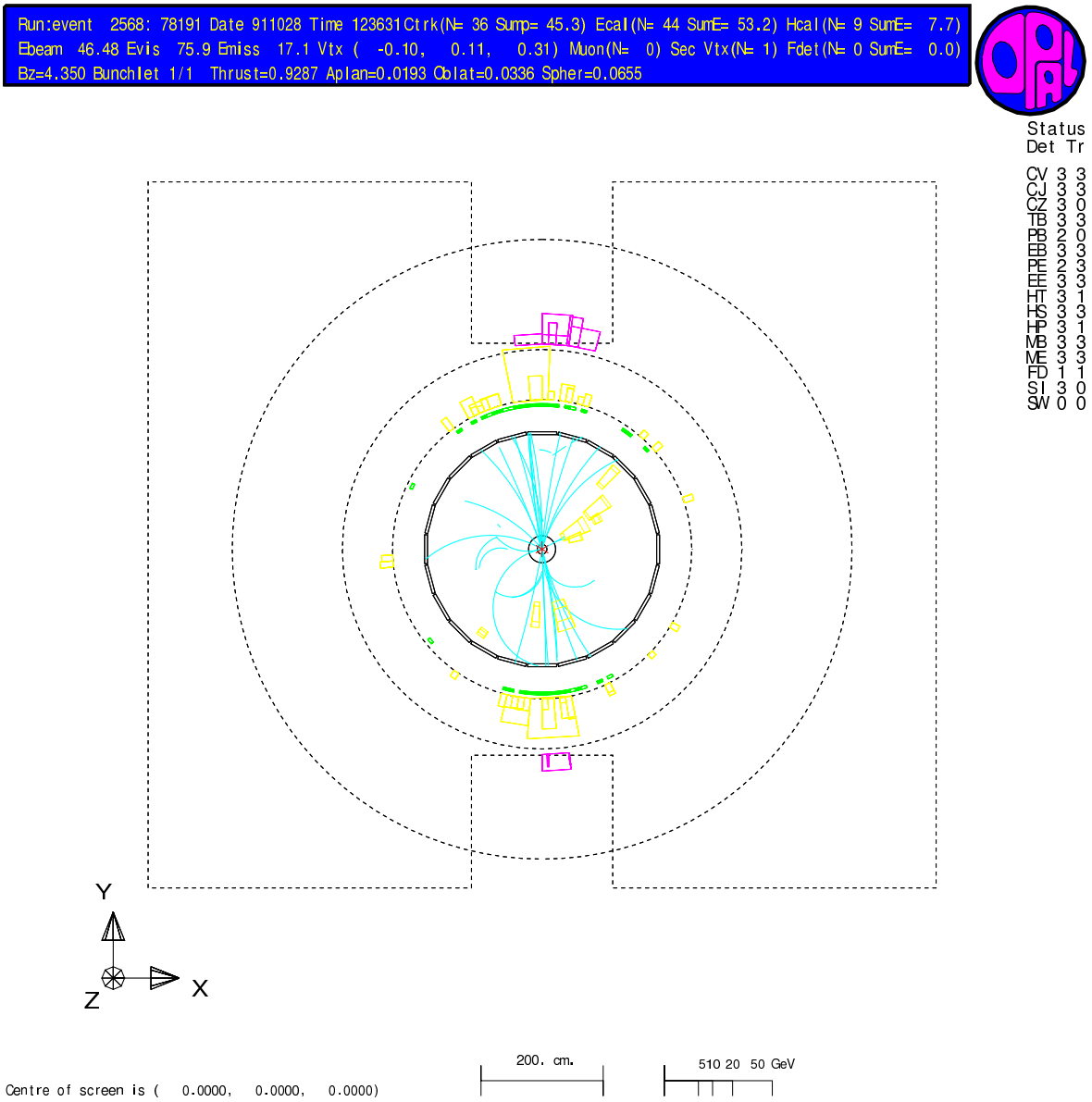

Figure 3.2.: OPAL eventdisplay „Grope“: cross sectional view of the most important detector components with the depiction of an event of the hadronic decay channel. The headline contains information like the run number, event number, date and measurement time and gives the most important measurands. Scales for length and energy input are given at the bottom, the right column gives an overview of the tigger status of the subdetectors.

3.2. Particle identification with the OPAL detector

In figure 3.2 and table 3.1, you can see which information the OPAL eventdisplay gives for each recorded event. Figure 3.3 shows schematically, how (and if) different kinds of particles are „seen“ by the individual subdetectors of OPAL.

How can this information – not only the values of the measurands, but also the topology of the traces left by the event – be used to reconstruct the decay channel? First, we look at charged and neutral particles seperately.

Table 3.1.: Detector components and their depiction in the graphical display of Grope (compare figure 3.2 and 3.3).

Detector component	**k**ind of particle and detection mechanism	**D**epiction in Grope
Vertex detector	charged (ionization)	line
Jet and Z chamber	charged (ionization)	line
TOF	charged (ionization)	rectangle at the piercing point
ECAL	electromagnetic cascade (bremsstrahlung; pair production)	trapezium: length $\propto$ deposited energy
HCAL	hadronic cascade (decay and nuclear reactions)	trapezium: length $\propto$ deposited energy
Muon chambers	charged	arrow in the flight direction of the muon

Charged Particles

In general, charged particles can be recognized by the signal they induce in the tracking detectors, while neutral particles are „invisible“ there.

Charged hadrons and electrons (and positrons respectively) can be distinguished by the shape and the starting point of the cascade in the electromagnetic calorimeter. The electromagnetic cascade of a e^+/e^- is contained entirely in the ECAL and has only a small lateral range. Hadronic cascades usually start later, are wider and expand into the HCAL. The core area of the energy deposition is in the HCAL most of the time. The differences between electromagnetic and hadronic cascades become smaller with lower particle energy, which means that charged hadrons and e^+/e^- below an energy of about 2 GeV can not be separated based on the cascade development. At low energies, it is however possible to identify the particles based on the specific energy loss $\mathrm{d}E/\mathrm{d}x$ in the jet chamber.

Muons don't induce a cascade while crossing the calorimeters and as minimal ionizing particles (because of $m_\mu \gg m_e$, compare Bethe-Bloch formula), they also loose little energy by means of inonization. Their trademark is, that they pass through thick layers of matter (compare figure 3.3) and leave a signal in the muon chambers all the way on the outside of the detector.

Neutral particles

Neutral particles are identified mainly based on the different cascade profiles. Neutral particles that decay or convert into charged particles in the tracking chambers show two traces in a typical V shape. The tip of the V, the decay or converson point of the neutral particle is outside of the primary vertex in this case.

The π^0 basically decays „instantly“ (after a mean lifetime of $\tau_{\pi^0} \approx 8 \cdot 10^{-17}$ s) to two photons, the opening angle of which depends on the energy of the π^0. With rising energy, the photons get closer due to the „Lorentz boost“ and can eventually not be distinguished from a single

photon that does not originate from a π^0 decay. Therefore, photons are identified by their electromagnetic cascade, neutral pions by two cascades close to each other. In both cases, no trace pointing to the cascade may be found.

Before entering the ECAL, photons can be converted into an e^+e^- pair in matter. Since basically all the matter (or the whole radiation length to be precise) is concentrated in the walls of the central detector and the solenoid, there is a high probability that the conversion takes place there. A converted photon can be identified by two charged traces in V hape and two electromagnetic cascades. Traces and cascades have to belong to each other without doubt.

Neutral hadrons with big flight length (e.g. K_L^0) can be identified by a hadronic cascade without a trace pointing at it. In figure 3.3, the decay of a K_S^0 in two charged pions is shown as an example for the signature of a short-lived neutral hadron.

What follows is a listing of the most important properties and recognition features of the individual reaction channels (invisible, leptonic, hadronic).

$e^+e^- \to \nu_x \overline{\nu}_x$

- Products of the decay (neutrinos) can not be detected in general: „invisible decay modes“.
- In case a bremsstrahlung photon was emitted at the beginning ($Z^0 \to \gamma\, \nu_x\, \overline{\nu}_x$), the decay mode is still detectable.

$e^+e^- \to e^+e^-$

- Two opposingly charged, almost collinear traces with total momentum (Ctrk(SumP)) approximately twice the beam momentum.
- Energy deposition in the ECAL also corresponds to twice the beam energy.
- In the lowest order, three Feynman graphs participate (compare figure 2.3 and 2.4 on the left). In the s channel close to the Z^0 resonance, the exchange of photons and the $\gamma\, Z^0$ interference term are suppressed by two to three orders of magnitude compared to the pure Z^0 exchange. More important, however, is the photon exchange in the t channel, that has a big cross section at small scattering angles and has to be reduced using suitable angle cuts when analysing Z^0 decay.

$e^+e^- \to \mu^+\mu^-$

- Differs from e^+e^- due to the fact, that the muons pass through both calorimeters basically without deposing any energy and give off additional signals in the muon chambers.
- Traces in the muon chambers have to be linked non-ambiguously to the traces in the central detector (remember the magnetic field when extrapolating the trace in the central detector).

$e^+e^- \to \tau^+\tau^-$

- The τ is a short-lived particle (mean lifetime $2.9 \cdot 10^{-13}$ s) and can only be verified by it's decay products. There are several possible decay channels, the most important ones are listed in table 3.2. Depending on the number n of charged traces, they are called „n-prong events“, the branching ratio of which decreases with increasing multiplicity (1-prong approx. 85%, 3-prong approx. 15%, 5-prong approx. 0.11%).
- To differentiate the $\tau^+\tau^-$ channels from the hadronic channels, one demands a small charged multiplicity, which in turn makes it harder to differentiate them from other leptonic events.
- An additional look at the energy (E_Ecal, Ctrk(SumP)) can help at this point, since a huge portion

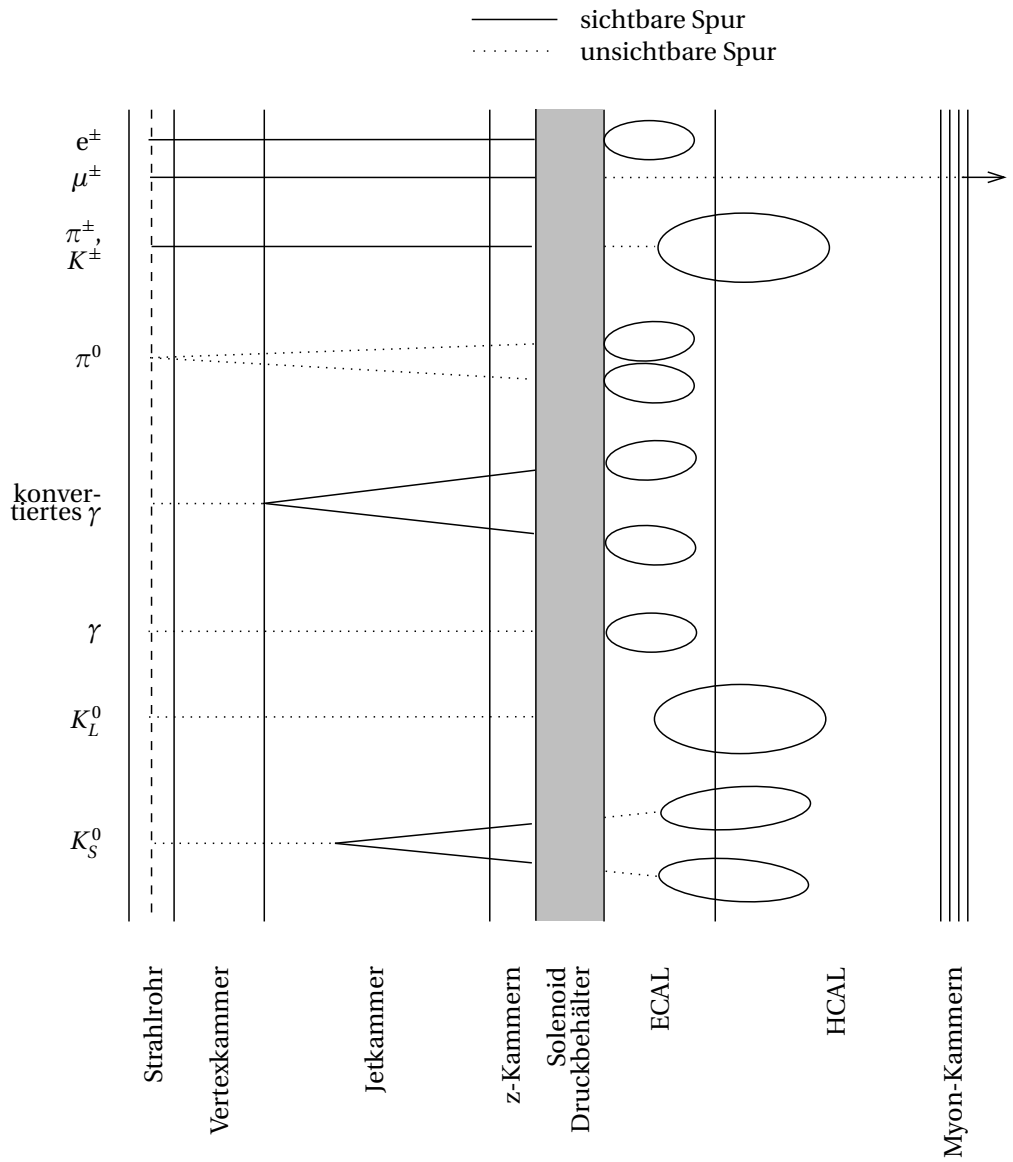

Figure 3.3.: Particle identification in OPAL based on the response behaviour of the subdetectors (Schematic drawing not true to scale). It is always possible to differentiate between charged and neutral particles: the former will be registered in the tracking detectors (solid lines), while the latter do not leave traces there (suggested by dotted lines). Electromagnetic and hadronic cascades are schematically indicated by „bubbles“ in the calorimeters. The grey area represents the parts that are not covered by detectors because of the magnet (solenoid) and pressure tank.

of energy ca nnot be detected because of the neutrinos that are emmitted at the τ decay.

$e^+e^- \to q\bar{q}$

- This is clearly the dominant decay channel with a branching ratio of $\frac{\Gamma_{had}}{\Gamma_{Z^0}} \approx 70\%$.
- Characteristic features are the huge number of charged traces (on average approx. 20) and the high values for the energy measured in both calorimeters.
- The charged hadrons form two or more bundles of particles (jets). During this process of fragmentation, neutral hadrons are formed as well (primarely π^0).
- Differentiating the different $q\bar{q}$ decay channels by the flavours is difficult and would demand too much for this practical.
- Two photon events (compare figure 3.4) with a $q\bar{q}$ pair as final state are background noise in principle, but the detected energy for these events is small in most cases, so they can be eliminated by a suitable energy cut. (Electrons and positrons are not visible normally, because they are scattered at small angles and stay in the beam tube or end up in the forward detector respectively.)

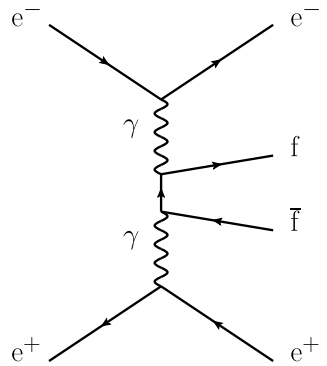

Figure 3.4.: Feynman diagram: two photon reaction.

Table 3.2.: Most important decay channels for the τ lepton (analogue for τ^+) [PDG08].

decay channel	branching ratio [%]	type
$\pi^-\pi^0\nu_\tau$	25.52 ± 0.10	1-prong
$e^-\bar{\nu}_e\nu_\tau$	17.85 ± 0.05	1-prong
$\mu^-\bar{\nu}_\mu\nu_\tau$	17.36 ± 0.05	1-prong
$\pi^-\nu_\tau$	10.91 ± 0.07	1-prong
$\pi^-\pi^-\pi^+\nu_\tau$	9.32 ± 0.07	3-prong
$\pi^-\pi^-\pi^+\pi^0\nu_\tau$	4.61 ± 0.06	3-prong
$\pi^-\pi^0\pi^0\pi^0\nu_\tau$	1.04 ± 0.07	1-prong

3.3. Cuts to separate the event classes

For the analysis in this practical, it is not as important to differentiate a K^0 from a π^0 as it is to differentiate electrons and muons from hadrons. On top of that, in the second and third part of the practical, we will look at so many events at once, that it is not feasible to take all details like

cascade shape or special geometry into account. Because of this these have to be merged to global variables.

The way these measurands are used is discussed in the following section.

As an example, the separation of $Z^0 \rightarrow e^+e^-$ events and $Z^0 \rightarrow \mu^+\mu^-$ events can be used. Both events differ little in the variables Ctrk(SumP) and Ctrk(N). Small differences are caused by the higher probabilityof emitting bremsstrahlung for $e^+e^- \rightarrow e^+e^-$ events. Bigger differences however can be seen in the total energy in the ECAL. For $e^+e^- \rightarrow e^+e^-$ events, the centre of mass energy should be measured on average. For the two muons in $e^+e^- \rightarrow \mu^+\mu^-$ events it is expected to see only a small energy deposition of ≈ 2 GeV in the ECAL. In $e^+e^- \rightarrow e^+e^-$ events, no energy is measured in the HCAL. The muons of the $e^+e^- \rightarrow \mu^+\mu^-$ events pass throught the ECAL and HCAL and deposit an energy of ≈ 5 GeV in the HCAL on average. Separation of the $e^+e^- \rightarrow e^+e^-$ events and $e^+e^- \rightarrow \mu^+\mu^-$ events can be done by a so called cut on the measurand E_ECAL. One demands that E_ECAL is bigger than a certain value that is to be determined by the experimenter (≡ participant of the practical).

Acceptance and background

The goal is to choose the cut on a suitable measurand or simultaneous cuts on multiple measurands in a way that an the partion of the „desired“ events that conform to the cut criteria is big as possible while the partion of the „undesired“ background events is as small as possible. The acceptance of one or more cuts is the quotient of the number of events in one chosen class that pass the criteria and the total number of events in that class. The reachable acceptance and background suppression depend on both the mean value and the width of the distributions. To illustrate this, figure 3.5 shows two hypothetical examples.

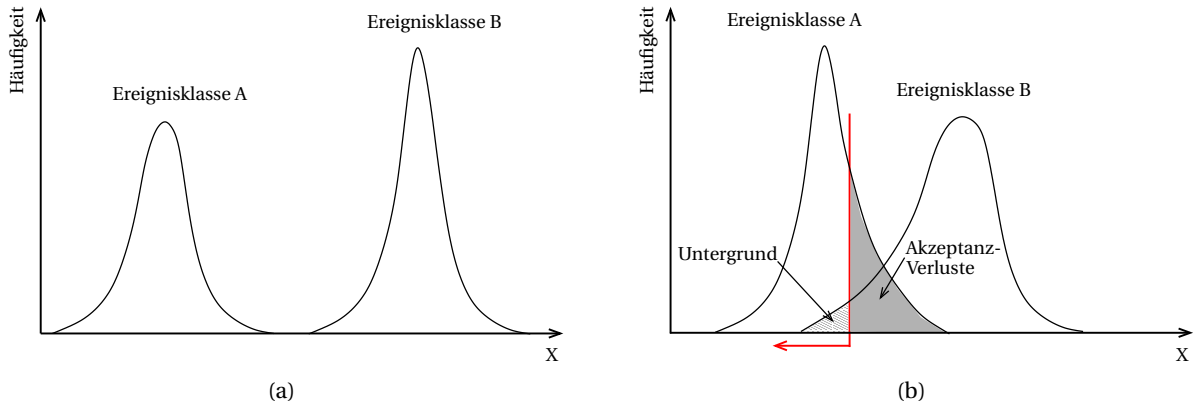

Figure 3.5.: Examples for the differentiation of events by the useage of cuts.

In the first example (figure 3.5(a)), the event classes A and B are completely separated when looking at variable X. An acceptance of 100% and a complete background suppression of the undesired event class is possible with a cut on variable X. This is the ideal case. The usual case is shown in the second example (figure 3.5(b)). With the choice of the cut, one determines the acceptance and the admixture of background. If it is important to have a highly pure amount of event class A, the cut has to be chosen small. If one wants to keep preferably all events of class A, the cut has to be chosen at a big value of X.

To separate an event class from the whole data, it is usually not sufficient to set cuts on only one measurand; multiple cuts on different measuands are required. Furthermore, cuts can be used

on composite measurands. If one demands $X^2 + Y^2 < \xi$ for example, one separates a circular area with the radius $\sqrt{\xi}$ in the two dimensional space X-Y. The goal of the cutting procedure is to determine the best variables and optimize the cut criteria to obtain a preferably pure portion of events.

In the practical, the cuts have to be determined manually, but it is also possible to use a mathematical optimisation procedure (Fisher's linear discriminant, neural network). When using these procedures, it is harder to determine systematic errors.

Event simulation (Monte-Carlo)

When using cuts, it is usually inevitable that one looses events of the relevant class while a portion of unwanted background events remains, as shown in figure 3.5. To calculate cross sections (which is also part of the practical), apart from the integrated luminosity, the „exact" number of events N in each class is needed. After the cuts, a number of registered events N_{obs} remains, that has to be corrected. Correcting N_{obs} based on data is not possible in the example shown in figure 3.5(b), as it is not possible to measure the variable X for the event classes A and B separately, but only their sum, in the experiment.

One possibility to determine the acceptance loss due to cuts are event simulations with computer programmes. For that, an as-large-as-possible number of events of a certain class is generated in the following way: First, the outbound fermion-antifermion pairs of a e^+e^-annihilation are generated. Then, the process of hadronisation for hadron-antihadron pairs is simmulated, followed by the decay of instable particles. In a last, complex step, all detector signals induced by the fictive particles are simulated, ensuring that the information is available in the same way as „real" events. Simulated and detected events can now be examined using the same analysis programs. For this event simulation, all available theoretical and experimental knowledge is used. The simulated data contains additional information about the particles that are involved on top of the information available in real data. This allows for testing the detector and it is reaction to specific events.

Simulating the event classes A and B in our example, the distributions for the variable X can be determined separately. Using the same cuts, that were used on the real data, one easily finds the value of the acceptance. In the same way, one can calculate the background. To do so, a relative standardisation between the distribution of the classes A and B is required. This can for example be done by matching the data with the combined distributions. The restult of the matching is the relative ratio of events of class A to class B.

When using Monte-Carlos, it is important to remember that a great deal of presumptions about the examined process are put into their generation. Therefore, it is important that the results are not correlated with the Monte-Carlos too much, because otherwise one will only find these presumptions as a result. This can lead to systematic errors, the evaluation of which is too complicated for you (not having the information about the generation of the Monte-Carlos) and exceeds the course of this practical.

4. Execution of the experiment

Practical parts

The experiment is divided into three main parts:

I. In the first part, characteristic properties of certain decay channels (e^+e^-, $\mu^+\mu^-$, $\tau^+\tau^-$, $q\overline{q}$) are studied based on preselected training datasets. For this, the measurements of individual events (20 per dataset) are shown in the OPAL event display Grope. The goal of this part is to find classification criteria regarding the available measurables that can be used to differentiate the four decay channels.

   To check your understanding and further train the particle identification, the criteria will be applied to mixed control datasets.

II. In the second part, the rough criteria found in part I are further examined using Monte-Carlo datasets (MC) with high statistics (approx. 100 000 events per dataset) and refined into identification cuts. Since the MC datasets consist of events of one type, it is possible to determine the cut efficiency and remaining background, which is needed for part III.

III. Now, the preparations are over and we can finally examine measured datasets (again > 100 000 events each) of the OPAL detector! With this data, different questions related to the physics of the Z^0 resonance can be examined. You can choose from several analysis tasks („experiments“). Only experiment E1 is mandatory, since it is the central challenge of the practical – the determination of the mass and lifetime of the Z^0 bosons. Please work on at least one additional experiment apart from E1.

4.1. Computational setup

The scripts and data needed are stored in `github` repository. The first step is to access this data and create a branch for your group, where you can freely edit the scripts just for yourself and later upload your results for the tutors to check.

First, go to the directory where everything will be done,

```
cd ~/Z0/ecap-fau-z0experiment
```

Activate the python environment with

```
conda activate z0-fp
```

Check the current branches with

```
git branch
```

If not in the main, please first move back to the main with

```
git checkout main
```

(There could be error messages if the previous group didn't save all their modifications, if so, run (`git stash`) and then rerun the command above.

Pull the repository. This makes sure that any further change made in the main repository (by the tutors for example), is up-to-date:

```
git pull
```

Finally, create your branch:

```
git checkout -b <groupnumber>
```

Whenever you want to save modifications (**AND FOR SURE BY THE END OF THE EXPERIMENT**), do

```
git add <file>
```

for every file that was modified, followed by

```
git push -u origin <groupnumber>
```

Don't forget to save your modifications, the next group may delete them if you don't (and it will not be their fault!).

Once the previous step is ready, open the jupyter notebook `MainNotebook.ipynb`. All the following steps can be performed in this notebook.

4.2. Classification of single events with Grope

The program Grope (Graphic Reconstruction of OPAL Events) was used back then for graphical analysis of events detected with OPAL. For this purpose, the information detected in the individual subdetectors and the geometry of the detector components are shown schematically; in addition, several measurands are given at the top of the image. At this point, it is too complicated and counter-productive to keep an installation on GROPE, given that it needs very old versions of Linux and several codes and libraries. For that reason, the screenshots of the corresponding were saved and will be used in this experiment.

1. First, you should practice the handling of the Grope screenshots and get familiar with the different information levels and sources of the event display. What indicator represents which detector information?
2. Discuss each event of the preselected training datasets (`ee`, `mm`, `tt`, `qq`) and note potential striking features.
3. Think of appropriate cut criteria to separate the decay modes based on the histograms. This rough classification should help you in the second part (section 4.3) as a basis for more refined cut criteria.

4. Now, look at the mixed testing dataset and identify the final states of the 20 events. Use this opportunity to verify and improve the identification criteria you found with the „pure“ datasets.
5. Sum up your experience with the training datasets and the testing dataset by putting down substantial separation criteria in the form of a matrix (compare table 4.1).

Table 4.1.: Separation of the different decay channels based on suitable parameters. Note the primary separation argument (either Ctrk(N), Ctrk(Sump), Ecal(SumE), Hcal(SumE) or a different criterion that you think is reasonable) as non-diagonal elements of the Matrix.

	$Z^0 \to e^+e^-$	$Z^0 \to \mu^+\mu^-$	$Z^0 \to \tau^+\tau^-$	$Z^0 \to q\overline{q}$
$Z^0 \to e^+e^-$	—			
$Z^0 \to \mu^+\mu^-$		—		
$Z^0 \to \tau^+\tau^-$			—	
$Z^0 \to q\overline{q}$				—

4.3. Determination of cut criteria based on MC datasets

(a) Familiarise yourselves with the Uproot commands on the notebook.

Table 4.2 sums up the parameters that are present in the Monte Carlo and OPAL data Ntuples. These are essentially parameters you already know from working with Grope, but some are named differently.

Table 4.2.: Parameters for event cuts in the high statistics Ntuples. Apart from the measurands given in this table, each event is assigned a run number and an event number, that is, however, not relevant for the statistical evaluation.

`run`	name for a continuous period of measurements
`event`	unique identification of an event in one period of measurements
`Ncharged`	„charged multiplicity“: number of charged traces in the central detector
`Pcharged`	„charged energy“: scalar sum of the measured momenta in the vertex/jet/Z chambers of all charged traces
`E_ecal`	total energy measured in the ECAL
`E_hcal`	total energy measured in the HCAL
`E_lep`	beam energy, read half the centre of mass energy
`cos_thet`	cosine of the polar angle θ between inbound e^+ and outbound positively charged fermions (only reasonable in decays with one destinct positive and negative trace each, meaning only $Z^0 \to e^+e^-$ and $Z^0 \to \mu^+\mu^-$)
`cos_thru`	cosine of the polar angle ϑ between thrust* and beam axis
*thrust	$\vec{n}(\vartheta,\varphi)$ defines an arbitrary axis through the vertex of an event, and $\max_\vartheta \left(\frac{\sum_{i=1}^{\text{Ncharged}} \vec{p}_i \cdot \vec{n}(\vartheta,\varphi)}{\sum_{i=1}^{\text{Ncharged}} \lvert\vec{p}_i\rvert} \right)$ is a measure for the diversification of the charged traces. The axis $\vec{n}(\vartheta,\varphi)$, that contains the maximum, is called thrust axis. It is usually consistent to the axis the primary fermion-antifermion pair flew apart on.

(b) Create histograms of the characteristic properties of the different MC datasets.

Think of a plan before you continue with the experiment. How can the cut criteria be optimized? Which information and distributions will be required to solve the following tasks?

(c) How can contributions from s and t channel be separated for e^+e^-events? Why is this important?

Compare the angular distribution of all channels for the OPAL data and the MC data, too. Of what significance is the result for the $\tau^+\tau^-$channel?

How do you have to change the cuts for the e^+e^- and $\tau^+\tau^-$ channel and what do these changes mean for the further analysis of these two and the other channels?

At the end of this part of the practical, you have decided on your final cut criteria. Discuss them with the advisor before continuing with the next part.

(d) Determine the probability of detection and the background contribution of the separate channels using the cuts derived in part (c) on the simulated events of the MC datasets.

Examples:

- By using the `ee` cuts on the `ee` MC datasets, the acceptance of the `ee` cuts can be determined (how many „good“ e^+e^- events are lost because of the cuts?).
- By using the `ee` cuts on the `tt` MC datasets, the remaining $\tau^+\tau^-$ background, that is not removed from the e^+e^- channel by the cuts, can be determined.

Present your results in a background acceptance matrix (= efficiency matrix) and think about the corrections that have to be applied to the rates when analysing the real OPAL data in part III.

How are statistical errors taken into account in this case?

4.4. Statistical analysis of measured data

4.4.1. Realisation of different experiments with the Z^0 decay

Experiment E1: Determination of decay parameters of the Z^0 boson

(a) Determine the number of events in the hadronic and leptonic channels for each of the seven centre of mass energies. Subtract the background and use the corrections to take the acceptance of your cuts into account.

Then calculate the partial cross sections σ_f for the hadronic and leptonic events. Remember that measurement results without uncertainty (error) hold no value.

(b) Determine the mass M_{Z^0} of the Z^0 boson, its decay width Γ_{Z^0} and the peak cross section of the three leptonic and the hadronic channels based on the partial cross sections with a χ^2 fit of a Breit-Wigner curve to the measured points of the four resonance curves.

Discussion of the quality of the fit: How many degrees of freedom does it have? How do you realize if the model agrees to your data? State a *c*onfidence level (C. L.).

(c) Determinating parameters of particle physics by evaluating the fit results:

(i) Calculate the weighted averages $\overline{\Gamma}_{Z^0}$ and $\overline{M}_{Z^0}$ from your individual results (Do not forget to give errors!). Compare them to the official results of the LEP experiments (see [PDG08] or figure C.2 in the supplementary materials for example) and to the

prediction of the theory (compare table 2.2) in case of $\overline{\Gamma}_{Z^0}$.

(ii) Calculate the mean lifetime τ_{Z^0} of the Z^0 boson from $\overline{\Gamma}_{Z^0}$ and give a quick subsumption of the value: How big is τ_{Z^0} compared with the lifetime of other instable particles and what physical meaning dioes this value hold?

(iii) Determine the partial width Γ_f from the measured peak cross sections σ_f^{peak} for each of the four channels. Try to think of a good partial width to start your calculations with. Where can your results be found compared to the theoretical values you calculated in preparation for the practical when you take the uncertainty of the measurement into account?

Choose at least one more experiment to conduct from the following suggestions (marked with *) after you finished experiment E1.

Experiment E2*: Testing lepton universality

Which meaning do your results (especially the partial peak cross sections in E1 (b) and the partial widths in E1 (c)) have, regarding lepton universality?

What is the ratio of the peak cross sections in the hadronic and leptonic channels?

Compare the result with the expected ratio of the branching ratios (Verzweigungsverhältnisse, BR) and discuss the differences if necessary.

Experiment E3*: Determination of the number of light neutrino generations

Determine the number of „light“ (read $m_\nu < M_{Z^0}/2$) neutrino generations from your results. Which measurand is used for this at best and which presumptions do you have to make for this?

Experiment E4*: Determination of the quark color rotation of the strong interaction

Look at the experimental value for Γ_{had} you determined in your analysis. The expected value according to the Standard Model is

$$\Gamma_{\text{had}}^{\text{SM}} = N_c \cdot \delta_{\text{QCD}} \cdot (2\Gamma_{\text{u}} + 3\Gamma_{\text{d}}). \tag{4.1}$$

The factor $\delta_{\text{QCD}} \approx 1 + \frac{\alpha_s}{\pi} \approx 1.05$ with the coupling constant α_s of the strong force takes gluon emission processes (processes of higher order) into account. The theoretical partial widths $\Gamma_{\text{u,d}}$ should be in the calculations you did in preparation for the practical. (Attention, the color rotation N_c is not to be included in the calculation of these theoretical values!) By comparing Γ_{had} and $\Gamma_{\text{had}}^{\text{SM}}$, N_c can be determined.

Experiment E5*: Determination of the Weinberg angle

Use the partial widths Γ_f established in E1 (c) to calculate the value $\sin^2\theta_W$ using equation (2.15). Using „natural units“ ($\hbar = 1$, $c = 1$) is often a good idea here. Compare your result with the literature value (e.g. in reference [PDG08]) and identify the reason for potential differences.

Evaluate, based on the reaction $e^2 = g^2 \cdot \sin^2\theta_W$ between the electromagnetic charge e and the „weak charge“ g, if the weak interaction lives up to its name compared to the electromagnetic interaction. (Remember: The important factor for the coupling strength are the constants $\alpha_{\text{em}} \propto e^2$ and $\alpha_{\text{schw}} \propto g^2$ respectively.)

4.4.2. Discussion of the results

Discuss thoroughly, which presumptions your analysis is based on and review your results sceptically, taking systematical uncertainties into account. Create a list of potential systematical errors.

Remember to integrate this discussion and evaluation of your results in your report.

We wish you plenty of fun and success with the execution of the practical!

Bibliography

[Bar89] R. J. Barlow: *S*tatistics. Wiley, 1989

[Ber06] Chr. Berger: *E*lementarteilchenphysik. Springer Verlag, 2006

[CERNlive] http://livefromcern.web.cern.ch

[CERNpub] http://public.web.cern.ch

[Gri87] D. Griffiths: *I*ntroduction to Elementary Particle Physics. John Wiley & Sons, 1987 (Neuauflage 2008 erschienen bei Wiley-VCH)

[Gru98] C. Grupen: *T*eilchendetektoren. Spektrum Akademischer Verlag, 1998

[Hal84] F. Halzen and A. D. Martin: *Q*uarks and Leptons. "John Wiley & Sons", 1984

[Leo94] W. R. Leo: *T*echniques for Nuclear and Particle Physics Experiments. Springer Verlag, 1994

[LHC08] *T*he Large Hadron Collider. LHC website at CERN: http://public.web.cern.ch/public/en/LHC/LHC-en.html (2008)

[LEP00] *T*he LEP story. CERN press release: http://press.web.cern.ch/press/PressReleases/Releases2000/PR10.00ELEPHistory.html (2000)

[LEP08] *T*he Z factory. LEP website at CERN: http://public.web.cern.ch/public/en/Research/LEP-en.html (2008)

[OPAL] *T*he OPAL detector. OPAL website at CERN: http://opal.web.cern.ch/Opal/tour/detector.html (2001)

[PDG08] C. Amsler *et al.* (Particle Data Group): *R*eview of Particle Physics. Physics Letters **B** 667 (2008) 1; Online verfügbar unter http://pdg.lbl.gov

[ROOT] ROOT website mit ausführlicher Dokumentation: http://root.cern.ch

[Scho09] H. Schopper: *L*EP – The Lord of the Collider Rings at CERN 1980–2000. The Making, Operation and Legacy of the World's Largest Scientific Instrument. Springer, 2009

[Sut04] Chr. Sutton and P. Zerwas: *T*he W and Z at LEP. CERN Courier: http://cerncourier.com/cws/article/cern/29076 (2004)

[ZRes06] The ALEPH, DELPHI, L3, OPAL, SLD Collaborations, the LEP Electroweak Working Group, the SLD Electroweak and Heavy Flavour Groups:
*P*recision electroweak measurements on the Z resonance. Phys. Rep. **4**27 (2006) 257 - 454.
Online verfügbar unter http://dx.doi.org/10.1016/j.physrep.2005.12.006 → (via SpringerLink, ggfs. nur aus der Uni-Bibliothek oder aus dem Uni-Netzwerk abrufbar)
bzw. http://arxiv.org/abs/hep-ex/0509008v3 → (pre-print, frei zugänglich)

Suplementory material for the

Practical M48:

Analysis of Z^0 decays

Physikalisches Institut

der Friedrich-Alexander-Universität Erlangen-Nürnberg

Last modification: March 2024

(Revision 1.06)

*r*odrigo.lang@fau.de

A. Kinematic formulary (scattering processes)

In general, to completely discribe scattering processes of the form

$$A + B \rightarrow C + D \tag{A.1}$$

two independant kinematic properties are needed, for example the energy and the scattering angle. It is, however, often useful to use variables, that behave invariant under Lorentz transormations (compare [Hal84], chapter 4.7 for example). One such set of parameters are the Mandelstam variables s, t and u:

$$\begin{aligned} s &= (p_A + p_B)^2 \\ t &= (p_A - p_C)^2 \\ u &= (p_A - p_D)^2. \end{aligned} \tag{A.2}$$

They are formed comprised of the four-momenta $p_i = \left(E_i, \vec{p}_i\right)$ (with $i \in \{A, B, C, D\}$). (To keep the discussion simple, we use $c = 1$ again.)

To make sure the variables are lorentz invariant one can simply use the invariance of the scalar product of four-vectors and $p_i^2 = m_i^2$. Using that and the preservation of energy and momentum in four-vector notation:

$$p_A + p_B = p_C + p_D, \tag{A.3}$$

one finds that only 2 of the 3 variables in equation (A.2) are independant.

The following applies:

$$s + t + u = m_A^2 + m_B^2 + m_C^2 + m_D^2. \tag{A.4}$$

In the centre of mass system (with $\vec{p}_A = -\vec{p}_B$), s is the total energy squared:

$$s = \left(p_A + p_B\right)^2 = \left(p_C + p_D\right)^2 = E_{\text{cm}}^2. \tag{A.5}$$

With the beam energy E_{beam} of the (symmetrical) particle beams, the following applies additionally:

$$E_{\text{cm}} = \sqrt{s} = 2E_{\text{beam}}. \tag{A.6}$$

The scattering angle θ is defined as the angle between the inbound particle A and the outbound particle C in the centre of mass system (compare adjecent sketch).

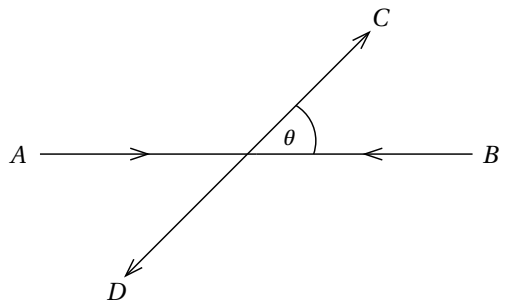

For the scattering event

$$\mathrm{e}^- + \mathrm{e}^+ \rightarrow \mathrm{e}^- + \mathrm{e}^+ \tag{A.7}$$

(compare figure A.1) θ can be calculated with the Mandelstamm variables t or u in the following way:

$$\begin{aligned} t &= \left(p_C - p_A\right)^2 &&= -2|\vec{p}|^2\,(1-\cos\theta) \\ &&&= -2E_{\text{beam}}^2\,(1-\cos\theta) &&\leq 0, \\ u &= \left(p_A - p_D\right)^2 &&= -2|\vec{p}|^2\,(1+\cos\theta) \\ &&&= -2E_{\text{beam}}^2\,(1+\cos\theta) &&\leq 0. \end{aligned} \tag{A.8}$$

Whereat $|\vec{p}| = |\vec{p}_{\text{in}}| = |\vec{p}_{\text{out}}|$ is the momentum of the inbound and scattered particles. Additionally, the following applies for this process:

$$s = 4(|\vec{p}|^2 + m^2). \tag{A.9}$$

The process (A.7) is also physically possible for $s \geq 4m^2$, $t \leq 0$ and $u \leq 0$ (compare figure A.2 too).

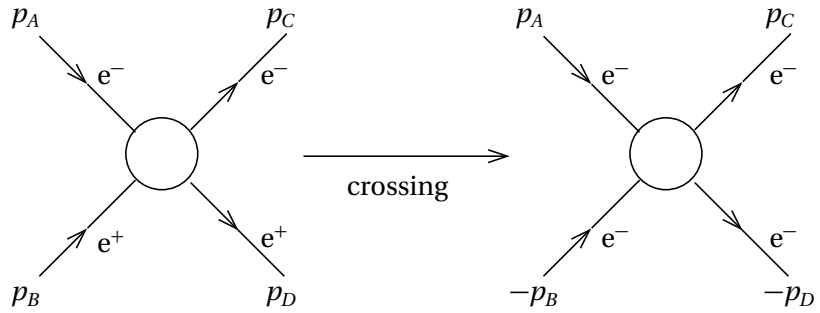

$A + B \rightarrow C + D$ — s-Kanal-Prozess

$A + \overline{D} \rightarrow C + \overline{B}$ — u-Kanal-Prozess

Figure A.1.: Mandelstam variables and „crossing“ (Vertauschung) of the particles B and D (in accordance with [Hal84]).

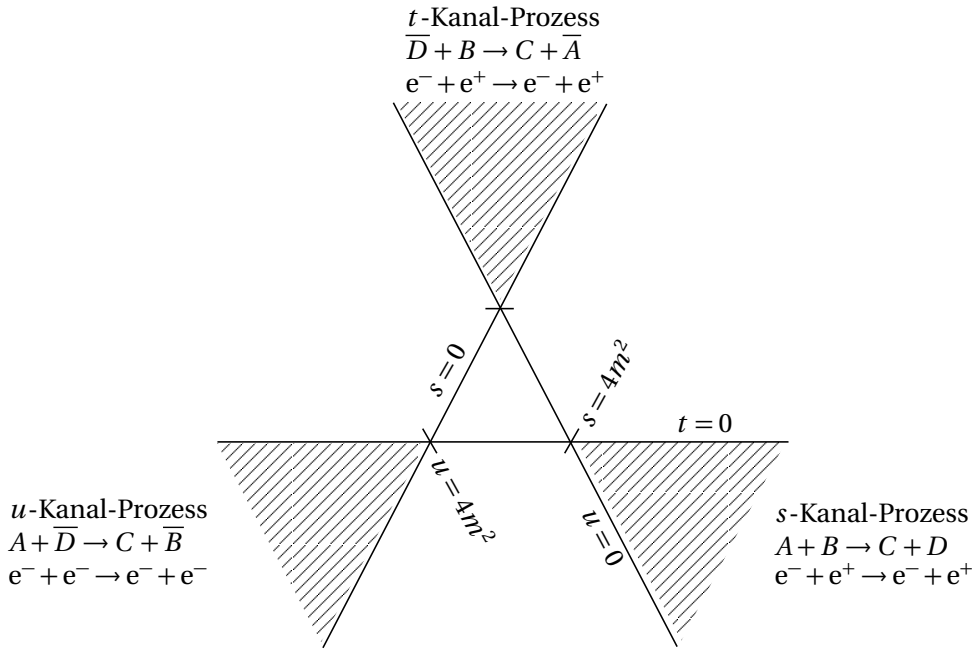

Figure A.2.: The Mandelstam diagram (according to [Hal84]) shows the physically permitted regions of the process $e^+ + e^- \to e^+ + e^-$ and both of the „crossed“ (vertauschten) reaktions.

B. The OPAL experiment: detector structure, measurands, event classification

As introduction to the detailed description of the OPAL experiment, a short overview of the environment is given, before the detector components ans their different measuring tasks are explained.

B.1. CERN – LEP – OPAL

Laboratory and accelerator The *European Organization for Nuclear Research* runs the european laboratory for core and particly physics (CERN) at the border between Switzerland and France near Geneva since 1954. The goal, to study the fundamental structure of mater down to ever smaller scales, requires the construction of ever more efficient particle accelerators, where the older machines are often used as pre-accelerator for the next stage (compare figure B.1). The peak in this chain of circular accelerators (*colliders*), for the time being, where two opposed particle beams are broight to collision at certain interaction points, is the *Large Hadron Collider* (LHC) [LHC08]. It was built in the 27 km long tunnel of the predecessor LEP (*Large Electron Positron Collider*) [LEP08, Sut04]. The e^+e^-collisions that were studied at the LEP accelerator are object of this practical.

Figure B.2 depicts an interior view of the LEP tunnel.

The LEP detectors The four LEP experiments (ALEPH, DELPHI, L3 and OPAL), that were designed as „general-purpose detectors“, are good examples of complex detector ystems in modern high energy physics. While they differ in details of their design ans their proportions – depending on the specific research question of each experiment – they consist of the same types of subdetectors, that are specialised to measure different measurands. The functioning of the most important types of subdetectors is described in section B.2.

One motivation for the simultaneous operation of multiple large-scale detectors is the redundancy (and in parts the complementarity) of the measurement. That way, not only the yield of measued data during the operation periods of the accelerator, that can be rather costly, but it is also possible to reduce sstematical errors by measuring the same measurands wih different detector systems. Likewise, the new major project of CERN, the LHC will have four experiments (ALICE, ATLAS, CMS and LHCb) with differently alligned goals.

The LEP accelerator was designed for precise measurements of the parameters of the Standard Model of elementary particles. For that kind of precision tests, detectors, that are designed to detect (as far as possible) all decays of the Z^0 ito fermion antifermion pairs and identify tha particles of the final state correctly, are required.

Electron positron collisions at high energies generally lead to events, that are characterized by a huge number of particles (charged ones as well as netral ones) emmitted in all direc-

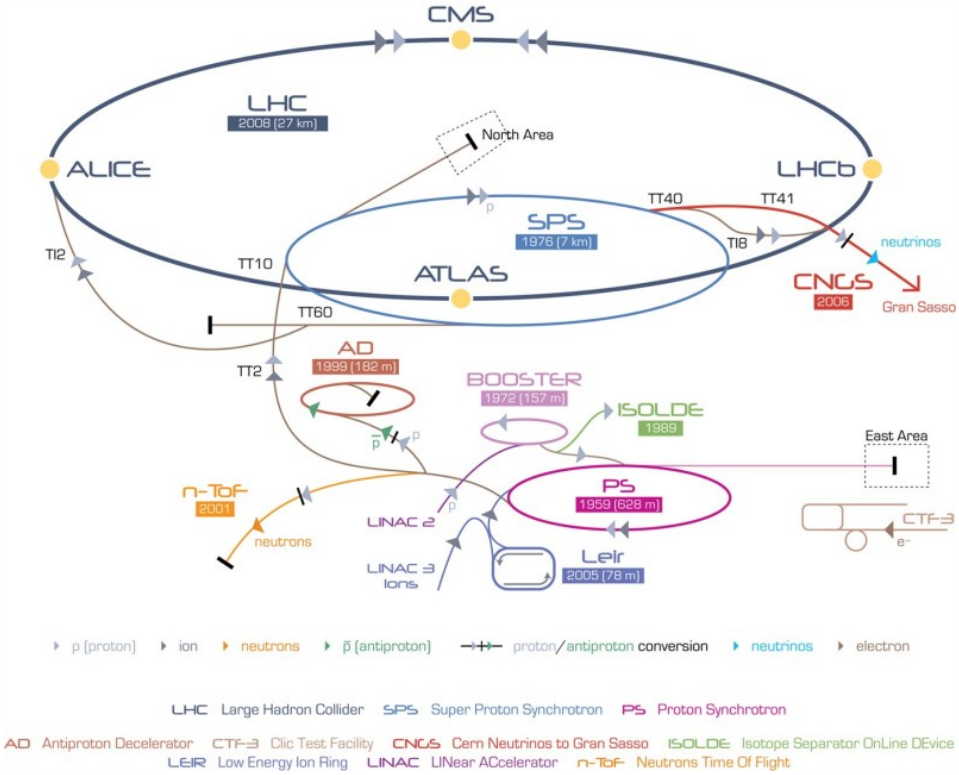

(a) Current state of construction of the accelerator facilities (not true to scale)

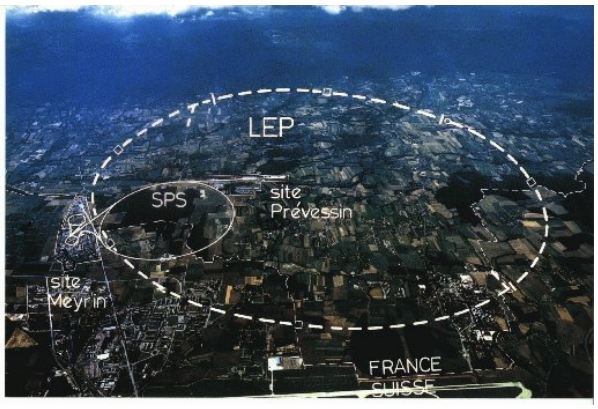

(b) Bird's eye view of the LEP accelerator area. The tunnel is roughly 100 m underground. At four interaction points, the LEP experiments ALEPH, DELPHI, L3 and OPAL are positioned.

Figure B.1.: Overview of the accelerator complex at CERN [CERNpub].

tions. A particle detector for that kind of events has to cover a huge solid angle, have a good spatial resolution and collect highly complete information of each event.

B.2. Functioning of important detector components

Especially important components, whose specifications are described below, are the tracking detectors, that, in junction with the stong magnetic field, allow for precise measurements of the

(a) Section of the LEP tunnel with magnets[CERNpub]

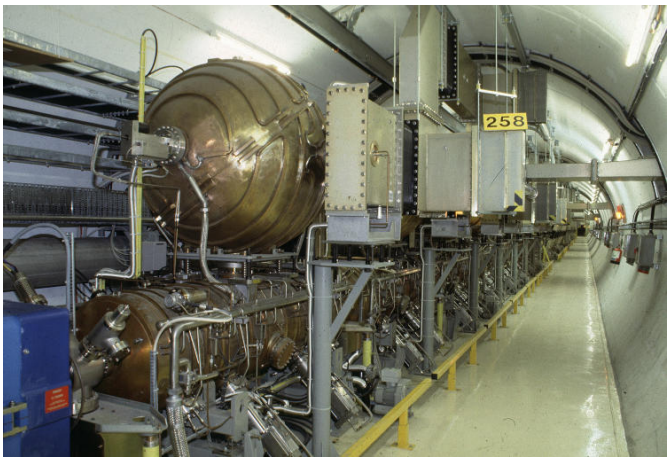

(b) RF cavity resonators [CERNlive]

Figure B.2.: View of the LEP tunnel.

momenta of charged particles, and the calorimeters for measurements of the energies of charged and neutral particles and for particle identification.

B.2.1. Proportional chambers

A charged particle, that passes a volume of gas, ionizes the gas, whereat electron ion pairs are created. The electrons („primary electrons“) fdrift to the thin, positively charged counting wires in the in the gas. In the high electrical field near the counting wire, the electrons gain enough energy between two collisions with gas atoms to ionize atoms themselves. This leads to an avalanche-like increasing number of electrons.

The multiwire proportional chamber (Nobel prize [1] 1992 for G. Charpak) is an advancement of the widely used proportional chamber. It consists of many anode wires that are hung tensely in a plane between two cathode planes. The individual wires are read out separately and give a spatial information with a precision that depends on the distance of the wires.

The time difference between the particles passage and the response of the wire is, if the drift velocity is constant, proportional to the distance between the trajectory of the particle and the counting wire. With the measurement of this time, one achieves a good spatial precision with a smaller number of counting wires.That's the principle of the drift chamber.

The jetchamber is basicly a big, cylindrical drift chamber. The special advantage of this chamber is it's good resolution of double traces, which is especially important for the analysis of hadronic events (jets)! Because OPAL's main tracking detector contains a jet chamber, this component will be explained more closely below.

The TPC (*t*ime projection chamber) is also a big, cylindrical dift chamber, both of its end caps equipped with a layer of proportional chambers. A particle passing through theTPC ionizes the

[1] Refer to information found at `http://nobelprize.org/nobel_prizes/physics/laureates/1992/` .

counter gas along its trace. The electrical field is aligned parallel to the magnetic field in axial direction. Because of that, the electrons released by the ionization drift along the field lines towards ne of the two end caps, where they are detected by the layer of wire chambers by means of secondary emmission. The electron cascade generated by the primary electrons moves to the anode. A signal is induced on the cathode, that consists of small *p*ads). The radial position r and the azimuth angle φ of the points on the primary particle trajectory can be reconstructed with high precision based on the information, which pads gave a response. The third component of the points, z, can be derived from the drift time of the electrons in the TPC.

B.2.2. Calorimeter / Cascade counters

The electromagnetic and strong interaction of particles with matter is used in cascade counters. They consist of either massive, transparent crystals, where the cascade particles generate light signals with szintillation and cherencov processes (so called *h*omogeneous calorimeters like the OPAL-ECAL for example), or passife plates of matter, where most of the interactions takes place, wih active detector elements inbetween (so called *s*ampling calorimeters like the OPAL-HCAL for example). The cascade counters have to be thick enough to allow the primary particles to denote their energy (or at least most of it) in a cascade of particles with ever smaller energies[2]. The interaction of the primary particle with the detector matter induces a cascade signal that is proportional to the initial particleenergy.

Cascade counters are used as particle detectors mainly because of the following reasons:

- thety are sensitive to both charged *a*nd neutral particles (except neutrinos);
- the cascade profile depends on the natur of the particle;
- they can be used at high event rates;
- it is possibleto achieve good spatial and directional resolution.

There are vast differences between an *e*lectromagnetic cascade (initiated by electrons and photons) and a *h*adronic cascade (initiated by p, n, $\pi^{\pm}$ for example) that reflect the nature of the cascade processes. Common to both cases, however, is the fact that the detector only has to grow logarithmical with the energy of the particles it has to detect.

Electronas with high energy loose it primarily by means of Bremsstrahlung, when they pass through matter. The photons that are produced in this process are mostly absorbed in the production of e^+e^-pairs. These generate additional photons with bremsstrahlung. This leads to a cascade („shower“) consisting of γ, e^+ and e^-, that only stops when the energy of electrons and positrons reaches a so called critical energy E_c. (E_c is the energy, where the energy loss by means of bremsstrahlung is as big as the energy loss by means of ionization.)

One important parameter to describe electromagnetic cascades is the radiation length X_0, that depends on the mean free path of an electron in matter. One can depict the development of the cascade roughly like this: An electron with an energy of E_0 generates on average one photon with an energy between E_0 and E_0/e (e = Euler's number) when passing through a layer thickness of X_0. Over the course of the next radiation length, the photon generates an /ee pair with a probability of 54% while the electron emmits another photon, so that there are on average four particles with an average enrgy of $E_0/4$ after 2 X_0.

Thus, the average energy rapidly decreases, the electrons are slowed down by ionization and the

[2] In contrast to what the name „calorimeter“ suggests, the increase of temperture by the energy that is transfomed to heat is rather small with roughly $\approx 10^{-5}$ degree and not usable for energy measurements.

further development of the cascade stops. Most of the energy of the incoming electron or photon is transformed to ionization energy that is proportional to the primary energy. The length of the cascade depends on the energy of the incoming particle logarithmically. The lateral expansion of the cascade is also limited. A characteristic measure is the Molière radius ρ_m:

$$\rho_m = \frac{21\,\text{MeV}}{E_c} X_0. \tag{B.1}$$

A counter (with infinite length) with a radius of $2\rho_m$ records basically the whole cascade energy ($\approx 95\%$) .

The uncertainty of the energy measurement is determined by statistical fluctuation in the cascade development. The best energy resolution can be achieved with blocks of heavy szintillator material (NaI or BGO for example). Most of the time, however, cascade counters with alternating layers of inactive absorber material (Pb for example) and active detector layers (szintillator) are used (in the *s*ampling technique described above). The detector layers record only part of the cascade energy that is measured on a random basis.

A hadronic cascade is induced when a strong interacting particle (hadron, e.g. p, n, $\pi^{\pm}$) hits an absorber and generates secondary hadrons in a series of inelastic core collisions, that scatter inelastically themselves. (Bremsstrahlung of the primary particles is not relevant here because of the high masses.) This cascade only stops when the cascade particles have energies small enough to allow for them to be absorbed or decellerated completely.

The description of a hadronic cascade is complex because of the high number of different particles that can be generated. It is, however, well understood today and can be modeled in Monte Carlo simulations. In contrast to cascade counters for electrons and positrons, in a hadronic calorimeter, not all od the energy of the particles is converted into ionization energy. It is partialy transferred onto neutrinos that no longer interact, used to generate muons that are no longer absorbed or axcites cores.

The characteristic dimensions of the cascade are determined by the Kernabsorptionslänge λ_0:

$$\lambda_0 = \frac{A}{N_A \cdot \rho \cdot \sigma_{\text{inel}}} \tag{B.2}$$

with the mass number A, the density ρ, the avogadro constant N_A and the cross section σ_{inel} for the inelastic scattering of hadrons at nuclei. The differences of hadronic and electromagnetic cascades are shown in table B.1.

Table B.1.: Characerization of electromagnetic and hadronic cascades.

	electromagn. cascade	**h**adronic cascade
multiplication process	bremsstrahlung and pair production	decays and nuclear reactions
secondary particles	electrons, positrons, photons	all kinds of particles, primarily nucleons and pions
cascade length	$\approx (10-30)\cdot X_0$	$\approx (5-10)\cdot \lambda_0$
cascade width	$\approx 2\cdot \rho_m$	$\approx \lambda_0$

B.2.3. Luminosity measurements

In order for the measured event rates for a specific final state (process) to be converted into a (partial) cross section, on ehas to *s*imultaneously measure the rate $\frac{dN}{dt}$ for another process with a known cross section $\sigma_{\text{bek.}}$. With this, the luminosity $\mathscr{L}$ can be derived, that is a measure for the interaction rate with a known cross section:

$$\begin{aligned} \frac{dN}{dt} &= \sigma_{\text{bek.}} \cdot \mathscr{L} \\ \Rightarrow \quad N &= \sigma_{\text{bek.}} \int \mathscr{L}\, dt. \end{aligned} \tag{B.3}$$

This equation defines the luminosity. It is determined using the elastic e^+e^-scattering (Bhabha scattering) at small scattering angles, which is the case for all e^+e^-storage ring experiments. In the extreme forward path, the scattering by photon exchange is dominating. The cross section can be calculated with a precission of approx. 1% in the context of quantum electro dynamics (QED).

Typical luminosity values for circular accelerators are given in table B.2.

Table B.2.: Luminosity values for some circular accelerators [PDG08].

accelerator	beam type	$\mathscr{L}$ $[10^{30}\,\text{cm}^{-2}\,\text{s}^{-1}]$	
LEP (CERN)	e^+e^-	24	at the pole of the Z^0 resonance
		100	bei $E_{\text{cm}} > 90\,\text{GeV}$
HERA (DESY)	$e^-\,p$	75	
TEVATRON (Fermilab)	$p\,\overline{p}$	286	
LHC (CERN)	$p\,p$	$1 \cdot 10^4$	(planned)
	Pb Pb	$1 \cdot 10^{-3}$	

B.2.4. Details to the OPAL subdetectors

The structure of the OPAL detector is shown scematically in figure 3.1 of the instructions.

First of all, the interaction point is enclosed by the central detector, that consists of the following components (beginning in the midle):

– Directly at the interaction point, the „micro vertex detector“ can be found, a semiconductor detector consisting of stripes of silicon.

– It is enclosed by the vertex detector, the jet chamber and the Z chambers.

The central detector is located in a pressure tank, that is filled with a mixture of 88.2% argon, 9.8% methane and 2.0% isobutane at a pressure of 4 bar. The pressure tank is sourounded by a cylindrical solenoid with a length of 6.3 m and a diameter of 4.36 m. It generates a homogenous magnetic field of 0.435 T in the direction of the beam on the inside. From the solenoid outward, the following components can be found:

– Adjacent to the solenoid in radial direction, the time of flight system (*T*OF, Flugzeitmesssystem) can be found. It consists of 160 szintillation counters, that are arranged parallel to the beam axis and have an conic profile. Each counter is 6.84 m long, 89 to 91 mm wide and 45 mm thick. The

szintillation light is detected at both ends of the counters. The signals of the TOF are used as trigger for the detector and to measure the time of flight of the particles.

– Around the TOF, the presampler (basicly a preliminary stage for the cascade counters), consisting of 16 streaming chambers, is mounted. It is used to check, if a cascade has already started in the relatively thick layer of material, that forms the pressure tank and solenoid.
– This is followed by the electromagnetic calorimeter (*E*CAL), with the forward calorimeter (*F*CAL) at its end caps, and the hadronic calorimeter (*H*CAL), that serves as yoke for the magnetic field of the solenoid.
– The outermost layer is formed by four layers of muon chambers (*M*UON), again consisting of a cylindrical part and two and caps.

What follows is a closer look at the characterisics of some of the detector components:

Vertex chamber The vertex chamber is a multi wire proportional chamber with high spatial resolution. It consists of an inner part, that, like the jet chamber, contains axial wires, arranged in 36 layers around the beam axis in this case. The outer part is responsible for the resolution in the z direction. Furthermore, the z coordinate is derived from the different drift times of the pulses on the wires to both ends. The spatial resolution of this vertex chamber is $55\,\mu$m on average.

Jet chamber The most important tracking detector in OPAL is the huge, cylindrical jet chamber with an outer diameter of 3.7 m, an inner diameter of 0.5 m and a length of 4 m. The chamber is divided into 24 identical sectors, where each sector contains a layer of 159 counting wires, that are stretched parallel to the beam axis. Between the anode wires, altering, field shaping potential wires are arranged. Between the layers of anode and potential wires, the layers of the cathode wires are placed. The distance between the anode and cathode layers (and with it the drift distance) varies from 3 cm close to the beam axis up to 25 cm for the outer wires. The signals from the counting wires are used for the position fixing and to measure the energy loss ($\mathrm{d}E/\mathrm{d}x$) of a charged trace.
The radial position r and the azimuth angle φ of the points on the primary trajectory of the particle can be determined from the drift times with high precision. In the $r\varphi$ plane, a resolution of $135\,\mu$m can be acieved. The third component of the point, z, is determined based on the quotient of the charge that reaches the ends of a counting wire. The resolution of the derivation of z is therefore determined by the length of the wires and is approx. 6 cm.

The jet chamber is then sourounded by 24 Z chambers (one for each sector of the jet chamber), where the wires are arranged radial, which leads to a good resolution for the z direction. It is about $100-200\,\mu$m.

The momentum of the particles is determined from the radius of curvature of their trace, that is bent by the axial magnetic field. Here, the transversal momentum (p_t, $r\varphi$ plane) and the longitudinal component (in the direction of the beam) have to be differnentiated.

The relative resolution for the transversal momentum is

$$\frac{\Delta p_t}{p_t} = \sqrt{(0.02)^2 + (0.0015 \cdot p_t)^2}, \tag{B.4}$$

which means that the relative error increases proportional with the momentum itself. (The constant term in the square root is not determined by the detector properties but by multiple scattering).

To give you a sense for the scales, you can find a small sample calculation here: For a paricle with $p_t = 45\,\mathrm{GeV/c}$, the relative error on the momentum is approx. 7% and the absoluteerror approx.

3 GeV/c respectiely. This should be kept in mind when interpreting the measured events.

For the z component, the momentum resolution is significantly worse. (Try to think of the reasons yourselves!)

Electromagnetic calorimeter The electromagnetic calorimeter (*E*CAL) consists of more than 10 000 blocks of lead glass. It is divided into a barrel shaped part sourounding the jet chamber (*b*arrel) and two *e*ndcaps, that cover 98% of the solid angle together. The blocks of lead glass have a density of 22 (endcaps) and 24.6 (barrel) radiation lengths X_0. At their back side, photomultipliers that detect the čerenkov light signals[3] generated by charged cascade particles in the lead glass, to determine the energy and position of the electromagnetic cascades. The energy resolution is approximately

$$\frac{\Delta E}{E} \approx \frac{5\%}{\sqrt{E/\mathrm{GeV}}}. \tag{B.5}$$

It is reduced because the particles have to pass through approx 2 radiation lengths of matter before entering the ECLA (elpecially the solenoid and pressure tankt, tat have to be inside the ECAL for technical reasons). Because of that, most electromagnetic cascades start *b*efore the ECAL, which can be scertained with the signals of the *p*re samplers and can be included for the energy determination.

Hadronic calorimeter The hadronic calorimeter (*H*CAL) is built similar to the ECAL with a central section and two end caps. It consists of layers of iron and ionization chambers, working in the „limited streamer mode“, as detection elements inbetween. Thety are constructed similar to proportional counters, but operate with a higher voltage which leads to a secondary ionization that is independant of the ionization density of the primary particle. The energy resolution achieved with this is approximately

$$\frac{\Delta E}{E} \approx \frac{120\%}{\sqrt{E/\mathrm{GeV}}}. \tag{B.6}$$

Again a small numerical example: The typical error on the measurement of a hadron with an energy of 25 GeV in the HCAL is 24%, or 6 GeV when looking at absolute numbers.

Forward calorimeter The luminosty measurement s done with two *f*orward calorimeters (*F*CAL). They are mounted very close to the beam tube and detect bhabha events with small angles by coincident measurement of electrons and positrons.

The FCAL consists of a lead glass wire chamber „sandwich“ with a thicknes of 24 radiation lengths. It covers an angular range of $58\,\mathrm{mrad} \leq \Theta \leq 120\,\mathrm{mrad}$, which corresponds to a bhabha cross section of approximately 24 nb and has an energy resolution of

$$\frac{\Delta E}{E} \approx \frac{17\%}{\sqrt{E}}. \tag{B.7}$$

Trigger The event rates at LEP resulted in great parts from so called „beam gass events“ (colisions of beam particles and gas atoms that remained in the beam tube despite the good vacuum condition) and beam particles that did not colide, leave the beam tube because of a differing momentum and hit the detector. The actual event rate of the desired process, $e^+e^- \to Z^0 \to f\bar{f}$, was only $\approx 1\,\mathrm{Hz}$, even though the beams hit each other 40 000 times per second.

[3] Often, cascade counters are built from szintillation crystals, likewise with photomultipliers to detect the light signals. Lead glass, however, is not a szintillator; the light signal is generated via the čerencov effect. Čerenkov light is emitted when charged particles pass through a medium with refractive index n with a velocity $v > c$ (with $c = c_{\mathrm{vac}}/n$).

The purpose of the trigger is the reduction of these background events as much as possible while allowing for the measurement of data for all desired events at the same time. The trigger conditions have to be set in a way that new, unknown decays of the Z^0 are accepted with high efficiency as well.

The trigger has make a decision on the selection of each event, befor the next bundle of particles (*b*unch) arrives and therefore uses fast signals of different detector components to define a vast range of trigger conditions that cover all possible physical processes together. That kind of fast signals can be provided by the (*t*ime-of-flight detector) on a time scale of some ns after the colision for example, while in the outer regions of the drift chambers, the ionization electrons did not reach the anode wires yet (the reconstruction of the traces is not even close to possible at this point).

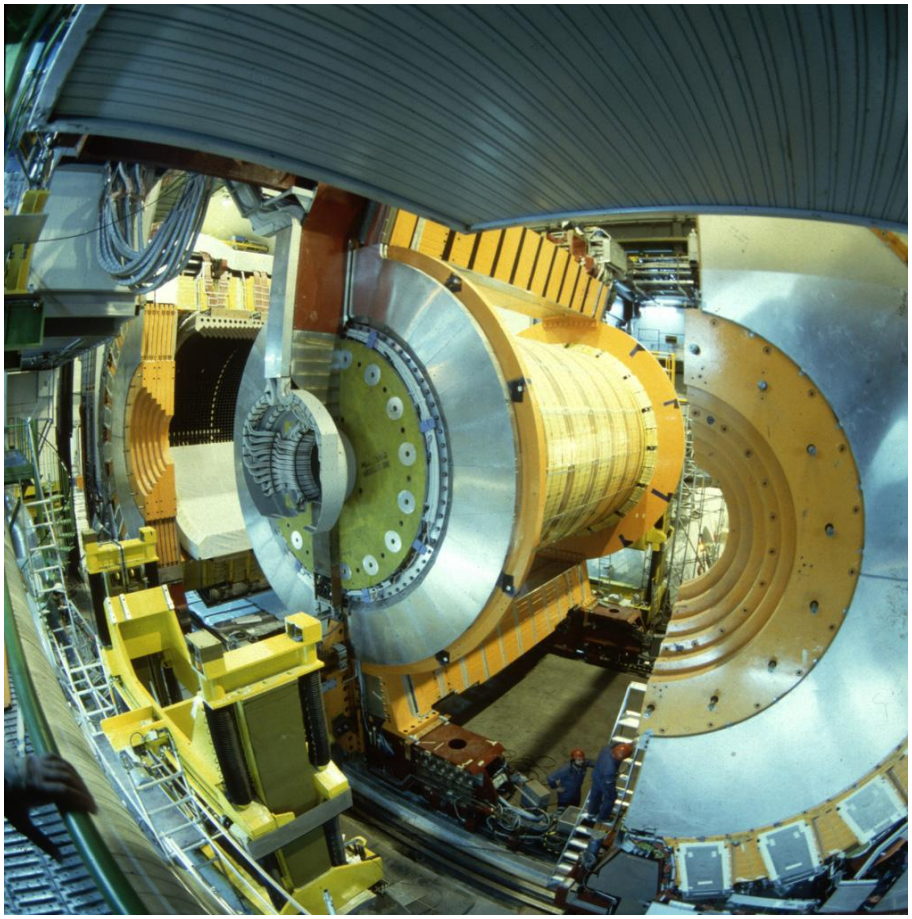

Figure B.3.: The OPAL detector at its construction [CERNpub]. In the background on the left side, a part of the electromagnetic calorimeter is visible (dark bricks of lead glass). The central detector is being placed between the two halves of the calorimeter.

C. Results of the LEP experiments

Some official results of the longtime precision measurements of the Z^0 characteristics and parameters of the Standard Model are shown in figure C.1 and C.2.

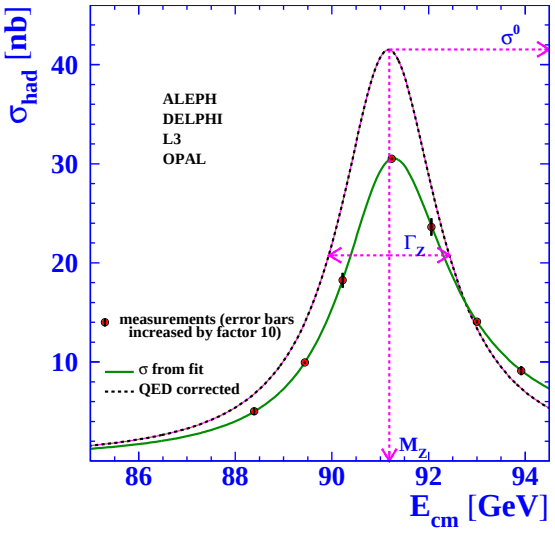

(a) Hadronic cross section (with and without QED radiation corrections) and extraction of the parameters Γ_Z, M_{Z^0} and $\sigma^{\text{peak}}_{\text{had}} \equiv \sigma^0$

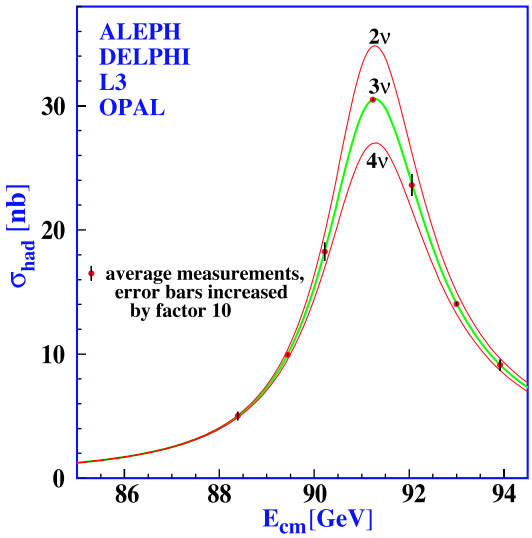

(b) Number of light neutrino generations

Figure C.1.: Results of the LEP experiments, part I: (a) example of the effect of QED radiation corrections on the measured resonance courve (hadronic final state) and (b) number of small neutrino generations [ZRes06].

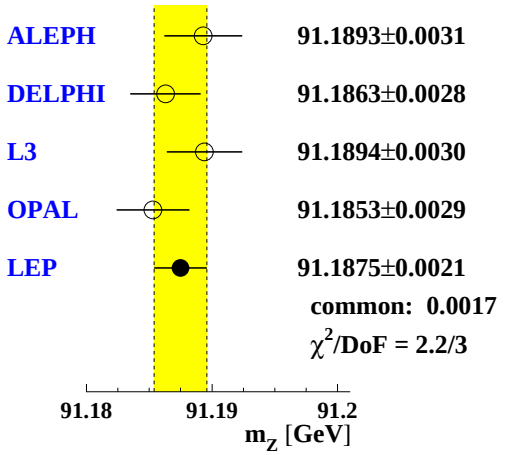

(a) Mass of the Z^0

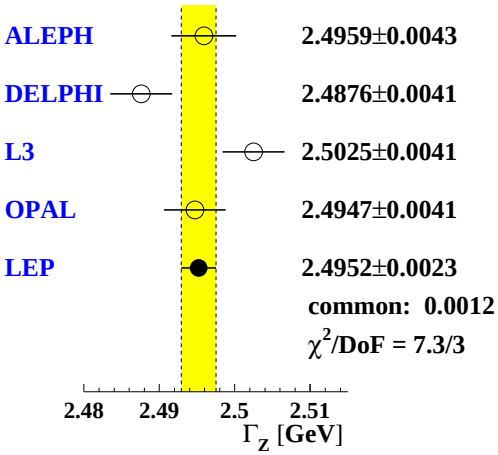

(b) Total decay width of the Z^0

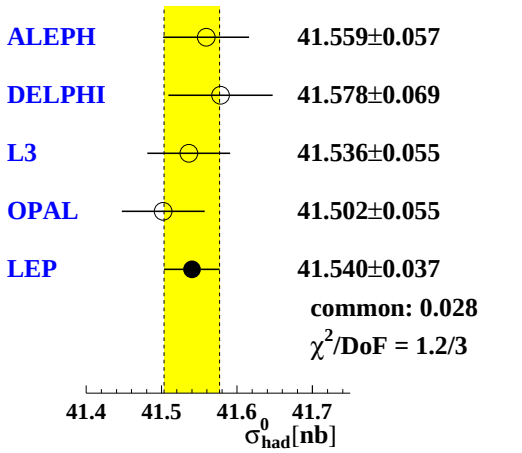

(c) Peak cross section hadr. channel

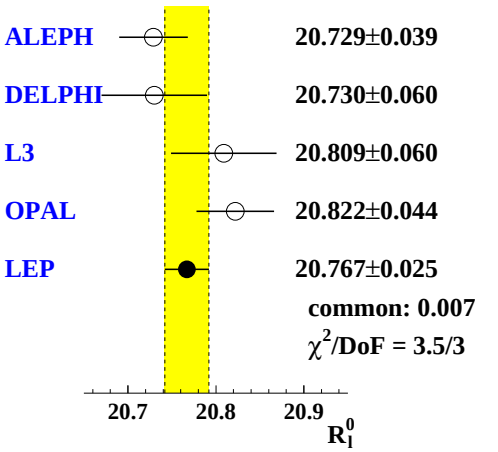

(d) Ratioof the hadr./lept. peak cross section

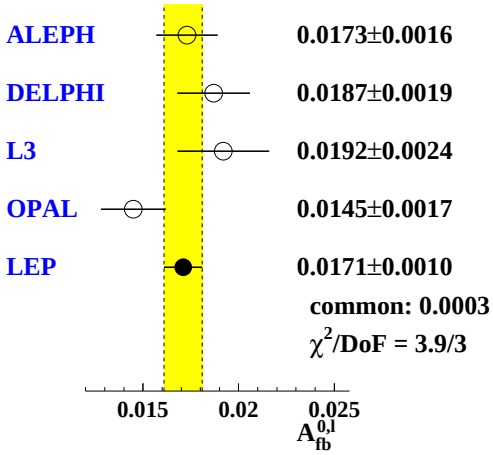

(e) Forwards backwards asymmetry at the peak

Figure C.2.: Results of the LEP experiments, part II [ZRes06]. Apart from the individual measurements of the four detectors, the average value is marked.

D. The Breit-Wigner distribution

D.1. Line width at the decay of instable particles

In case of a damped harmonic oszillator with the differential equation

$$m\ddot{x} - \beta\dot{x} + Kx = 0, \tag{D.1}$$

when using the driving force

$$F(t) = F_0 e^{i\omega t}$$

and the approach

$$x(t) = a e^{i(\omega t - \phi)} \tag{D.2}$$

one finds the following correlation:

$$\left(\frac{a}{F_0}\right)^2 = \frac{1}{m^2} \frac{1}{[(\omega-\omega_0)(\omega+\omega_0)]^2 + \frac{\beta^2\omega^2}{m^2}}, \tag{D.3}$$

and for $\omega \sim \omega_0$:

$$\left(\frac{a}{F_0}\right)^2 \sim \frac{1}{4\omega_0^2 m^2} \cdot \frac{1}{(\omega-\omega_0)^2 + \beta^2/4m^2} \tag{D.4}$$

with

$$\omega = \sqrt{\frac{K}{m} - \frac{\beta^2}{4m^2}} \qquad \text{und} \qquad \omega_0 = \sqrt{\frac{K}{m}}.$$

Using $E = \hbar\omega$ and $E_0 = \hbar\omega_0$, one finds the quantum mechanical equivalent

$$\sim \frac{1}{(E-E_0)^2 + \Gamma^2/4} \tag{D.5}$$

with $\Gamma = \frac{\hbar\beta}{m}$ = width of the resonance.

This special kind of energy dependancy is called *Breit-Wigner courve*. The width of the resonance is given by the number of possible decay channels in particle physics. It is correlated to the life time via the uncertainty principle:

$$\Gamma \cdot \tau = \hbar.$$

This energy dependant beaviour, analogous to the harmonic oszillator, justifies the name „resonance“ fir instable particles with a defined, invariant mass m, width Γ and mean life time τ.

In non relativistic quantum mechanics, the energy distribution of an instable state is already a Breit-Wigner distribution as described above. This can be seen with the following train of thought:

Instable particles follow the decay law

$$N(t) = N(0)e^{-\lambda t}. \tag{D.6}$$

The wave function of a particle at rest is given by

$$\psi(t) = \psi(0)e^{-iEt/\hbar}, \qquad |\psi(t)|^2 = |\psi(0)|^2, \tag{D.7}$$

which means that the particle does not decay for a purely real E.
Therefore, one adds a small imaginary part to the real part of the energy:

$$E = E_0 - \frac{1}{2}i\Gamma \qquad \text{mit} \qquad \Gamma = \lambda\hbar. \tag{D.8}$$

The time dependancy of the wave function of an instable particle is then given by:

$$\psi(t) = \psi(0)e^{-iE_0t/\hbar}e^{-\Gamma t/2\hbar}. \tag{D.9}$$

Energy is a measurable quantity – does an imaginary part make sense? To find this out, one has to look at the fourier transformation $\phi(\omega)$ of the wave function:

$$\phi(\omega) = \frac{1}{\sqrt{2\pi}}\int_{-\infty}^{+\infty}\psi(t)e^{+i\omega t}\,\mathrm{d}t \tag{D.10}$$

$$= \frac{\psi(0)}{\sqrt{2\pi}}\frac{i\hbar}{(\hbar\omega - E_0) + i\Gamma/2}. \tag{D.11}$$

With $E = \hbar\omega$, one finds the Brei-Wigner formula described above by squaring and normalizing to 1:

$$P(E) = \frac{\Gamma}{2\pi}\frac{1}{(E-E_0)^2 + (\Gamma/2)^2}, \tag{D.12}$$

which means that the imaginary part of the energy leads to decay **and** widenes the state. The width of the state caused by decay is called *natural line width*. Γ is the width at half of the maximum.

D.2. Breit-Wigner formula for resonante cross sections

Resonante cross sections can generally be expressed by the Breit-Wigner formula:

$$\sigma(E) = \frac{2J+1}{(2s_1+1)(2s_2+1)}\frac{4\pi}{k^2}\left[\frac{\Gamma^2/4}{(E-E_0)^2 + \Gamma^2/4}\right]B_{\text{in}}\,B_{\text{out}}. \tag{D.13}$$

With

E	the energy in the centre of mass system,
J	the spin of the resonating state,
s_i $(i = 1, 2)$	the spin of the beam particles
	($2s_i + 1$ is the number of polarization states of the beam particles),
k	the centre of mass momentum in the initial state,
E_0	the energy of the resonance and
Γ	the width (FWHM) of the resonance.

Furthermore, B_{in} and B_{out} are the *branching ratios* for the reactions that are looked at in the initial and final state respectively. In our case, B_{in} is the branching ratio for the reaction

$$\mathrm{e}^+ + \mathrm{e}^- \to Z^0,$$

while B_{out} is the corrsponding parameter for the decay channels

$$Z^0 \to \begin{pmatrix} \mathrm{e}^+ + \mathrm{e}^- \\ \mu^+ + \mu^- \\ \tau^+ + \tau^- \\ \nu_x + \overline{\nu}_x \\ \mathrm{q} + \overline{\mathrm{q}} \end{pmatrix}$$

for example.

E. Radiation corrections

To compare the measured data of the experiment with the predictions of the theory, the experimental results have to be corrected to take signal loss due to detector inefficiency and selective cuts. On the other hand, Born approximation is no longer sufficient due to the high centre of mass energy of LEP and the desired precision tests on the Standard Model and additional graphs of higher order (radiation corrections) have to be taken into account, which leads to a modification of the cross section. One differs between real, virtuel (electroweak) and QCD corrections.

The real radiation processes (QED) consist of the initial bremsstrahlung (*i*nitial state radiation), the final bremsstrahlung (*f*inal state radiation) and the interference of these two effects (compare figure E.1).

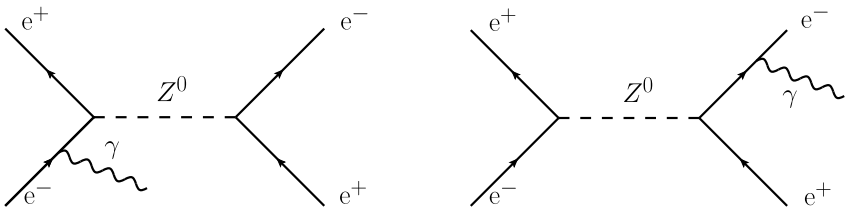

Figure E.1.: Examples for Feynman diagrams for real QED radiation corrections.

Both the line shape and the maximum value of the resonance courve are modified by these radiation correlations. In case of photon emission in the initial state this can be understood easily: This emission lowers the energy of the electron, the positron or both, which is why the centre of mass energy of the e^+e^-system at the time of interaction $\sqrt{s'}$ is no longer $\sqrt{s}$. Because of that, the cross section at the peak ($E_{cm} = 91\,\text{GeV}$) will be significantly lower compared to the value with Born approximation (an order of 25%), while it is measured higher at higher energies (because of $\sqrt{s'} \sim$91 GeV). The last case is called *r*adiative return.

Virtual radiation processes (vertex and propagator corrections, compare figure E.2) are, in contrast to bremsstrahlung corrections, characterized by the same final state as in Born approximation, while the path is different. The additional contribution of more Feynman diagrams changes the cross section. This effect is also responsible for the running of the coupling constant.

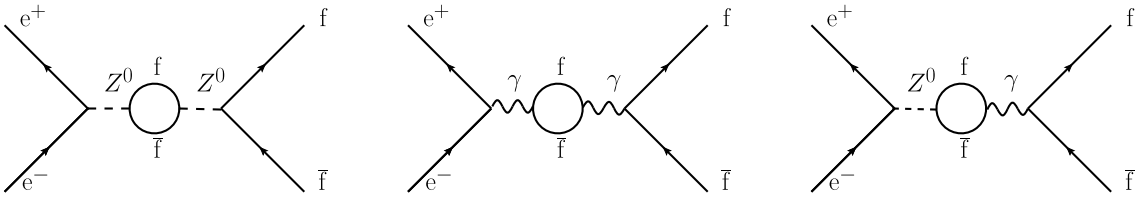

Figure E.2.: Examples for Feynman diagrams for virtual radiation corrections.

These non photonic corrections are especially interesting, as in these fermion loops, heavy virtual particles (for example top quarks at LEP) can appear. This gives valuable hints for the search for

new particles like the Higgs boson. When taking terms of higher order into account, the coupling of g_V^f and g_A^f, among other things, are affected by a coefficient that contains M_t^2 and $\ln(M_{\text{Higgs}}^2/M_W^2)$.

In case of hadronic final states, additional QCD corrections have to be considered, that consist of vertex corrections and gluon emission processes (compare figure E.3).

As gluons carry the color charge, they fragment similar to quarks. Gluon emission processes can be identified by a jet, indicating the direction of the gluon, in addition to the two jets of the quarks.

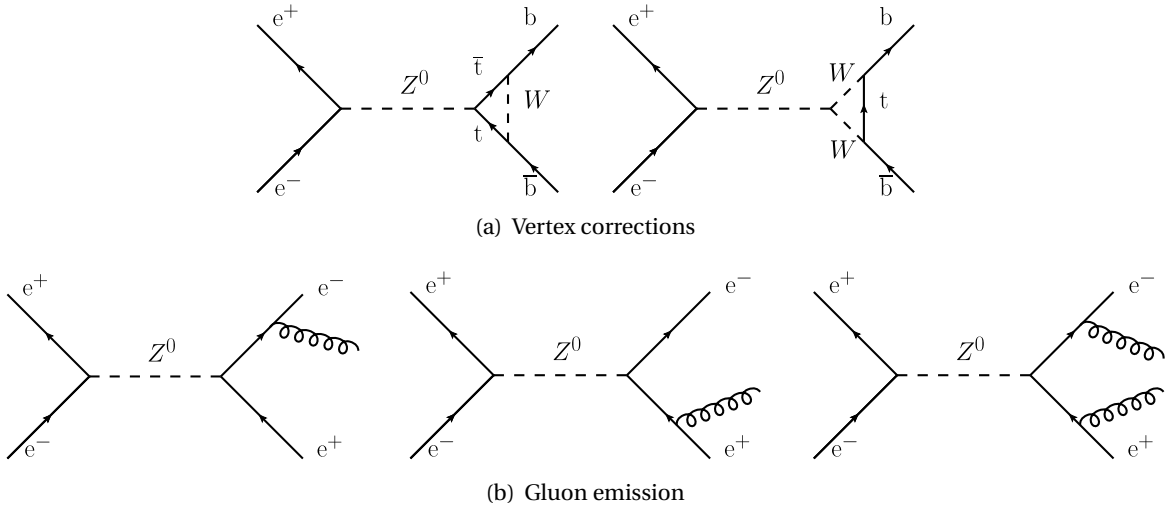

(a) Vertex corrections

(b) Gluon emission

Figure E.3.: Examples for Feynman diagrams for vertex corrections (a) and gluon emission processes (b).

In practice, the exact calculation of the radiation corrections is very complex due to the processes (Feynman graphs) of higher rder that are involved. For this practical, the energy dependant radiation corrections are provided in a table for the different values of the centre of mass energy.

F. Luminosity values

Table F.1.: Values for the integrated luminosity and corresponding errors for the OPAL datasets 1 to 6.

Dataset	$\sqrt{s}$ [GeV]	$\mathscr{L}\,\mathrm{d}t$ [nb^{-1}]	stat. error [nb^{-1}]	syst. error [nb^{-1}]	total error [nb^{-1}]
daten_1	88.48021	675.8590	3.502185	4.524100	5.721257
	89.47158	543.6270	3.179205	3.637000	4.830643
	90.22720	419.7760	2.810879	2.810400	3.974844
	91.23223	3122.204	7.786547	20.91518	22.31760
	91.97109	639.8380	3.567344	4.287300	5.577354
	92.97091	479.2400	3.121618	3.216000	4.481870
	93.71841	766.8380	3.972102	5.142000	6.497519
daten_2	88.47777	371.9800	2.594937	2.488100	3.595044
	89.46906	488.5300	3.009684	3.273000	4.446429
	90.22324	378.5461	2.670417	2.533900	3.681273
	91.23965	2072.793	6.334670	13.87960	15.25684
	91.96968	540.6800	3.274401	3.620000	4.881198
	92.97059	369.4000	2.737608	2.480000	3.693900
	93.71714	353.5000	2.695570	2.371000	3.589950
daten_3	88.47630	403.1200	2.702073	2.700000	3.819843
	89.46658	545.0066	3.174455	3.650900	4.837999
	90.21986	542.7271	3.200826	3.637500	4.845275
	91.22910	2080.004	6.346789	13.92980	15.30755
	91.96428	493.6100	3.126548	3.302000	4.547362
	92.96229	340.7600	2.630304	2.284000	3.483555
	93.71362	622.4900	3.579958	4.180000	5.503499
daten_4	88.47939	463.9790	2.902361	3.104100	4.249604
	89.46793	667.5236	3.521166	4.471900	5.691792
	90.22266	486.7641	3.033955	3.261500	4.454466
	91.22430	2246.568	6.603405	15.04780	16.43293
	91.96648	535.9080	3.265110	3.585300	4.849260
	92.96465	450.6000	3.027953	3.020000	4.276552
	93.71712	709.6980	3.819882	4.762000	6.104764
daten_5	88.47939	463.9790	2.902361	3.104100	4.249604
	89.46957	472.6636	2.964559	3.161900	4.334307
	90.23120	510.2150	3.099458	3.414400	4.611373
	91.23193	3898.628	8.694719	26.11330	27.52277
	91.97322	518.6880	3.213012	3.475300	4.732985
	92.96836	624.5900	3.564113	4.190000	5.500818
	93.71712	709.6980	3.819882	4.762000	6.104764
daten_6	88.48021	675.8590	3.502185	4.524100	5.721257
	89.46928	800.8436	3.855322	5.364900	6.606486
	90.22604	873.7021	4.057872	5.851900	7.121170
	91.24186	7893.498	12.37099	52.87910	54.30692
	91.96859	825.2780	4.051215	5.527300	6.852984
	92.96836	624.5900	3.564113	4.190000	5.500818
	93.71685	942.2280	4.403135	6.322000	7.704238

G. GROPE – Graphic Reconstruction of OPal Events

G.1. Execution of the program and important commands

Grope is executed from the command line interface with the command

grope *d*ataset

where *d*ataset is either one of the preselected (pure) learning datasets `ee`, `mm`, `tt`, `qq` or one of the mixed testing datasets `test1` to `test4`.

At execution, four windows are opened:

GROPE executive window:
input and output interface in the console – useful for the practical;

GROPE main browser:
command menu for advanced users – not important for the practical;

GROPE 'handy commands' panel:
graphical user interface (GUI) – contains most, but not all functions of the command line; while many of the existing buttons are not used! (Compare the command reference in table G.1);

GROPE gphigs:
main window for the graphical output.

The last three windows are shown in figure G.1 and G.2.

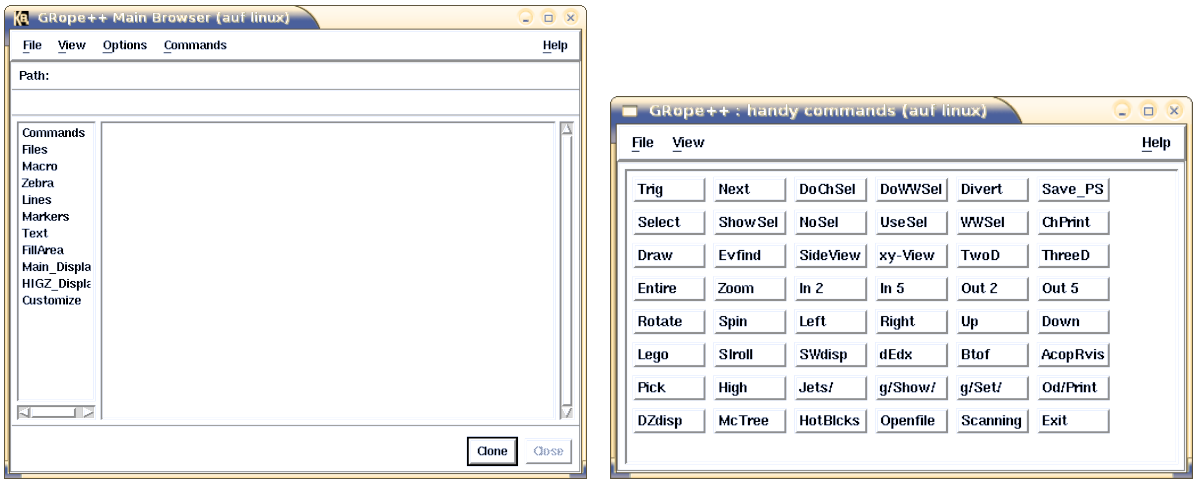

(a) Grope main browser

(b) Grope 'handy commands' panel

Figure G.1.: Grope display, part I

The **c**ommand input in Grope can be done – depending on preferences – either directly in the con-

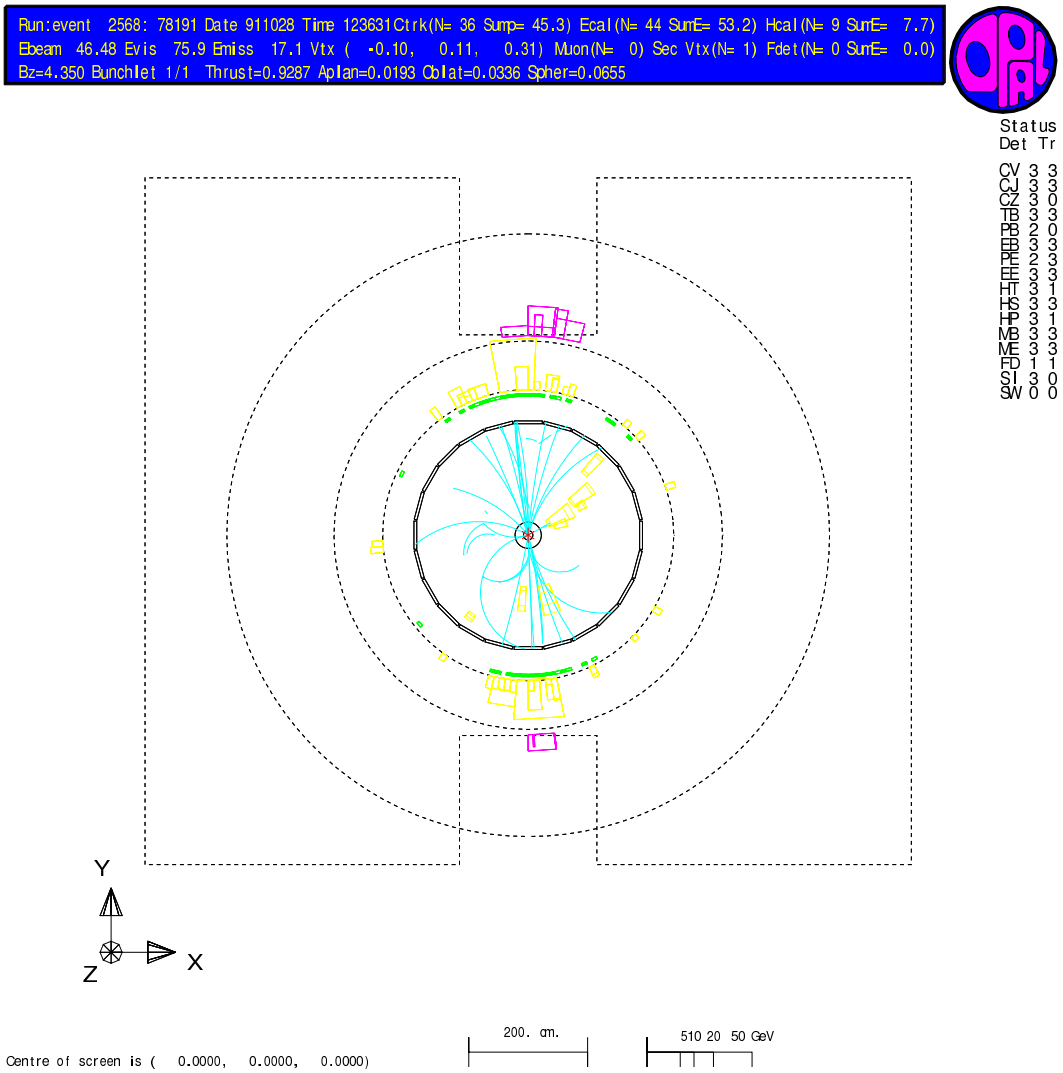

Figure G.2.: Grope display, part II

sole (in the „Grope executive window“) or using the mouse and buttons in the GUI GUI („Grope command panel“).[1] The most important commands can be found in table G.1.

Comments:

- It is often helpful to look at an event from different perspectives. You should use the posibility to switch between the projections offered by Grope.
- The GUI contains additional buttons for commands, that you will not need for the practical. Some of them are not implemented in the existing installation and can lead to crashes of the program. It is best to stick to the commands listed above.

[1] Grope is not case sensitive. This means you can type in the commands in the console like they are displayd in the GUI or – to keep it simple – using small letters.

Table G.1.: Grope command reference

command line	GUI	description
`next`	**N**ext	loads and displays the next event
`draw`	**D**raw	displays the current event again from scratch
`xy`,	**x**y-View	display of different projections
`xz`, `yz`	—	
`in` *z*ahl	**I**n *z*ahl	zoom in by a factor of *z*ahl
`out` *z*ahl	**O**ut *z*ahl	zoom out by a factor of *z*ahl
`entire`	**E**ntire	switch to *x y* view and eset of the zoom factor to the default value
`side`	**S**ide	switch to the view of the plane given by the beam and thrust axis

G.2. Definition of the used variables

In the gphigs window, on top of the graphical output, there is a *header*, that contains the following information for each event:

variable		explanation
Run		used as labels for the event
Event		
Date		
Time		
Ctrk	*charged tracks*	number (**N**) and sum of the momenta (**S**ump) of the charged traces
Ecal	*electromagnetic calorimeter*	number (**N**) and sum of the energies (**S**umE)
Hcal	*hadronic calorimeter*	number (**N**) and sum of the energies (**S**umE)
Ebeam	*beam energy*	beam energy, read half of the centre of mass energy
Evis	*visible energy*	„visible energy“ calculated from the charged traces and the calorimeter entries
Emiss	*missing energy*	„missing energy“ calculated as difference of Ebeam and Evis
Vtx	*vertex*	coordinates of the reconstructed interaction point
Muon		number of entries in the muon detector

Therein, all momenta are given in GeV/c, likewise, energies are given in GeV.

G.3. Additional tools

Apart from the visualization of the event geometry, Grope some more analysis tools. They are, however, if minor relevance for the tasks in this practical. Typing one of the following commands in the Grope console (or clicking the respective button in the GUI) for example, will open an additional grafical output window (GRope Graphics 1):

command line	GUI	description
`lego`	**l**ego	Lego plot with the parameters **C**trk, Ecal, Hcal, Fdet+SiW displayd in the $(\cos\theta, \varphi)$ plane.
`dedx`	**d**Edx	Display of the energy loss $\frac{dE}{dx}$ against the particle momentum p: typical courves for protons, electrons, muons,pions and kaons are given as comparison. Useful for the identification/differentiation of different particle types.
`btof`	**B**tof	Display of the value for $\beta = v/c$, derived from the *time of flight* (*TOF*), as function of the particle momentum p. This plot can also be used for particle identification.

H. Working with the data alalysis package ROOT

Brief instruction

The data analysis package ROOT [ROOT] was developed at CERN to analyze huge amounts of data regarding different aspects. One can study the influence of cuts on one or more properties on the distibution of another variable and display the result graphically, for example. The fit of a model courve to the measured data is also possible with ROOT.
The package is complex and vast; the structure is object-oriented and the syntax is close to that of C++. Root can do much more than what can be described in this sbrief instruction, which is why the realization of some simple tasks can look rather complicated. To use ROOT for this practical, however, only a small number of commands are important. They are summarized below.

General

An interactive ROOT session is started from the Linux terminal with the command

`root -l`

(The option –l supresses the display of the graphical start display with the ROOT and does nothing else.) This command opens the ROOT console, where interactive commands can be executed and a macro, that has been prepared beforehand, (basically a set of consecutive commands) can be loaded/executed.

The ROOT session can be terminated with the command

`.q`

Execution of a ROOT macro

An example of a ROOT macro is the file

/home/fpraktikum/analysis_scripts/part3/fit_breitwigner.C

With the command

`.x fit_breitwigner.C("resultfile")`

in the ROOT console, the commands in the macro are processed step by step.

Instead of the ROOT console, macros can be executed (most of the time) directly from the Linux terminal:

`root -l mc_histos.C`

Opening and inspecting a ROOT file

ROOT saved files in its own format, which can be reckognized by its suffix .root. How to open a ROOT file from the Linux terminal and interactively display its contents with the commans .ls is demonstrated in the listing H.1.

Listing H.1: This is how to open a ROOT file and display its contents. The file daten_6.root contains a tree with the name h33, its contents are shown in figure H.1 .

```
root -l daten_6.root

root [0]
Attaching file daten_6.root as _file0...
root [1] .ls
TFile**         daten_6.root    HBOOK file: daten_6.rz converted to ROOT
 TFile*         daten_6.root    HBOOK file: daten_6.rz converted to ROOT
  KEY: TTree    h33;1   OPAL
```

A ROOT file can contain different objects. The following object types are of relevance to us primarely:

- datasets, often in a matrix like, so called ntuple (Ger.: *N*-Tupel). They are organized in a tree structure (ROOT class: TTree, see ROOT Users Guide as Reference [ROOT] and the tutorial-page for tree objects at `http://root.cern.ch/root/html/tutorials/tree/index.html`). An example of a root tree can be found in figure H.1.
- complete plots, typically histograms or graphs (see the ROOT Users Gide and the corresponding tutorials again) can be saved as ROOT file right after their generation by a macro. The same goes for a drawing surface (*c*anvas), that can contain multiple histograms or graphs. The macro `fit_breitwigner.C` mentioned above generates a ROOT file with the following content for example:

Listing H.2: Contents of another ROOT file. This time, a tree (name for a ntuple) and a canvas with the name c1 has been saved.

```
root -l z0_results_errors.root

root [0]
Attaching file z0_results_errors.root as _file0...
root [1] .ls
TFile**         z0_results_errors.root
 TFile*         z0_results_errors.root
  KEY: TCanvas  c1;1      Fit der partiellen Wirkungsquerschnitte
  KEY: TNtuple  ntuple;1  Energie und part. Wirkungsquerschnitte
```

The content of a ROOT file can be displayd with a GUI browser. This is doen with the command

new TBrowser

after launching ROOT. A typical browser window is shown in figure H.2. Both TreeViewer and TBrowser can be used to access histograms/graphs, canvas data container (...) in a ROOT file interactively using the mouse. One usually does not achieve the same functionality and flexibility compared to executing the same operations in the ROOT command line.

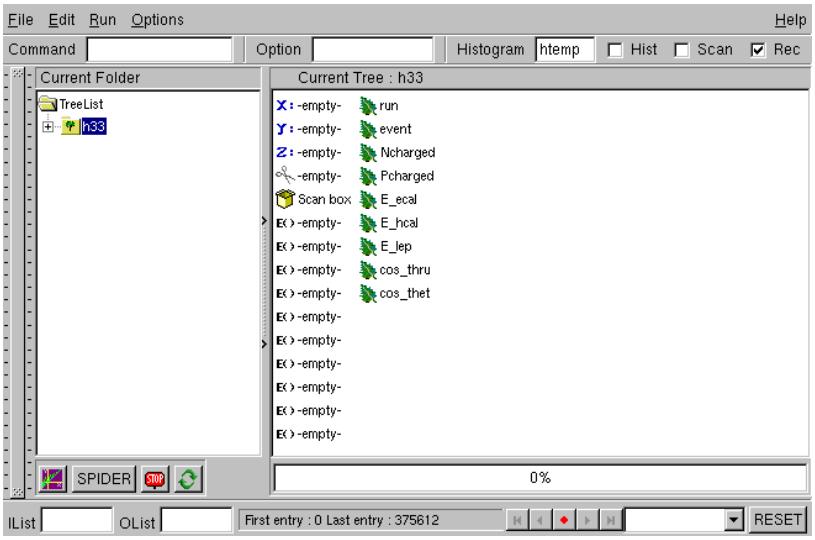

Figure H.1.: Example of a ROOT tree object. The contents of the tree can be displayed ith the command `treename->StartViewer()`. (In this example, h33 is, like in listing H.1, the `treename`).

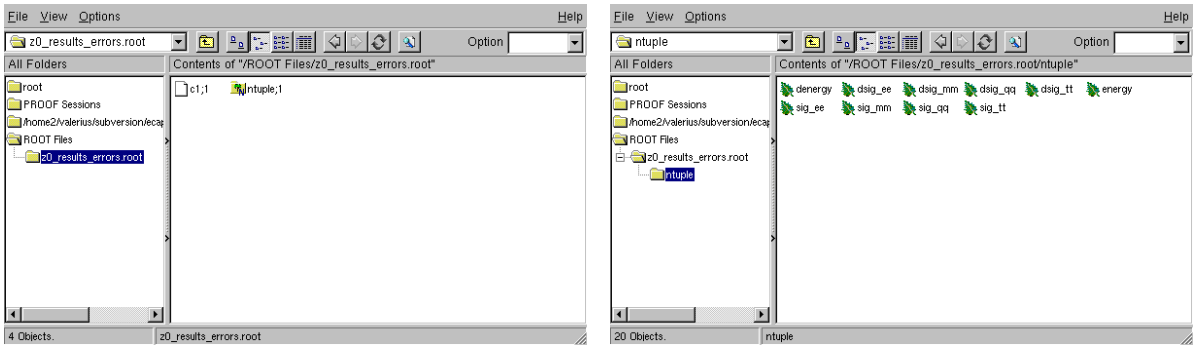

(a) whole file

(b) only ntuple

Figure H.2.: ROOT object browser „TBrowser“.

Moreuseful commands

- open the file example.root from an existing ROOT session:
  TFile *f1 = TFile::Open(“example.root”)
- draw the histogram hist1, that has been generated before:
  hist1->Draw()
- choose color for the histogram hist1:
  hist1->SetLineColor(X), with X=1: black, 2: red, 3: green, 4: blue, 5: yellow, 6: pink
- set the axis titles:
  hist1->SetXTitle(“title1”); hist1->SetYTitle(“title2”)
- normalization of the histogram hist1 to an event number defined by the user:
  hist1->SetNormFactor(Ereigniszahl)
- integrate over the histogram from BinNr_min to BinNr_max:

hist1->Integral(BinNr_min, BinNr_max)

- subtract the histogram hist2, scaled down half, from hist1:

  hist1->Add(hist2, -0.5)

- draw another histogram into an existing one:

  hist2->Draw("same")

- a cut can be defined like this:

  TCut cut1 = "Ncharged < 4" or Tcut cut2 = "E_ECAL < 82"

  The execution of the cut ona ntuple is donw with

  ntuplename->Draw("Pcharged", cut1)

  Different cuts can be combined freely, for example with

  ntuplename->Draw("Pcharged", cut1&&cut2)

  (The logical operations AND and OR are indicated in ROOT using C++ style, which is && and || respectively.)

- saving the contents of a canvas canvas1 in a postscript file (other output formats work analogue):

  canvas1->Print("outputfile.ps")

- work with two histograms from different root files, for example hist1 in file1.root and hist2 in file2.root:

  - load file file1.root, set hist1 a vname for a variable: var1 = hist1
  - load file file2.root, draw histogram hist2: hist2->Draw()
  - draw hist1 in the already existing histogram: var1->Draw("same")

- Similar actions are possible for complete trees or ntuples from different root files:

  - load file ee.root, set an unique name for h3 in it:

    TFile *ee = TFile::Open("~/data/mc/ee.root")

    TTree *eetree = h3
  - load file mm.root, set an unique name for h3 in it:

    TFile *mm = TFile::Open("~/data/mc/mm.root")

    TTree *mmtree = h3
  - ... analogue for additional files ...
  - Use the same, previously defined, cuts on different trees:

    eetree->Draw("Ncharged", cut1&&cut2)

    mmtree->Draw("Ncharged", cut1&&cut2)

  This allows for efficient working when determining the background and acceptance of the cuts on MC datasets.

I. Particle Data Booklet

What follows are excerpts from the *R*eview of Particle Properties (kurz: *R*PP) [PDG08]. The RPP is a wide collection of data and overview articles related to particle physics, released every two years as updated version by the Particle Data Group. Although the number of elementary particles could be reduced by reducing the mesons and baryons to their constituents, the RPP contains all particles that have been found so far. All known quantum numbers as well as their mass, charge, mean life time (and decay width respectively) and additional data is included. In addition to these general properties, the individual decay channels along with their branching ratio are listed.

For reasons of space, only the tables for leptons, quarks and gauge bosons are included here; the listings in the whole RPP are far more extensive. The overview articles, that are included in addition to the tables, cover vast complexes of themes like particle detection technique, accelerator systems, probability theory and statistics, but also the big bang model and modern cosmology.

Apart from the website (`http://pdg.lbl.gov`), the *P*article Data Booklet, that contains the most important data in compressed form and is available for this practical, can come in handy to look things up quickly.

LEPTONS

e

$J = \frac{1}{2}$

Mass $m = (548.57990943 \pm 0.00000023) \times 10^{-6}$ u
Mass $m = 0.510998910 \pm 0.000000013$ MeV
$|m_{e^+} - m_{e^-}|/m < 8 \times 10^{-9}$, CL = 90%
$|q_{e^+} + q_{e^-}|/e < 4 \times 10^{-8}$
Magnetic moment anomaly
$(g-2)/2 = (1159.65218073 \pm 0.00000028) \times 10^{-6}$
$(g_{e^+} - g_{e^-}) / g_{\text{average}} = (-0.5 \pm 2.1) \times 10^{-12}$
Electric dipole moment $d = (0.07 \pm 0.07) \times 10^{-26}$ $e$cm
Mean life $\tau > 4.6 \times 10^{26}$ yr, CL = 90% [a]

μ

$J = \frac{1}{2}$

Mass $m = 0.1134289256 \pm 0.0000000029$ u
Mass $m = 105.658367 \pm 0.000004$ MeV
Mean life $\tau = (2.197034 \pm 0.000021) \times 10^{-6}$ s (S = 1.2)
$\tau_{\mu^+}/\tau_{\mu^-} = 1.00002 \pm 0.00008$
$c\tau = 658.654$ m
Magnetic moment anomaly $(g-2)/2 = (11659208 \pm 6) \times 10^{-10}$
$(g_{\mu^+} - g_{\mu^-}) / g_{\text{average}} = (-0.11 \pm 0.12) \times 10^{-8}$
Electric dipole moment $d = (3.7 \pm 3.4) \times 10^{-19}$ $e$cm

Decay parameters [b]

$\rho = 0.7503 \pm 0.0004$
$\eta = 0.001 \pm 0.024$ (S = 2.0)
$\delta = 0.7504 \pm 0.0006$
$\xi P_\mu = 1.0007 \pm 0.0035$ [c]
$\xi P_\mu \delta/\rho > 0.99682$, CL = 90% [c]
$\xi' = 1.00 \pm 0.04$
$\xi'' = 0.7 \pm 0.4$
$\alpha/A = (0 \pm 4) \times 10^{-3}$
$\alpha'/A = (0 \pm 4) \times 10^{-3}$
$\beta/A = (4 \pm 6) \times 10^{-3}$
$\beta'/A = (1 \pm 5) \times 10^{-3}$
$\overline{\eta} = 0.02 \pm 0.08$

μ^+ modes are charge conjugates of the modes below.

μ^- DECAY MODES		Fraction (Γ_i/Γ)	Confidence level	p (MeV/c)
$e^- \overline{\nu}_e \nu_\mu$		$\approx 100\%$		53
$e^- \overline{\nu}_e \nu_\mu \gamma$	[d]	(1.4±0.4) %		53
$e^- \overline{\nu}_e \nu_\mu e^+ e^-$	[e]	$(3.4\pm0.4) \times 10^{-5}$		53
Lepton Family number (LF) violating modes				
$e^- \nu_e \overline{\nu}_\mu$	LF	[f] < 1.2 %	90%	53
$e^- \gamma$	LF	$< 1.2 \times 10^{-11}$	90%	53
$e^- e^+ e^-$	LF	$< 1.0 \times 10^{-12}$	90%	53
$e^- 2\gamma$	LF	$< 7.2 \times 10^{-11}$	90%	53

τ

$J = \frac{1}{2}$

Mass $m = 1776.84 \pm 0.17$ MeV
$(m_{\tau^+} - m_{\tau^-})/m_{\text{average}} < 2.8 \times 10^{-4}$, CL = 90%
Mean life $\tau = (290.6 \pm 1.0) \times 10^{-15}$ s
$c\tau = 87.11$ μm
Magnetic moment anomaly > -0.052 and < 0.013, CL = 95%
$\text{Re}(d_\tau) = -0.22$ to 0.45×10^{-16} $e$cm, CL = 95%
$\text{Im}(d_\tau) = -0.25$ to 0.008×10^{-16} $e$cm, CL = 95%

Weak dipole moment

$\text{Re}(d_\tau^w) < 0.50 \times 10^{-17}$ $e$cm, CL = 95%
$\text{Im}(d_\tau^w) < 1.1 \times 10^{-17}$ $e$cm, CL = 95%

Weak anomalous magnetic dipole moment

$\text{Re}(\alpha_\tau^w) < 1.1 \times 10^{-3}$, CL = 95%
$\text{Im}(\alpha_\tau^w) < 2.7 \times 10^{-3}$, CL = 95%

Decay parameters

See the τ Particle Listings for a note concerning τ-decay parameters.

$\rho(e \text{ or } \mu) = 0.745 \pm 0.008$
$\rho(e) = 0.747 \pm 0.010$
$\rho(\mu) = 0.763 \pm 0.020$
$\xi(e \text{ or } \mu) = 0.985 \pm 0.030$
$\xi(e) = 0.994 \pm 0.040$
$\xi(\mu) = 1.030 \pm 0.059$
$\eta(e \text{ or } \mu) = 0.013 \pm 0.020$
$\eta(\mu) = 0.094 \pm 0.073$
$(\delta\xi)(e \text{ or } \mu) = 0.746 \pm 0.021$
$(\delta\xi)(e) = 0.734 \pm 0.028$
$(\delta\xi)(\mu) = 0.778 \pm 0.037$
$\xi(\pi) = 0.993 \pm 0.022$
$\xi(\rho) = 0.994 \pm 0.008$
$\xi(a_1) = 1.001 \pm 0.027$
$\xi(\text{all hadronic modes}) = 0.995 \pm 0.007$

τ^+ modes are charge conjugates of the modes below. "$h^\pm$" stands for $\pi^\pm$ or $K^\pm$. "ℓ" stands for e or μ. "Neutrals" stands for γ's and/or π^0's.

τ^- DECAY MODES		Fraction (Γ_i/Γ)	Scale factor/ Confidence level	p (MeV/c)
Modes with one charged particle				
particle$^- \geq 0$ neutrals $\geq 0 K^0 \nu_\tau$ ("1-prong")		(85.36±0.08) %	S=1.3	–
particle$^- \geq 0$ neutrals $\geq 0 K_L^0 \nu_\tau$		(84.72±0.08) %	S=1.4	–
$\mu^- \overline{\nu}_\mu \nu_\tau$	[g]	(17.36±0.05) %		885
$\mu^- \overline{\nu}_\mu \nu_\tau \gamma$	[e]	$(3.6 \pm 0.4) \times 10^{-3}$		885
$e^- \overline{\nu}_e \nu_\tau$	[g]	(17.85±0.05) %		888
$e^- \overline{\nu}_e \nu_\tau \gamma$	[e]	(1.75±0.18) %		888
$h^- \geq 0 K_L^0 \nu_\tau$		(12.13±0.07) %	S=1.1	883
$h^- \nu_\tau$		(11.61±0.06) %	S=1.1	883
$\pi^- \nu_\tau$	[g]	(10.91±0.07) %	S=1.1	883
$K^- \nu_\tau$	[g]	$(6.96\pm0.23) \times 10^{-3}$	S=1.1	820
$h^- \geq 1$ neutrals ν_τ		(37.06±0.10) %	S=1.2	–
$h^- \geq 1\pi^0 \nu_\tau$ (ex. K^0)		(36.54±0.11) %	S=1.2	–
$h^- \pi^0 \nu_\tau$		(25.94±0.09) %	S=1.1	878
$\pi^- \pi^0 \nu_\tau$	[g]	(25.51±0.09) %	S=1.1	878
$\pi^- \pi^0$ non-$\rho(770) \nu_\tau$		$(3.0 \pm 3.2) \times 10^{-3}$		878
$K^- \pi^0 \nu_\tau$	[g]	$(4.29\pm0.15) \times 10^{-3}$		814

$h^- \geq 2\pi^0 \nu_\tau$		(10.85±0.12) %	S=1.3	–
$h^- 2\pi^0 \nu_\tau$		(9.51±0.11) %	S=1.2	862
$h^- 2\pi^0 \nu_\tau$ (ex. K^0)		(9.35±0.11) %	S=1.2	862
$\pi^- 2\pi^0 \nu_\tau$ (ex. K^0)	[g]	(9.29±0.11) %	S=1.2	862
$\pi^- 2\pi^0 \nu_\tau$ (ex. K^0), scalar		$< 9 \times 10^{-3}$	CL=95%	862
$\pi^- 2\pi^0 \nu_\tau$ (ex. K^0), vector		$< 7 \times 10^{-3}$	CL=95%	862
$K^- 2\pi^0 \nu_\tau$ (ex. K^0)	[g]	$(6.5 \pm 2.3) \times 10^{-4}$		796
$h^- \geq 3\pi^0 \nu_\tau$		(1.34±0.07) %	S=1.1	–
$h^- \geq 3\pi^0 \nu_\tau$ (ex. K^0)		(1.25±0.07) %	S=1.1	–
$h^- 3\pi^0 \nu_\tau$		(1.18±0.08) %		836
$\pi^- 3\pi^0 \nu_\tau$ (ex. K^0)	[g]	(1.04±0.07) %		836
$K^- 3\pi^0 \nu_\tau$ (ex. K^0, η)	[g]	$(4.9 \pm 2.3) \times 10^{-4}$	S=1.1	765
$h^- 4\pi^0 \nu_\tau$ (ex. K^0)		$(1.5 \pm 0.4) \times 10^{-3}$		800
$h^- 4\pi^0 \nu_\tau$ (ex. K^0, η)	[g]	$(1.1 \pm 0.4) \times 10^{-3}$		800
$K^- \geq 0\pi^0 \geq 0 K^0 \geq 0\gamma \nu_\tau$		(1.57±0.04) %	S=1.1	820
$K^- \geq 1$ (π^0 or K^0 or γ) ν_τ		$(8.72\pm0.32) \times 10^{-3}$	S=1.1	–
Modes with K^0's				
K_S^0 (particles)$^- \nu_\tau$		$(9.2 \pm 0.4) \times 10^{-3}$	S=1.5	–
$h^- \overline{K}^0 \nu_\tau$		(1.00±0.05) %	S=1.8	812
$\pi^- \overline{K}^0 \nu_\tau$	[g]	$(8.4 \pm 0.4) \times 10^{-3}$	S=2.1	812
$\pi^- \overline{K}^0$ (non-$K^*(892)^-$) ν_τ		$(5.4 \pm 2.1) \times 10^{-4}$		812
$K^- K^0 \nu_\tau$	[g]	$(1.59\pm0.16) \times 10^{-3}$		737
$K^- K^0 \geq 0\pi^0 \nu_\tau$		$(3.18\pm0.24) \times 10^{-3}$		737
$h^- \overline{K}^0 \pi^0 \nu_\tau$		$(5.5 \pm 0.4) \times 10^{-3}$		794
$\pi^- \overline{K}^0 \pi^0 \nu_\tau$	[g]	$(4.0 \pm 0.4) \times 10^{-3}$		794
$\overline{K}^0 \rho^- \nu_\tau$		$(2.2 \pm 0.5) \times 10^{-3}$		612
$K^- K^0 \pi^0 \nu_\tau$	[g]	$(1.59\pm0.20) \times 10^{-3}$		685
$\pi^- \overline{K}^0 \geq 1\pi^0 \nu_\tau$		$(3.2 \pm 1.0) \times 10^{-3}$		–
$\pi^- \overline{K}^0 \pi^0 \pi^0 \nu_\tau$		$(2.6 \pm 2.4) \times 10^{-4}$		763
$K^- K^0 \pi^0 \pi^0 \nu_\tau$		$< 1.6 \times 10^{-4}$	CL=95%	619
$\pi^- K^0 \overline{K}^0 \nu_\tau$		$(1.7 \pm 0.4) \times 10^{-3}$	S=1.6	682
$\pi^- K_S^0 K_S^0 \nu_\tau$	[g]	$(2.4 \pm 0.5) \times 10^{-4}$		682
$\pi^- K_S^0 K_L^0 \nu_\tau$	[g]	$(1.2 \pm 0.4) \times 10^{-3}$	S=1.7	682
$\pi^- K^0 \overline{K}^0 \pi^0 \nu_\tau$		$(3.1 \pm 2.3) \times 10^{-4}$		614
$\pi^- K_S^0 K_S^0 \pi^0 \nu_\tau$		$< 2.0 \times 10^{-4}$	CL=95%	614
$\pi^- K_S^0 K_L^0 \pi^0 \nu_\tau$		$(3.1 \pm 1.2) \times 10^{-4}$		614
$K^0 h^+ h^- h^- \geq 0$ neutrals ν_τ		$< 1.7 \times 10^{-3}$	CL=95%	760
$K^0 h^+ h^- h^- \nu_\tau$		$(2.3 \pm 2.0) \times 10^{-4}$		760

Modes with three charged particles

$h^-h^-h^+ \geq 0$ neutrals $\geq 0K^0_L\nu_\tau$		(15.19±0.08) %		S=1.4	861
$h^-h^-h^+ \geq 0$ neutrals ν_τ (ex. $K^0_S \to \pi^+\pi^-$) ("3-prong")		(14.56±0.08) %		S=1.3	861
$h^-h^-h^+\nu_\tau$		(9.80±0.08) %		S=1.4	861
$h^-h^-h^+\nu_\tau$(ex.K^0)		(9.46±0.07) %		S=1.3	861
$h^-h^-h^+\nu_\tau$(ex.K^0,ω)		(9.42±0.07) %		S=1.3	861
$\pi^-\pi^+\pi^-\nu_\tau$		(9.32±0.07) %		S=1.2	861
$\pi^-\pi^+\pi^-\nu_\tau$(ex.K^0)		(9.03±0.06) %		S=1.2	861
$\pi^-\pi^+\pi^-\nu_\tau$(ex.K^0), non-axial vector		< 2.4 %	CL=95%		861
$\pi^-\pi^+\pi^-\nu_\tau$(ex.K^0,ω)	[g]	(9.00±0.06) %		S=1.2	861
$h^-h^-h^+ \geq 1$ neutrals ν_τ		(5.38±0.07) %		S=1.2	–
$h^-h^-h^+ \geq 1\pi^0\nu_\tau$(ex. K^0)		(5.08±0.06) %		S=1.1	–
$h^-h^-h^+\pi^0\nu_\tau$		(4.75±0.06) %		S=1.2	834
$h^-h^-h^+\pi^0\nu_\tau$(ex.K^0)		(4.56±0.06) %		S=1.2	834
$h^-h^-h^+\pi^0\nu_\tau$(ex. K^0, ω)		(2.79±0.08) %		S=1.2	834
$\pi^-\pi^+\pi^-\pi^0\nu_\tau$		(4.61±0.06) %		S=1.1	834
$\pi^-\pi^+\pi^-\pi^0\nu_\tau$(ex.$K^0$)		(4.48±0.06) %		S=1.2	834
$\pi^-\pi^+\pi^-\pi^0\nu_\tau$(ex.$K^0$,$\omega$)	[g]	(2.70±0.08) %		S=1.2	834
$h^-h^-h^+ \geq 2\pi^0\nu_\tau$(ex. K^0)		(5.18±0.33) $\times 10^{-3}$			–
$h^-h^-h^+2\pi^0\nu_\tau$		(5.06±0.32) $\times 10^{-3}$			797
$h^-h^-h^+2\pi^0\nu_\tau$(ex.K^0)		(4.95±0.32) $\times 10^{-3}$			797
$h^-h^-h^+2\pi^0\nu_\tau$(ex.K^0,ω,η)	[g]	(10 ±4) $\times 10^{-4}$			797
$h^-h^-h^+3\pi^0\nu_\tau$	[g]	(2.3 ±0.7) $\times 10^{-4}$		S=1.3	749
$K^-h^+h^- \geq 0$ neutrals ν_τ		(6.24±0.24) $\times 10^{-3}$		S=1.5	794
$K^-h^+\pi^-\nu_\tau$(ex.K^0)		(4.27±0.20) $\times 10^{-3}$		S=2.4	794
$K^-h^+\pi^-\pi^0\nu_\tau$(ex.K^0)		(8.7 ±1.2) $\times 10^{-4}$		S=1.1	763
$K^-\pi^+\pi^- \geq 0$ neutrals ν_τ		(4.78±0.21) $\times 10^{-3}$		S=1.3	794
$K^-\pi^+\pi^- \geq 0\pi^0\nu_\tau$(ex.$K^0$)		(3.68±0.20) $\times 10^{-3}$		S=1.4	794
$K^-\pi^+\pi^-\nu_\tau$		(3.42±0.17) $\times 10^{-3}$		S=1.8	794
$K^-\pi^+\pi^-\nu_\tau$(ex.K^0)	[g]	(2.87±0.16) $\times 10^{-3}$		S=2.1	794
$K^-\rho^0\nu_\tau \to K^-\pi^+\pi^-\nu_\tau$		(1.4 ±0.5) $\times 10^{-3}$			–
$K^-\pi^+\pi^-\pi^0\nu_\tau$		(1.36±0.14) $\times 10^{-3}$			763
$K^-\pi^+\pi^-\pi^0\nu_\tau$(ex.$K^0$)		(8.1 ±1.2) $\times 10^{-4}$			763
$K^-\pi^+\pi^-\pi^0\nu_\tau$(ex.$K^0$,$\eta$)	[g]	(7.7 ±1.2) $\times 10^{-4}$			763
$K^-\pi^+\pi^-\pi^0\nu_\tau$(ex.$K^0$,$\omega$)		(3.7 ±0.9) $\times 10^{-4}$			763
$K^-\pi^+K^- \geq 0$ neut. ν_τ		< 9 $\times 10^{-4}$	CL=95%		685
$K^-K^+\pi^- \geq 0$ neut. ν_τ		(1.46±0.06) $\times 10^{-3}$		S=1.6	685
$K^-K^+\pi^-\nu_\tau$	[g]	(1.40±0.05) $\times 10^{-3}$		S=1.7	685

$K^-K^+\pi^-\pi^0\nu_\tau$	[g]	(6.1 ±2.5) $\times 10^{-5}$		S=1.4	618
$K^-K^+K^- \geq 0$ neut. ν_τ		< 2.1 $\times 10^{-3}$	CL=95%		472
$K^-K^+K^-\nu_\tau$		(1.58±0.18) $\times 10^{-5}$			472
$K^-K^+K^-\nu_\tau$(ex. ϕ)		< 2.5 $\times 10^{-6}$	CL=90%		–
$K^-K^+K^-\pi^0\nu_\tau$		< 4.8 $\times 10^{-6}$	CL=90%		345
$\pi^-K^+\pi^- \geq 0$ neut. ν_τ		< 2.5 $\times 10^{-3}$	CL=95%		794
$e^-e^-e^+\overline{\nu}_e\nu_\tau$		(2.8 ±1.5) $\times 10^{-5}$			888
$\mu^-e^-e^+\overline{\nu}_\mu\nu_\tau$		< 3.6 $\times 10^{-5}$	CL=90%		885

Modes with five charged particles

$3h^-2h^+ \geq 0$ neutrals ν_τ (ex. $K^0_S \to \pi^-\pi^+$) ("5-prong")		(1.02±0.04) $\times 10^{-3}$		S=1.1	794
$3h^-2h^+\nu_\tau$(ex.K^0)	[g]	(8.39±0.35) $\times 10^{-4}$		S=1.1	794
$3h^-2h^+\pi^0\nu_\tau$(ex.K^0)	[g]	(1.78±0.27) $\times 10^{-4}$			746
$3h^-2h^+2\pi^0\nu_\tau$		< 3.4 $\times 10^{-6}$	CL=90%		687

Miscellaneous other allowed modes

$(5\pi)^-\nu_\tau$		(7.6 ±0.5) $\times 10^{-3}$			800
$4h^-3h^+ \geq 0$ neutrals ν_τ ("7-prong")		< 3.0 $\times 10^{-7}$	CL=90%		682
$4h^-3h^+\nu_\tau$		< 4.3 $\times 10^{-7}$	CL=90%		682
$4h^-3h^+\pi^0\nu_\tau$		< 2.5 $\times 10^{-7}$	CL=90%		612
$X^-(S{=}-1)\nu_\tau$		(2.86±0.07) %		S=1.3	–
$K^*(892)^- \geq 0$ neutrals $\geq 0K^0_L\nu_\tau$		(1.42±0.18) %		S=1.4	665
$K^*(892)^-\nu_\tau$		(1.20±0.07) %		S=1.8	665
$K^*(892)^-\nu_\tau \to \pi^-\overline{K}^0\nu_\tau$		(7.8 ±0.5) $\times 10^{-3}$			–
$K^*(892)^0K^- \geq 0$ neutrals ν_τ		(3.2 ±1.4) $\times 10^{-3}$			542
$K^*(892)^0K^-\nu_\tau$		(2.1 ±0.4) $\times 10^{-3}$			542
$\overline{K}^*(892)^0\pi^- \geq 0$ neutrals ν_τ		(3.8 ±1.7) $\times 10^{-3}$			655
$\overline{K}^*(892)^0\pi^-\nu_\tau$		(2.2 ±0.5) $\times 10^{-3}$			655
$(\overline{K}^*(892)\pi)^-\nu_\tau \to \pi^-\overline{K}^0\pi^0\nu_\tau$		(1.0 ±0.4) $\times 10^{-3}$			–
$K_1(1270)^-\nu_\tau$		(4.7 ±1.1) $\times 10^{-3}$			433
$K_1(1400)^-\nu_\tau$		(1.7 ±2.6) $\times 10^{-3}$		S=1.7	335
$K^*(1410)^-\nu_\tau$		(1.5 $^{+1.4}_{-1.0}$) $\times 10^{-3}$			326
$K^*_0(1430)^-\nu_\tau$		< 5 $\times 10^{-4}$	CL=95%		317
$K^*_2(1430)^-\nu_\tau$		< 3 $\times 10^{-3}$	CL=95%		317
$\eta\pi^-\nu_\tau$		< 1.4 $\times 10^{-4}$	CL=95%		797
$\eta\pi^-\pi^0\nu_\tau$	[g]	(1.39±0.10) $\times 10^{-3}$		S=1.4	778
$\eta\pi^-\pi^0\pi^0\nu_\tau$		(1.5 ±0.5) $\times 10^{-4}$			746
$\eta K^-\nu_\tau$	[g]	(1.61±0.11) $\times 10^{-4}$		S=1.1	719
$\eta K^*(892)^-\nu_\tau$		(1.38±0.15) $\times 10^{-4}$			511

$\eta K^-\pi^0\nu_\tau$		(4.8 ±1.2) $\times 10^{-5}$			665
$\eta K^-\pi^0$(non-$K^*(892)$)ν_τ		< 3.5 $\times 10^{-5}$	CL=90%		–
$\eta\overline{K}^0\pi^-\nu_\tau$		(9.3 ±1.5) $\times 10^{-5}$			661
$\eta\overline{K}^0\pi^-\pi^0\nu_\tau$		< 5.0 $\times 10^{-5}$	CL=90%		590
$\eta K^-K^0\nu_\tau$		< 9.0 $\times 10^{-6}$	CL=90%		430
$\eta\pi^+\pi^-\pi^- \geq 0$ neutrals ν_τ		< 3 $\times 10^{-3}$	CL=90%		744
$\eta\pi^-\pi^+\pi^-\nu_\tau$(ex.$K^0$)		(1.64±0.12) $\times 10^{-4}$			744
$\eta a_1(1260)^-\nu_\tau \to \eta\pi^-\rho^0\nu_\tau$		< 3.9 $\times 10^{-4}$	CL=90%		–
$\eta\eta\pi^-\nu_\tau$		< 7.4 $\times 10^{-6}$	CL=90%		637
$\eta\eta\pi^-\pi^0\nu_\tau$		< 2.0 $\times 10^{-4}$	CL=95%		559
$\eta\eta K^-\nu_\tau$		< 3.0 $\times 10^{-6}$	CL=90%		382
$\eta'(958)\pi^-\nu_\tau$		< 7.2 $\times 10^{-6}$	CL=90%		620
$\eta'(958)\pi^-\pi^0\nu_\tau$		< 8.0 $\times 10^{-5}$	CL=90%		591
$\phi\pi^-\nu_\tau$		(3.4 ±0.6) $\times 10^{-5}$			585
$\phi K^-\nu_\tau$		(3.70±0.33) $\times 10^{-5}$		S=1.3	445
$f_1(1285)\pi^-\nu_\tau$		(3.6 ±0.7) $\times 10^{-4}$			408
$f_1(1285)\pi^-\nu_\tau \to \eta\pi^-\pi^+\pi^-\nu_\tau$		(1.11±0.08) $\times 10^{-4}$			–
$\pi(1300)^-\nu_\tau \to (\rho\pi)^-\nu_\tau \to (3\pi)^-\nu_\tau$		< 1.0 $\times 10^{-4}$	CL=90%		–
$\pi(1300)^-\nu_\tau \to ((\pi\pi)_{S-\text{wave}}\,\pi)^-\nu_\tau \to (3\pi)^-\nu_\tau$		< 1.9 $\times 10^{-4}$	CL=90%		–
$h^-\omega \geq 0$ neutrals ν_τ		(2.41±0.09) %		S=1.2	708
$h^-\omega\nu_\tau$	[g]	(1.99±0.08) %		S=1.3	708
$K^-\omega\nu_\tau$		(4.1 ±0.9) $\times 10^{-4}$			610
$h^-\omega\pi^0\nu_\tau$	[g]	(4.1 ±0.4) $\times 10^{-3}$			684
$h^-\omega2\pi^0\nu_\tau$		(1.4 ±0.5) $\times 10^{-4}$			644
$h^-2\omega\nu_\tau$		< 5.4 $\times 10^{-7}$	CL=90%		250
$2h^-h^+\omega\nu_\tau$		(1.20±0.22) $\times 10^{-4}$			641

Lepton Family number (*LF*), Lepton number (*L*), or Baryon number (*B*) violating modes

L means lepton number violation (*e.g.* $\tau^- \to e^+\pi^-\pi^-$). Following common usage, *LF* means lepton family violation *and not* lepton number violation (*e.g.* $\tau^- \to e^-\pi^+\pi^-$). *B* means baryon number violation.

$e^-\gamma$	*LF*	< 1.1	$\times 10^{-7}$	CL=90%	888
$\mu^-\gamma$	*LF*	< 4.5	$\times 10^{-8}$	CL=90%	885
$e^-\pi^0$	*LF*	< 8.0	$\times 10^{-8}$	CL=90%	883
$\mu^-\pi^0$	*LF*	< 1.1	$\times 10^{-7}$	CL=90%	880
$e^-K^0_S$	*LF*	< 3.3	$\times 10^{-8}$	CL=90%	819
$\mu^-K^0_S$	*LF*	< 4.0	$\times 10^{-8}$	CL=90%	815
$e^-\eta$	*LF*	< 9.2	$\times 10^{-8}$	CL=90%	804
$\mu^-\eta$	*LF*	< 6.5	$\times 10^{-8}$	CL=90%	800

$e^-\rho^0$	*LF*	< 6.3	$\times 10^{-8}$	CL=90%	719
$\mu^-\rho^0$	*LF*	< 6.8	$\times 10^{-8}$	CL=90%	715
$e^-\omega$	*LF*	< 1.1	$\times 10^{-7}$	CL=90%	716
$\mu^-\omega$	*LF*	< 8.9	$\times 10^{-8}$	CL=90%	711
$e^-K^*(892)^0$	*LF*	< 7.8	$\times 10^{-8}$	CL=90%	665
$\mu^-K^*(892)^0$	*LF*	< 5.9	$\times 10^{-8}$	CL=90%	659
$e^-\overline{K}^*(892)^0$	*LF*	< 7.7	$\times 10^{-8}$	CL=90%	665
$\mu^-\overline{K}^*(892)^0$	*LF*	< 1.0	$\times 10^{-7}$	CL=90%	659
$e^-\eta'(958)$	*LF*	< 1.6	$\times 10^{-7}$	CL=90%	630
$\mu^-\eta'(958)$	*LF*	< 1.3	$\times 10^{-7}$	CL=90%	625
$e^-f_0(980) \to e^-\pi^+\pi^-$	*LF*	< 3.2	$\times 10^{-8}$	CL=90%	–
$\mu^-f_0(980) \to \mu^-\pi^+\pi^-$	*LF*	< 3.4	$\times 10^{-8}$	CL=90%	–
$e^-\phi$	*LF*	< 7.3	$\times 10^{-8}$	CL=90%	596
$\mu^-\phi$	*LF*	< 1.3	$\times 10^{-7}$	CL=90%	590
$e^-e^+e^-$	*LF*	< 3.6	$\times 10^{-8}$	CL=90%	888
$e^-\mu^+\mu^-$	*LF*	< 3.7	$\times 10^{-8}$	CL=90%	882
$e^+\mu^-\mu^-$	*LF*	< 2.3	$\times 10^{-8}$	CL=90%	882
$\mu^-e^+e^-$	*LF*	< 2.7	$\times 10^{-8}$	CL=90%	885
$\mu^+e^-e^-$	*LF*	< 2.0	$\times 10^{-8}$	CL=90%	885
$\mu^-\mu^+\mu^-$	*LF*	< 3.2	$\times 10^{-8}$	CL=90%	873
$e^-\pi^+\pi^-$	*LF*	< 1.2	$\times 10^{-7}$	CL=90%	877
$e^+\pi^-\pi^-$	*L*	< 2.0	$\times 10^{-7}$	CL=90%	877
$\mu^-\pi^+\pi^-$	*LF*	< 2.9	$\times 10^{-7}$	CL=90%	866
$\mu^+\pi^-\pi^-$	*L*	< 7	$\times 10^{-8}$	CL=90%	866
$e^-\pi^+K^-$	*LF*	< 3.2	$\times 10^{-7}$	CL=90%	813
$e^-\pi^-K^+$	*LF*	< 1.6	$\times 10^{-7}$	CL=90%	813
$e^+\pi^-K^-$	*L*	< 1.8	$\times 10^{-7}$	CL=90%	813
$e^-K^0_SK^0_S$	*LF*	< 2.2	$\times 10^{-6}$	CL=90%	736
$e^-K^+K^-$	*LF*	< 1.4	$\times 10^{-7}$	CL=90%	738
$e^+K^-K^-$	*L*	< 1.5	$\times 10^{-7}$	CL=90%	738
$\mu^-\pi^+K^-$	*LF*	< 2.6	$\times 10^{-7}$	CL=90%	800
$\mu^-\pi^-K^+$	*LF*	< 3.2	$\times 10^{-7}$	CL=90%	800
$\mu^+\pi^-K^-$	*L*	< 2.2	$\times 10^{-7}$	CL=90%	800
$\mu^-K^0_SK^0_S$	*LF*	< 3.4	$\times 10^{-6}$	CL=90%	696
$\mu^-K^+K^-$	*LF*	< 2.5	$\times 10^{-7}$	CL=90%	699
$\mu^+K^-K^-$	*L*	< 4.4	$\times 10^{-7}$	CL=90%	699
$e^-\pi^0\pi^0$	*LF*	< 6.5	$\times 10^{-6}$	CL=90%	878
$\mu^-\pi^0\pi^0$	*LF*	< 1.4	$\times 10^{-5}$	CL=90%	867
$e^-\eta\eta$	*LF*	< 3.5	$\times 10^{-5}$	CL=90%	699
$\mu^-\eta\eta$	*LF*	< 6.0	$\times 10^{-5}$	CL=90%	653
$e^-\pi^0\eta$	*LF*	< 2.4	$\times 10^{-5}$	CL=90%	798
$\mu^-\pi^0\eta$	*LF*	< 2.2	$\times 10^{-5}$	CL=90%	784
$\overline{p}\gamma$	*L*,*B*	< 3.5	$\times 10^{-6}$	CL=90%	641
$\overline{p}\pi^0$	*L*,*B*	< 1.5	$\times 10^{-5}$	CL=90%	632

$\overline{p}2\pi^0$	L,B	$<$	3.3	$\times 10^{-5}$	CL=90%	604
$\overline{p}\eta$	L,B	$<$	8.9	$\times 10^{-6}$	CL=90%	475
$\overline{p}\pi^0\eta$	L,B	$<$	2.7	$\times 10^{-5}$	CL=90%	360
$\Lambda\pi^-$	L,B	$<$	7.2	$\times 10^{-8}$	CL=90%	525
$\overline{\Lambda}\pi^-$	L,B	$<$	1.4	$\times 10^{-7}$	CL=90%	525
e^- light boson	LF	$<$	2.7	$\times 10^{-3}$	CL=95%	–
μ^- light boson	LF	$<$	5	$\times 10^{-3}$	CL=95%	–

Heavy Charged Lepton Searches

$L^\pm$ – charged lepton

Mass $m >$ 100.8 GeV, CL = 95% [h] Decay to νW.

$L^\pm$ – stable charged heavy lepton

Mass $m >$ 102.6 GeV, CL = 95%

Neutrino Properties

See the note on "Neutrino properties listings" in the Particle Listings.

Mass $m <$ 2 eV (tritium decay)
Mean life/mass, $\tau/m >$ 300 s/eV, CL = 90% (reactor)
Mean life/mass, $\tau/m > 7 \times 10^9$ s/eV (solar)
Mean life/mass, $\tau/m >$ 15.4 s/eV, CL = 90% (accelerator)
Magnetic moment $\mu < 0.54 \times 10^{-10}\ \mu_B$, CL = 90% (solar)

Number of Neutrino Types

Number $N = 2.984 \pm 0.008$ (Standard Model fits to LEP data)
Number $N = 2.92 \pm 0.05$ (S = 1.2) (Direct measurement of invisible Z width)

Neutrino Mixing

The following values are obtained through data analyses based on the 3-neutrino mixing scheme described in the review "Neutrino mass, mixing, and flavor change" by B. Kayser in this *Review*.

$\sin^2(2\theta_{12}) = 0.87 \pm 0.03$
$\Delta m^2_{21} = (7.59 \pm 0.20) \times 10^{-5}$ eV^2
$\sin^2(2\theta_{23}) > 0.92$ [i]
$\Delta m^2_{32} = (2.43 \pm 0.13) \times 10^{-3}$ eV^2 [j]
$\sin^2(2\theta_{13}) < 0.19$, CL = 90%

Heavy Neutral Leptons, Searches for

For excited leptons, see Compositeness Limits below.

Stable Neutral Heavy Lepton Mass Limits

Mass $m >$ 45.0 GeV, CL = 95% (Dirac)
Mass $m >$ 39.5 GeV, CL = 95% (Majorana)

Neutral Heavy Lepton Mass Limits

Mass $m >$ 90.3 GeV, CL = 95%
(Dirac ν_L coupling to e, μ, τ; conservative case(τ))
Mass $m >$ 80.5 GeV, CL = 95%
(Majorana ν_L coupling to e, μ, τ; conservative case(τ))

NOTES

[a] This is the best limit for the mode $e^- \to \nu\gamma$. The best limit for "electron disappearance" is 6.4×10^{24} yr.

[b] See the "Note on Muon Decay Parameters" in the μ Particle Listings for definitions and details.

[c] P_μ is the longitudinal polarization of the muon from pion decay. In standard $V-A$ theory, $P_\mu = 1$ and $\rho = \delta = 3/4$.

[d] This only includes events with the γ energy > 10 MeV. Since the $e^-\overline{\nu}_e\nu_\mu$ and $e^-\overline{\nu}_e\nu_\mu\gamma$ modes cannot be clearly separated, we regard the latter mode as a subset of the former.

[e] See the relevant Particle Listings for the energy limits used in this measurement.

[f] A test of additive vs. multiplicative lepton family number conservation.

[g] Basis mode for the τ.

[h] $L^\pm$ mass limit depends on decay assumptions; see the Full Listings.

[i] The limit quoted corresponds to the projection onto the $\sin^2(2\theta_{23})$ axis of the 90% CL contour in the $\sin^2(2\theta_{23})-\Delta m^2_{32}$ plane.

[j] The sign of Δm^2_{32} is not known at this time. The range quoted is for the absolute value.

QUARKS

The u-, d-, and s-quark masses are estimates of so-called "current-quark masses," in a mass-independent subtraction scheme such as $\overline{\text{MS}}$ at a scale $\mu \approx 2$ GeV. The c- and b-quark masses are the "running" masses in the $\overline{\text{MS}}$ scheme. For the b-quark we also quote the 1S mass. These can be different from the heavy quark masses obtained in potential models.

u

$I(J^P) = \frac{1}{2}(\frac{1}{2}^+)$

Mass $m = 1.5$ to 3.3 MeV [a] Charge $= \frac{2}{3}\,e$ $I_z = +\frac{1}{2}$

$m_u/m_d = 0.35$ to 0.60

d

$I(J^P) = \frac{1}{2}(\frac{1}{2}^+)$

Mass $m = 3.5$ to 6.0 MeV [a] Charge $= -\frac{1}{3}\,e$ $I_z = -\frac{1}{2}$

$m_s/m_d = 17$ to 22

$\overline{m} = (m_u + m_d)/2 = 2.5$ to 5.0 MeV

s

$I(J^P) = 0(\frac{1}{2}^+)$

Mass $m = 104^{+26}_{-34}$ MeV [a] Charge $= -\frac{1}{3}\,e$ Strangeness $= -1$

$(m_s - (m_u + m_d)/2)/(m_d - m_u) = 30$ to 50

c

$I(J^P) = 0(\frac{1}{2}^+)$

Mass $m = 1.27^{+0.07}_{-0.11}$ GeV Charge $= \frac{2}{3}\,e$ Charm $= +1$

b

$I(J^P) = 0(\frac{1}{2}^+)$

Charge $= -\frac{1}{3}\,e$ Bottom $= -1$

Mass $m = 4.20^{+0.17}_{-0.07}$ GeV ($\overline{\text{MS}}$ mass)

t

$I(J^P) = 0(\frac{1}{2}^+)$

Charge $= \frac{2}{3}\,e$ Top $= +1$

Mass $m = 171.2 \pm 2.1$ GeV [b] (direct observation of top events)

t DECAY MODES	Fraction (Γ_i/Γ)	Confidence level	p (MeV/c)
$W\,q\,(q = b,\ s,\ d)$			–
$W\,b$			–
$\ell\,\nu_\ell$ anything	[c,d] (9.4±2.4) %		–
$\gamma\,q\,(q=u,c)$	[e] < 5.9 $\times 10^{-3}$	95%	–

$\Delta T = 1$ weak neutral current ($T1$) modes					
$Z\,q\,(q=u,c)$	$T1$	[f] < 13.7	%	95%	–

b′ (4th Generation) Quark, Searches for

Mass $m >$ 190 GeV, CL = 95% ($p\overline{p}$, quasi-stable b')
Mass $m >$ 199 GeV, CL = 95% ($p\overline{p}$, neutral-current decays)
Mass $m >$ 128 GeV, CL = 95% ($p\overline{p}$, charged-current decays)
Mass $m >$ 46.0 GeV, CL = 95% (e^+e^-, all decays)

t′ (4th Generation) Quark, Searches for

Mass $m >$ 256 GeV, CL = 95% ($p\overline{p}$, $t'\overline{t}'$ prod., $t' \to W\,q$)

Free Quark Searches

All searches since 1977 have had negative results.

NOTES

[a] The ratios m_u/m_d and m_s/m_d are extracted from pion and kaon masses using chiral symmetry. The estimates of u and d masses are not without controversy and remain under active investigation. Within the literature there are even suggestions that the u quark could be essentially massless. The s-quark mass is estimated from SU(3) splittings in hadron masses.

[b] Based on published top mass measurements using data from Tevatron Run-I and Run-II. Including also the most recent unpublished results from Run-II, the Tevatron Electroweak Working Group reports a top mass of $172.6 \pm 0.8 \pm 1.1$ GeV. See the note "The Top Quark" in the Quark Particle Listings of this *Review*.

[c] ℓ means e or μ decay mode, not the sum over them.

[d] Assumes lepton universality and W-decay acceptance.

[e] This limit is for $\Gamma(t \to \gamma\,q)/\Gamma(t \to W\,b)$.

[f] This limit is for $\Gamma(t \to Z\,q)/\Gamma(t \to W\,b)$.

GAUGE AND HIGGS BOSONS

γ

$I(J^{PC}) = 0,1(1^{--})$

Mass $m < 1 \times 10^{-18}$ eV
Charge $q < 1 \times 10^{-35}$ e
Mean life τ = Stable

g or gluon

$I(J^{P}) = 0(1^{-})$

Mass $m = 0$ [a]
SU(3) color octet

W

$J = 1$

Charge $= \pm 1$ e
Mass $m = 80.398 \pm 0.025$ GeV
$m_Z - m_W = 10.4 \pm 1.6$ GeV
$m_{W^+} - m_{W^-} = -0.2 \pm 0.6$ GeV
Full width $\Gamma = 2.141 \pm 0.041$ GeV
$\langle N_{\pi^\pm} \rangle = 15.70 \pm 0.35$
$\langle N_{K^\pm} \rangle = 2.20 \pm 0.19$
$\langle N_p \rangle = 0.92 \pm 0.14$
$\langle N_{\text{charged}} \rangle = 19.39 \pm 0.08$

W^- modes are charge conjugates of the modes below.

W^+ DECAY MODES		Fraction (Γ_i/Γ)	Confidence level	p (MeV/c)
$\ell^+\nu$	[b]	(10.80 ± 0.09) %		–
$e^+\nu$		(10.75 ± 0.13) %		40199
$\mu^+\nu$		(10.57 ± 0.15) %		40199
$\tau^+\nu$		(11.25 ± 0.20) %		40179
hadrons		(67.60 ± 0.27) %		–
$\pi^+\gamma$		$< 8 \times 10^{-5}$	95%	40199
$D_s^+\gamma$		$< 1.3 \times 10^{-3}$	95%	40175
$c\text{X}$		(33.4 ± 2.6) %		–
$c\overline{s}$		$(31\ ^{+13}_{-11})$ %		–
invisible	[c]	(1.4 ± 2.8) %		–

Z

$J = 1$

Charge $= 0$
Mass $m = 91.1876 \pm 0.0021$ GeV [d]
Full width $\Gamma = 2.4952 \pm 0.0023$ GeV
$\Gamma(\ell^+\ell^-) = 83.984 \pm 0.086$ MeV [b]
$\Gamma(\text{invisible}) = 499.0 \pm 1.5$ MeV [e]
$\Gamma(\text{hadrons}) = 1744.4 \pm 2.0$ MeV
$\Gamma(\mu^+\mu^-)/\Gamma(e^+e^-) = 1.0009 \pm 0.0028$
$\Gamma(\tau^+\tau^-)/\Gamma(e^+e^-) = 1.0019 \pm 0.0032$ [f]

Average charged multiplicity

$\langle N_{charged} \rangle = 20.76 \pm 0.16$ (S = 2.1)

Couplings to leptons

$g_V^\ell = -0.03783 \pm 0.00041$
$g_V^u = 0.29^{+0.10}_{-0.08}$
$g_V^d = -0.33^{+0.05}_{-0.07}$
$g_A^\ell = -0.50123 \pm 0.00026$
$g_A^u = 0.50^{+0.04}_{-0.07}$
$g_A^d = -0.524^{+0.050}_{-0.030}$
$g^{\nu_\ell} = 0.5008 \pm 0.0008$
$g^{\nu_e} = 0.53 \pm 0.09$
$g^{\nu_\mu} = 0.502 \pm 0.017$

Asymmetry parameters [g]

$A_e = 0.1515 \pm 0.0019$
$A_\mu = 0.142 \pm 0.015$
$A_\tau = 0.143 \pm 0.004$
$A_s = 0.90 \pm 0.09$
$A_c = 0.670 \pm 0.027$
$A_b = 0.923 \pm 0.020$

Charge asymmetry (%) at Z pole

$A_{FB}^{(0\ell)} = 1.71 \pm 0.10$
$A_{FB}^{(0u)} = 4 \pm 7$
$A_{FB}^{(0s)} = 9.8 \pm 1.1$
$A_{FB}^{(0c)} = 7.07 \pm 0.35$
$A_{FB}^{(0b)} = 9.92 \pm 0.16$

Z DECAY MODES		Fraction (Γ_i/Γ)	Scale factor/ Confidence level	p (MeV/c)
e^+e^-		(3.363 ±0.004) %		45594
$\mu^+\mu^-$		(3.366 ±0.007) %		45594
$\tau^+\tau^-$		(3.370 ±0.008) %		45559
$\ell^+\ell^-$	[b]	(3.3658±0.0023) %		–
invisible		(20.00 ±0.06) %		–
hadrons		(69.91 ±0.06) %		–
$(u\overline{u}+c\overline{c})/2$		(11.6 ±0.6) %		–
$(d\overline{d}+s\overline{s}+b\overline{b})/3$		(15.6 ±0.4) %		–
$c\overline{c}$		(12.03 ±0.21) %		–
$b\overline{b}$		(15.12 ±0.05) %		–
$b\overline{b}b\overline{b}$		(3.6 ±1.3) $\times 10^{-4}$		–
ggg		< 1.1 %	CL=95%	–
$\pi^0\gamma$		$< 5.2 \times 10^{-5}$	CL=95%	45594
$\eta\gamma$		$< 5.1 \times 10^{-5}$	CL=95%	45592
$\omega\gamma$		$< 6.5 \times 10^{-4}$	CL=95%	45590
$\eta'(958)\gamma$		$< 4.2 \times 10^{-5}$	CL=95%	45589
$\gamma\gamma$		$< 5.2 \times 10^{-5}$	CL=95%	45594
$\gamma\gamma\gamma$		$< 1.0 \times 10^{-5}$	CL=95%	45594
$\pi^\pm W^\mp$	[h]	$< 7 \times 10^{-5}$	CL=95%	10150
$\rho^\pm W^\mp$	[h]	$< 8.3 \times 10^{-5}$	CL=95%	10125
$J/\psi(1S)\text{X}$		$(3.51\ ^{+0.23}_{-0.25}) \times 10^{-3}$	S=1.1	–
$\psi(2S)\text{X}$		(1.60 ±0.29) $\times 10^{-3}$		–
$\chi_{c1}(1P)\text{X}$		(2.9 ±0.7) $\times 10^{-3}$		–
$\chi_{c2}(1P)\text{X}$		$< 3.2 \times 10^{-3}$	CL=90%	–

$\Upsilon(1S)\text{X} + \Upsilon(2S)\text{X} + \Upsilon(3S)\text{X}$		(1.0 ±0.5) $\times 10^{-4}$		–
$\Upsilon(1S)\text{X}$		$< 4.4 \times 10^{-5}$	CL=95%	–
$\Upsilon(2S)\text{X}$		$< 1.39 \times 10^{-4}$	CL=95%	–
$\Upsilon(3S)\text{X}$		$< 9.4 \times 10^{-5}$	CL=95%	–
$(D^0/\overline{D}^0)\text{X}$		(20.7 ±2.0) %		–
$D^\pm\text{X}$		(12.2 ±1.7) %		–
$D^*(2010)^\pm\text{X}$	[h]	(11.4 ±1.3) %		–
$D_{s1}(2536)^\pm\text{X}$		(3.6 ±0.8) $\times 10^{-3}$		–
$D_{sJ}(2573)^\pm\text{X}$		(5.8 ±2.2) $\times 10^{-3}$		–
$D^{*\prime}(2629)^\pm\text{X}$		searched for		–
$B^+\text{X}$	[i]	(6.08 ±0.13) %		–
$B_s^0\text{X}$	[i]	(1.59 ±0.13) %		–
$B_c^+\text{X}$		searched for		–
$\Lambda_c^+\text{X}$		(1.54 ±0.33) %		–
$\Xi_c^0\text{X}$		seen		–
$\Xi_b\text{X}$		seen		–
b-baryon X	[i]	(1.38 ±0.22) %		–
anomalous γ + hadrons	[j]	$< 3.2 \times 10^{-3}$	CL=95%	–
$e^+e^-\gamma$	[j]	$< 5.2 \times 10^{-4}$	CL=95%	45594
$\mu^+\mu^-\gamma$	[j]	$< 5.6 \times 10^{-4}$	CL=95%	45594
$\tau^+\tau^-\gamma$	[j]	$< 7.3 \times 10^{-4}$	CL=95%	45559
$\ell^+\ell^-\gamma\gamma$	[k]	$< 6.8 \times 10^{-6}$	CL=95%	–
$q\overline{q}\gamma\gamma$	[k]	$< 5.5 \times 10^{-6}$	CL=95%	–
$\nu\overline{\nu}\gamma\gamma$	[k]	$< 3.1 \times 10^{-6}$	CL=95%	45594
$e^\pm\mu^\mp$	LF [h]	$< 1.7 \times 10^{-6}$	CL=95%	45594
$e^\pm\tau^\mp$	LF [h]	$< 9.8 \times 10^{-6}$	CL=95%	45576
$\mu^\pm\tau^\mp$	LF [h]	$< 1.2 \times 10^{-5}$	CL=95%	45576
pe	L,B	$< 1.8 \times 10^{-6}$	CL=95%	45589
$p\mu$	L,B	$< 1.8 \times 10^{-6}$	CL=95%	45589

Higgs Bosons — H^0 and $H^\pm$, Searches for

The limits for H_1^0 and A_0 refer to the m_h^{max} benchmark scenario for the supersymmetric parameters.

H^0 Mass $m > 114.4$ GeV, CL = 95%

H_1^0 in Supersymmetric Models ($m_{H_1^0} < m_{H_2^0}$)

Mass $m > 92.8$ GeV, CL = 95%

A^0 Pseudoscalar Higgs Boson in Supersymmetric Models [f]

Mass $m >$ 93.4 GeV, CL = 95% $\tan\beta > 0.4$

$H^\pm$ Mass $m >$ 79.3 GeV, CL = 95%

See the Particle Listings for a Note giving details of Higgs Bosons.

Heavy Bosons Other Than Higgs Bosons, Searches for

Additional W Bosons

W' with standard couplings decaying to $e\nu$

Mass $m >$ 1.000×10^3 GeV, CL = 95%

Additional Z Bosons

$Z'_{\rm SM}$ with standard couplings

Mass $m >$ 923 GeV, CL = 95% ($p\overline{p}$ direct search)

Mass $m >$ 1500 GeV, CL = 95% (electroweak fit)

Z_{LR} of $SU(2)_L \times SU(2)_R \times U(1)$ (with $g_L = g_R$)

Mass $m >$ 630 GeV, CL = 95% ($p\overline{p}$ direct search)

Mass $m >$ 860 GeV, CL = 95% (electroweak fit)

Z_χ of $SO(10) \rightarrow SU(5) \times U(1)_\chi$ (with $g_\chi = e/\cos\theta_W$)

Mass $m >$ 822 GeV, CL = 95% ($p\overline{p}$ direct search)

Mass $m >$ 781 GeV, CL = 95% (electroweak fit)

Z_ψ of $E_6 \rightarrow SO(10) \times U(1)_\psi$ (with $g_\psi = e/\cos\theta_W$)

Mass $m >$ 822 GeV, CL = 95% ($p\overline{p}$ direct search)

Mass $m >$ 475 GeV, CL = 95% (electroweak fit)

Z_η of $E_6 \rightarrow SU(3) \times SU(2) \times U(1) \times U(1)_\eta$ (with $g_\eta = e/\cos\theta_W$)

Mass $m >$ 891 GeV, CL = 95% ($p\overline{p}$ direct search)

Mass $m >$ 619 GeV, CL = 95% (electroweak fit)

Scalar Leptoquarks

Mass $m >$ 256 GeV, CL = 95% (1st generation, pair prod.)

Mass $m >$ 298 GeV, CL = 95% (1st gener., single prod.)

Mass $m >$ 316 GeV, CL = 95% (2nd gener., pair prod.)

Mass $m >$ 73 GeV, CL = 95% (2nd gener., single prod.)

Mass $m >$ 229 GeV, CL = 95% (3rd gener., pair prod.)

(See the Particle Listings for assumptions on leptoquark quantum numbers and branching fractions.)

Axions (A^0) and Other Very Light Bosons, Searches for

The standard Peccei-Quinn axion is ruled out. Variants with reduced couplings or much smaller masses are constrained by various data. The Particle Listings in the full *Review* contain a Note discussing axion searches.

The best limit for the half-life of neutrinoless double beta decay with Majoron emission is $> 7.2 \times 10^{24}$ years (CL = 90%).

NOTES

[a] Theoretical value. A mass as large as a few MeV may not be precluded.

[b] ℓ indicates each type of lepton (e, μ, and τ), not sum over them.

[c] This represents the width for the decay of the W boson into a charged particle with momentum below detectability, p< 200 MeV.

[d] The Z-boson mass listed here corresponds to a Breit-Wigner resonance parameter. It lies approximately 34 MeV above the real part of the position of the pole (in the energy-squared plane) in the Z-boson propagator.

[e] This partial width takes into account Z decays into $\nu\overline{\nu}$ and any other possible undetected modes.

[f] This ratio has not been corrected for the τ mass.

[g] Here $A \equiv 2g_V g_A/(g_V^2+g_A^2)$.

[h] The value is for the sum of the charge states or particle/antiparticle states indicated.

[i] This value is updated using the product of (i) the $Z \rightarrow b\overline{b}$ fraction from this listing and (ii) the b-hadron fraction in an unbiased sample of weakly decaying b-hadrons produced in Z-decays provided by the Heavy Flavor Averaging Group (HFAG, http://www.slac.stanford.edu/xorg/hfag/osc/PDG_2009/#FRACZ).

[j] See the Z Particle Listings for the γ energy range used in this measurement.

[k] For $m_{\gamma\gamma} = (60 \pm 5)$ GeV.

[l] The limits assume no invisible decays.

J. Glossary

Antiproton: The negatively charged antiparticle to the proton.

Antiparticle: An antiparticle has identical properties like the corresponding particle in many cases, except some quantum numbers like the charge and baryon number, that have exactly opposite values.

Barn: Unit of the cross section: 1 Barn = $10^{-24}\,\mathrm{cm}^2$.

Baryons: Collective name of all *h*adrons, that are *F*ermionen and have a mass $\geq m_p$.

Accelerator: An instrument, that increases the velocity – and with it the energy – of charged particles. Only stable particles like electrons, protons and ions can be accelerated.

Bhabha scattering: Elastical scattering $e^+e^- \rightarrow e^+e^-$.

Borns approximation: (Here:) processes of lower order.

Boson: Every particle is either a boson or a fermion. Bosons are particles with integer numbered spin, they conform to Bose-Einstein statistics. The carriers of fundamental interactions are all bosons. (see also *F*ermion).

Breit-Wigner resonance: refer to section D, suplementary materials.

Bremsstrahlung: the radiation (photons) emitted by charged particles in an electromagnetic field..

CERN: before **C**onseil **E**uropéen pour la **R**echerche **N**ucléaire, today: European Organization for Nuclear Research. European centre for elementray particle physics in Geneva. Refer to the extensive homepage at `http://www.cern.ch`.

Confinement: Describes the fact that quarks can not exist as free particles.

DESY: (**D**eutsches **E**lektronen **S**Ynchrotron)
German centre for elementary particle physics in Hamburg.

Detector: An instrument to detectparticles and measure their properties.

Drift chamber: Detector for measuring the trajectory of particles, advancement from the *p*roportional chamber.

Gauge bosons: *V*ektor bosons, that carry the fundamental forces between the fundamental *f*ermions. 12 gauge bosons are known: 8 *g*luons, the photon, W^+, W^- and Z^0.

Electromagnetic calorimeter: An incoming γ, e^+ or e^- gives off all of its energy ina cascade. With the calorimeter, the energy of the particle can be measured.

Electromagnetic interaction: The longrange force that affects electrical charges, currents and magnets. Carrier of the force is the photon.

Electron: Spin 1/2 fermion. The lightest of the charged leptons. It only has 1/1836 of the mass of a proton.

Electroweak interaction: A fundamental interaction. Unifiation of the electromagnetic and weak interaction.

Elementary particle: A particle, that can not be devided into other particles. According to our current state of understanding, quarks, leptons and the gauge bosons are elementary.

Color: Name for a quantum number of quarks and gluons. There are three colors (red, geen, blue).

Fermion: see also *B*oson. Fermions are particles with half integer spin, they conform to Fermi-Dirac statistics. The fundamental components (quarks and leptons) are all fermions.

Feynman diagrams: Diagrams, that were introduced by R. P. Feynman to describe the mechanisms of the elementary interactions. There is a set of corresponding rules for calculations.

Flavor: A term to describe the kind of a quark (up, down, strange, charm, bottom, top).

Shape factor: A shape factor in the formula of the cross section, that takes the difference of the charge distribution from a point into account,

Fragmentation: The process, that generates bundles of colorles particles from colored quarks and gluons.

Fundamentale Wechselwirkungen: Zu diesen zählen die *s*tarke Wechselwirkung, die *e*lektroschwache Wechselwirkung und die *G*ravitation.

Charged (weak) current: The part of the *w*eak interaction, that is described by the exchange of $W^{\pm}$gauge bosons.

GeV (Giga-eV): 10^9 eV.

Gluon: massless *v*ektor boson. Conveys the *s*trong interaction. There are 8 different gluons, that each carry a color and an anticolor.

Gravitation: A longranged force, that affects all particles. It is, however, weak and only affects macroscopic objects.

Graviton: The hypothetical massless boson that serves as carrier of gravitation.

GUT (Grand Unified Theories): A mathematical farmalism to unify all fundamental interactions.

Hadrons: Particles, that are affected by the *s*trong interaction. This includes the *m*esons and the *b*aryons. Components of these particles are *q*uarks and *a*ntiquarks.

Higgs boson: the spin 0 particle demanded by theory, that has to exist if the *H*iggs mechanism is responsible for the gauge bosons $W^{\pm}$, Z^0 having mass.

Higgs mechanism: A mechanism, that gives a field particle mass withot breaking the gauge symmetry using the existance of a spin 0 particle

JET chamber: Big drift chamber at OPAL.

Coupling constant: A measure for the strength of an interaction. the coupling constants of the gauge theories are not constant, but depend on the momentum transfer.

Cosmic radiation: Radiation of extremely high energy, that hits earth from space. Muons with high energy, generated by interactions of the cosmic radiation with the atmosphere, typically lead to background events in experiments on particle physics.

Critical energy: Kinetic energy of a charged particle, where the energy loss via bremsstrahlung is the same as the energy loss via ionization. At higher energies, bremsstrahlung is predominate.

LEP: (**L**arge **E**lectron-**P**ositron storage ring), e^+e^- storage ring at CERN with 27 km tunnel length.

Lepton: Spin 1/2 fermion. One of six elementary particles (that are known to date) that are af-

fected by the weak, but not the strong interacion: the electron, the muon, the tau lepton along with their respective neutinos.

Luminosity: A term introduced to describe the intensity of interaction of a storage ring. A higher luminosity corresponds to a higher rate of interaction.

Mandelstam variable: see section **??**, suplementary materials

Muon: Spin 1/2 *f*ermion. A charged lepton like the electron, but with roughly 200 times its mass.

Neutral (weak) current: The part of the weak interaction that is described by the exchange of Z^0gauge bosons.

Neutrino: Spin 1/2 fermion. One of the three neutral leptonswith very small mass, each associated with a charged lepton. Neutrinos are only affected by the weak force.

Neutron: A neutral hadron with a mass slightly larger than that of the proton. Like the proton, it is built from three quarks and belongs to the nucleons.

OPAL: (**O**mni-**P**urpose-**A**pparatus for **L**EP), name of one of the four experiments at LEP. The others are ALEPH, DELPHI and L3.

Partial cross section: Cross section for an interaction with a specific final state.

Photon: A massless spin 1 boson, that carries the electromagnetic force. Electromagnetic radiation consists of photons.

Positron: The positive antiparticle to the electron.

Proportional chamber: Detector for inonization measurements, based on the principle of the Geiger-Müller counter. Often used as *m*ulti-wire proportional chamber (*M*WPC) at accelerator experiments, that can measure particle tracks and, combined with a magnetic fielsd, momenta.

Proton: A positively charged hadron. The lightest baryon consists of three quarks and is constituent of all nuclei.

QCD (**Q**uantum-**C**hromo-**D**ynamics), theory of the *s*trong interaction. Describes the interaction between *q*uarks and *g*luons using the color field.

QED (**Q**uantum-**E**lectro-**D**ynamics), theory of the electromagnetic force. Describes the interaction of charged particles in the electromagnetic field.

Quarks (antiquarks): Spin 1/2 fermions. The six different quarks (see *F*lavor) and their antiquarks are elementary particles with an electrical charge that is a fraction (1/3 or 2/3) of the elementary charge e. They do not exist as free particles but are bound as quark antiquark pair (*m*esons, e.g. pions, kaons) or as three quark states (*b*aryons, e.g. proton, neutron) by the stron interaction. Each quark has three additional degrees of freedom (*F*arbe).

Real photons: Only real photons can be independant of their ource. They conform to the condition $E^2 = m^2 + \vec{p}^2$. As photons do not have mass, momentum and energy are the same.

Weak interaction: A weak, short ranged force, that affects all quarks and leptons. It is responsible for the decay of many particles (the β decay of neutrons for example).

Storage ring (collider): An accelerator, where wo opposed particle beams are brought to colision.

Standard Model: The combined theory of the strong, electromagnetic and weak forces. The Standard Model describes basically describes everything we know about core and particle physics today.

Strong interaction: A short ranged interaction, the strongest of all fundamental interactions. It affects quarks and all particles consisting of quarks (hadrons), but not leptons. It is described by QCD. Its carriers are the gluons.

Radiation length: Traversed length in a material, after which the number of remaining original electrons (in a cascade) is only $1/e$ of the original number.

Synchrotron radiation: Electromagnetic radiation, that is emitterd by charged particles, when they are deviated from their original path, like in a acircular accelerator like LEP for example.

Tau (τ) lepton: Spin 1/2 fermion. the heaviest of the known leptons.

Particle physics: Goal of particle physics is the analysis of subnuclear particles, both elementary and composed, and forces, that describe their interactions.

Thrust: $T = \max_{\vec{n}} \frac{\sum_i |\vec{p}_i \cdot \vec{n}|}{\sum_i |\vec{p}_i|}$, where $\vec{n}$ is an unit vector, that gives the direction of the thrust axis and $\vec{p}_i$ are the momenta of all participating particles.

Totale cross section: The cross section of an interaction, integrated over all possible final states.

TPC: (**T**ime **P**rojection **C**hamber), Advancement of the *d*rift chamber.

Vektor bosons: Bosons with spin 1. The *g*auge bosons belong to these particles.

Vektor mesons: *H*adrons with spin parity $J^P = 1^-$.

Virtual photons: Virtual photons can be time-like ($E > p$) or space-like ($E < p$). As quasi free particles, they can only exist for a short period of time, that is given by the uncertainty relation. They are carriers of the electromagnetic force between charged particles.

Virtual particles: see also *v*irtual photon. The three heavy (virtual) spin 1 bosons $\boldsymbol{W^+, W^-}$**a**nd $\boldsymbol{Z^0}$ are carriers of the weak interaction.

Interaction: Process, where only energy and momentum are transferred between two particles (elastic scattering) or particles are generated and anihilated (inelastic scattering).

Weinberg angle: Mixing angle (θ_W) in the theory of the *e*lectroweak interaction.